Sensitivity analysis in key parameters related to wind power production

Master's Thesis in Energy

Astrid Fonnes Myren
June 2021

University of Bergen
Geophysical Institute

Acknowledgements

I would first like to thank my supervisor, Finn Gunnar Nielsen, for the guidance in finding an interesting research topic and for all the great ideas and improvements.

Secondly, I want to express my gratitude to my co-supervisor, Ida Marie Solbrekke, for providing wind speed data and insight to wind energy meteorology, for great advice and for help with proofreading.

Thanks to Hilde Haakenstad for providing temperature data, and to Marte Godvik for access to industry standards.

I also want to thank Jochen Reuder and Birgitte Furevik for their advice on the vertical wind speed profile.

Thanks to my fellow students for making the past two years memorable, and a special thanks to Victor for always helping me with Python.

Lastly, I want to thank my boyfriend Øystein and my family for the endless support and cheering.

Abstract

The development of the offshore wind industry leads to wind turbines increasing in size and height. The aim of this thesis is to investigate how the power output and temporal power variability of an offshore wind turbine change when key parameters related to wind power production are altered. A sensitivity analysis is performed by considering the offshore reference wind turbines NREL 5 MW and NREL 15 MW. The parameters analysed are the hub height, the rotor diameter, the shape and wind speed limits of the power curve, the choice of wind speed extrapolation model, and the wind shear over the rotor disk. The new hindcast data set NORA3 is compared to the established hindcast data set NORA10 at seven sites in the North Sea and the Norwegian Sea. The analysis finds that NORA3 and NORA10 are in close agreement when used to calculate the capacity factor of the wind turbine NREL 5 MW. The wind shear coefficient α is found to be on average 0.070 for NORA3 and 0.058 for NORA10 and to vary in time, with wind speed, and with latitude. The monthly mean α and the mean temperature difference between 100 m asl and the sea surface temperature (SST) were found to be closely related. By using the NREL 15 MW wind turbine instead of the NREL 5 MW wind turbine, the capacity factor will increase by 5.1 percentage points and the temporal power variability will increase. The use of a fixed, time- and space independent $\alpha = 0.12$ to extrapolate the wind speed from 10 m to hub height results in an average overestimation of the capacity factor of 5.8 percentage points for NREL 5 MW and 7 percentage points for NREL 15 MW. The implantation of a storm control can increase the power output and will decrease the temporal power variability.

Contents

Nomenclature

Abbreviations

Abbreviation	Full name
CF	Capacity factor
ECMWF	European Centre for Medium-Range Weather Forecasts
HIRLAM	High Resolution Limited Area Model
NORA3	Norwegian 3 km Reanalysis Archive
NORA10	Norwegian 10 km Reanalysis Archive
NREL	National Renewable Energy Laboratory
NWP	Numerical weather prediction model
REWS	Rotor equivalent wind speed
SC1	Storm control 1
SC2	Storm control 2
SST	Sea surface temperature

Symbols

Symbol	Full name [Unit]
α	Wind shear coefficient
ρ	Air density [kg/m^3]
u	Wind speed [m/s]
A	Area of rotor disk [m^2]
D	Rotor diameter [m]
R	Rotor radius [m]
H	Hub height [m]
C_p	Capacity factor
P	Power [W]
P_N	Normalized power
t	Time [h]
μ	Arithmetic mean
σ	Arithmetic standard deviation

1 Introduction

1.1 Background

The new, improved climate targets in the EU are to reduce greenhouse gas emissions by 55 % by 2030 (compared to 1990) and make Europe the first climate-neutral continent by 2050 (European Commission, 2019). Offshore wind power will play a key role in reaching the ambitious climate target due to the high capacity factors (CF) that can be obtained, the large sites available, technological advances, and the rapid cost reduction of offshore wind power (European Commission, 2020a; CarbonBrief, 2020). In 2020, the European Commission launched a strategy to reach 60 GW of offshore wind in the EU by 2030, increasing to 300 GW by 2050 (European Commission, 2020b). The large increase from 12 GW of offshore wind in the EU in 2020 demands a massive scale-up of the offshore wind industry in Europe.

The offshore wind industry development leads to wind turbines growing in size and power, allowing the wind turbines to utilise stronger winds higher in the atmosphere. The number of wind turbines in a wind farm can be reduced if the power output of each wind turbine is increased, leading to a reduction in construction costs. The average rated capacity of offshore horizontal-axis wind turbines installed in Europe was 8.2 MW in 2020, 5 % higher than in 2019 (WindEurope, 2021). The offshore wind turbines are expected to increase to 17 MW by 2035 with rotor diameters of 250 m and hub heights of 150 m (Wiser et al., 2021). The large height of the wind turbines gives rise to challenges not experienced for smaller wind turbines.

One challenge related to the height of the wind turbines is access to wind data. To find the best location for a potential wind farm, the wind characteristics at the site must be known for the whole height range of the wind turbine (Emeis, 2018). The wind speed distribution, the wind direction, the vertical wind shear, and temporal wind speed variation are important wind parameters influencing the wind power output. Traditionally, these parameters have been investigated by measurement devices mounted on meteorological masts. Today, the heights of modern offshore wind turbines have exceeded

the heights of offshore meteorological masts, making the masts unable to cover the full height of the turbine. An alternative to using measurement devices is to use data from models. Two data sets from such models produced by the Norwegian Meteorological Institute are the well established Norwegian Reanalysis Archive 10 km (NORA10) (Reistad et al., 2011) and the new, state-of-the-art Norwegian Reanalysis Archive 3 km (NORA3) (Haakenstad, Breivik, Furevik, et al., 2021). NORA10 and NORA3 can provide wind characteristics for sites and heights not accessed previously, and the improved temporal and spatial resolution of NORA3 compared to NORA10 can give a better power estimate.

Another challenge is to obtain information of the wind characteristics at the desired height, and the increased height of offshore wind turbines complicates it. For wind energy purposes models are often used to extrapolate or interpolate the wind speed from a known height, usually 10 m, to hub height. A commonly used extrapolation model for offshore wind energy purposes is the empirical power law, which depends on the static stability of the atmosphere and the surface roughness of the ocean (Emeis, 2018). According to Gualtieri (2019), the most widely used variety of the power law in the literature is the power law with a fixed exponent (α), which assumes a time and space independent vertical wind speed profile. In addition to being the most widely used model, the power law with a fixed exponent is also one of the most incorrect models, with the largest wind speed difference between the estimated and the actual wind speed (Gualtieri, 2019). The utilisation of the power law with a fixed exponent can give a wrong estimate of the wind speed, and therefore a wrong estimate of the potential power output of a wind turbine. As the wind turbines keep increasing in height, the difference in estimated wind power output using the power law with a fixed power exponent and actual power output will increase.

A third challenge related to the increased height of offshore wind turbines is the validity of the assumption that the wind speed at hub height is representative of the whole rotor disk (Wagner et al., 2011). For small rotor diameters, the vertical difference in wind speed (wind shear) over the rotor disk is small, and the assumption that the wind speed at hub height is representative for the whole rotor disk can be used. The validity of this assumption will become more erroneous as the rotor disk continues to increase in size. In the new IEC 61400-12-1 standard for estimating the power output from a wind turbine, a new method for estimating the wind speed that affects the wind turbine is presented which takes into account the vertical wind shear (International Electrotechnical Commission, 2017). The method is called Rotor Equivalent Wind Speed (REWS) and gives an equivalent wind speed based on an area weighting of the wind speeds at multiple heights of

the rotor disk.

In addition to the challenges related to the larger turbine size, the increased share of variable power in the electrical grid is a challenge. Offshore wind power is variable on time scales ranging from seconds to years. This variability is a challenge when electricity from offshore wind is added to the electrical grid. The generated power and the consumed power must always be equal in magnitude, but the rapid fluctuations in offshore wind power require balancing measures. An option for reducing the challenge of variability is to reduce the variability of the power output itself. The standard wind turbine is abruptly shut off from full power to zero power at high wind speeds to prevent damage to the turbine, and is started again at full power when the wind speed is lower. The shutdown and startup make the power output variable, and this can be reduced if a storm control is implemented. A hysteresis storm control can reduce the frequency of the shutdowns and startups of the wind turbine and thereby reduce the variability of the power output (Cutululis et al., 2012). A soft cut-out storm-control allows the wind turbine to generate power at higher wind speeds (Markou et al., 2009; Bossanyi et al., 2012), thus eliminating the events of abrupt shutdowns and startups due to high wind speeds.

1.2 Motivation

The motivation of this thesis is to see the increased turbine height, the choice of wind speed model, the wind shear, and the use of a storm control in relation, and to investigate how they affect each other. The power curve of a wind turbine indicates the power output at a certain wind speed, and is limited by the cut-in wind speed after which the wind turbine is started, the rated wind speed after which the power output is held constant, and the cut-out wind speed after which the wind turbine is shut off to prevent damage. These wind speed limits can be altered by increasing the size of the wind turbine or by implementing a storm control. When the height of a wind turbine increases, the turbine will experience higher wind speeds which can result in the turbine shutting down more often, and I therefore expect that the gain of implementing a storm control will increase when the turbine size increases. The larger turbine height also results in the rotor disk covering a much larger section of the vertical wind profile, and the importance of knowing the wind shear and how it affects the power output increases. I also expect that using a model with an improved temporal and spatial resolution such as NORA3 will give a more accurate power estimate than the coarser NORA10. I expect that choice of extrapolation model for the vertical wind

shear will affect the power estimate of using a storm control.

1.3 Objectives

In this master thesis I aim to investigate how the capacity factor (CF) and the temporal variability of an offshore wind turbine changes when the size of the turbine increases, and how they change by implementing a storm control. I also aim to investigate how the increased size affects the importance of modelling the vertical wind shear over the rotor disk and how the choice of wind speed model affects CF.

The main objective is to perform a sensitivity analysis in key parameters related to offshore wind power production. The parameters in the analysis are the hub height, the rotor diameter, the shape and wind speed limits of the power curve, the choice of extrapolation model, and the wind shear over the rotor disk. The parameters will be studied by considering the power output and temporal power variability from the 5 MW and 15 MW reference wind turbines for offshore conditions developed by the National Renewable Energy Laboratory (NREL) (Jonkman et al., 2009; Gaertner et al., 2020), and how the power output and temporal power variability change by changing the parameters.

The secondary objectives are as follows:

- Investigate the wind speeds modelled by the new data set NORA3 compared to the data set NORA10, and investigate how the power output of a theoretical wind turbine is affected by the choice of model.
- Investigate the difference in wind power output using wind speed at hub height versus using REWS.

In the thesis, I will investigate a theoretical wind turbine located at seven sites in the North Sea and the Norwegian Sea. Due to the temporal resolution of the data sets, I will not investigate turbulent effects on time scales less than 1 hour. I will neither consider the wind direction, nor the vertical component of the wind speed.

1.4 Thesis overview

Chapter 2 presents the theoretical background for the thesis, including the vertical wind speed profile, data sources for wind power generation and how the wind power can be extracted. Chapter 3 describes the data sets NORA10

and NORA3, the reference wind turbines NREL 5 MW and NREL 15 MW, the power curves and the statistics used. Chapter 4 presents and discusses the results, and it consists of two parts. The first part will compare wind speeds and CF using the data sets NORA3 and NORA10. In the second part, the sensitivity analysis be performed using the wind turbines NREL 5 MW and NREL 15 MW. Chapter 5 concludes the findings and provides suggestions for further work.

2 | Theoretical background

When assessing a site for deployment of an offshore horizontal-axis wind turbine, the wind characteristics at the site must be known in order to estimate the power output. Important wind characteristics include the wind speed distribution, the temporal and spatial variability of the wind flow, and the vertical wind speed profile in the height range of the wind turbine. The wind flow can be investigated using measurements or models, and the wind data obtained can be used to estimate the power output of the chosen wind turbine from a power curve, which is defined for the wind speed at hub height or the area weighted wind speed of the rotor disk. The estimated power output can be used to calculate the capacity factor, which is a measure of the efficiency of the wind turbine.

2.1 Wind characteristics

Wind turbines extract energy from the wind. The wind is a three-dimensional flow, and can be divided into wind speed and wind direction. The wind speed u can further be divided into a mean wind speed component (usually 10 min mean) $\bar{u}$ and a turbulent deviation u'.

On a spatial scale, the wind variation can be divided into three different regimes: the primary atmospheric circulation, the synoptic regime and the tertiary circulation. The primary atmospheric circulation is driven by the excess insolation at the equator. The resulting transportation of thermal energy towards the poles determines the prevailing winds. The wind patterns in the synoptic regime are determined by the cyclones and anticyclones which form due to temperature differences. The tertiary circulations are wind patterns that arise due to geography. Examples are land and sea breezes which form due to the difference in heating of landmasses and the ocean.

The wind varies at different timescales ranging from seconds to years. The annual, synoptic, diurnal and turbulent are the timescales most important for wind energy. On timescales smaller than one minute, the wind speed varies

due to turbulence, which causes stress on the wind turbines. The changes on a diurnal scale are caused by the heating and cooling of the surface and are of lesser importance offshore than onshore. The variations on a synoptic scale (several days) are caused by the passing of cyclones and anticyclones. The variations on longer scales are caused by seasonal differences and interannual variations.

2.2 Marine atmospheric boundary layer

The vertical section of the atmosphere that impacts offshore wind turbines the most is called the marine atmospheric boundary layer (MABL) (Emeis, 2018; Jaffe et al., 2018). The MABL is the part of the atmosphere directly influenced by the surface, and the wind patterns here are complex. The height of the MABL may extend up to a level of 100-1000 m above sea level (asl), depending on the conditions in the atmosphere. MABL consists of three layers: the sublayer, the surface layer, and the Ekman layer, illustrated in figure 2.1. The lowest level is called the sublayer and is influenced by single waves. The second layer is the surface layer, also called the Prandtl layer or the constant-flux sublayer. Here the turbulent mixing is strong and the wind speed starts increasing from zero, and is assumed to have a constant direction due to the small influence of the Coriolis force. The sublayer and surface layer are located in the lowest approximately 10 % of the MABL. The third layer is called the Ekman layer and constitutes approximately 90 % of the MABL. The wind speed continues to increase in the Ekman layer and the wind direction rotates due to the Coriolis force until the wind at the top of the layer is equal to the geostrophic winds. The geostrophic winds above the MABL are located in the free troposphere, where the winds are stronger than in the MABL, no longer affected by the surface friction. For wind turbines with large hub heights and rotor diameters, the wind speed in both the MABL and the free troposphere may affect the rotor disk.

2.3 Static stability

The static stability (stability further on) is a measure of how vertical movements in the atmosphere are accelerated or decelerated. A very simple stability measure in the MABL is ΔT, the temperature difference between the air and the sea surface. Dry air cools at approximately 1 K/100 m when moved adiabatically upwards while moist air cools at approximately 0.6 K/100 m (Spiridonov et al., 2021; Emeis, 2018). If the temperatures are evaluated at 0

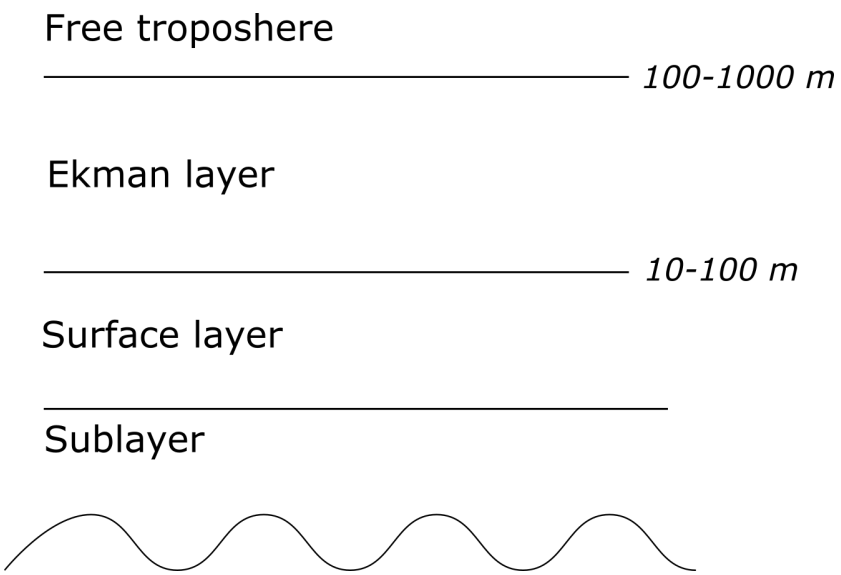

Figure 2.1: Illustration of the marine atmospheric boundary layer (MABL). Adapted from (Emeis, 2018).

m and 100 m asl, the stability of the atmosphere can roughly be determined as follows: The atmosphere is unstable when $\Delta T < -1$, neutral or conditionally unstable when $-1 \leq \Delta T \leq -0.6$, and stable when $\Delta T > -0.6$. A more precise stability measure is the Richardson number (Stull, 1988), but it will not be evaluated in this thesis.

2.4 Vertical wind speed profile

The variation of the wind speed with height in the MABL is called the vertical wind shear, and is illustrated in figure 2.2. The shape of the vertical wind shear depends on the atmospheric stability and the roughness of the sea surface. In unstable conditions, the wind shear is small due to vertical mixing. Reversely, the wind shear is large during stable conditions due to little or no vertical mixing. The roughness of the sea surface affects how quickly the wind speed decreases towards the sea surface and where it becomes zero. The surface roughness is measured by the roughness length z_0. Over water, z_0 increases with increasing wind speed due to the growing waves which make the surface rougher. The surface roughness is in general smaller offshore than onshore, resulting in a smaller wind shear over the ocean than for the same height onshore.

To be able to calculate the power of a wind turbine it is necessary to

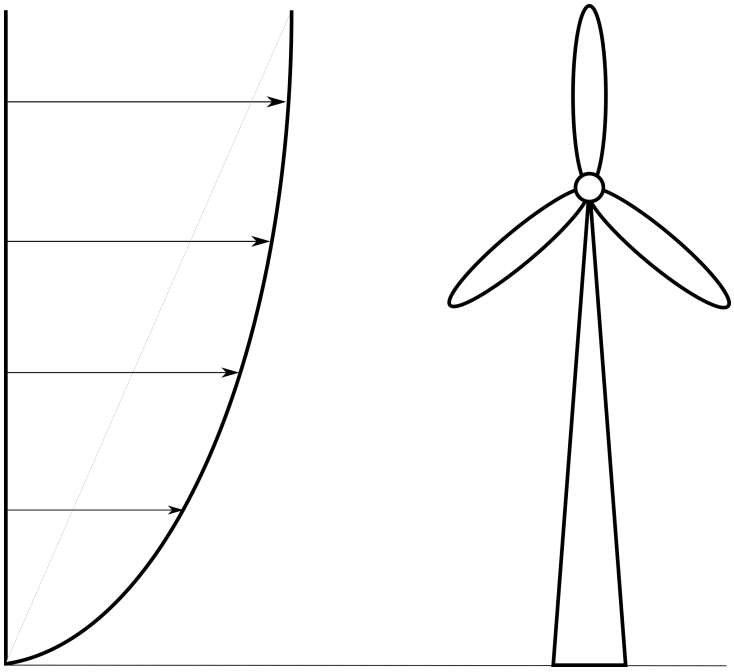

Figure 2.2: Illustration of the wind shear incident on a wind turbine. The arrows represent the wind speed at each height.

know the wind speed in the area covered by the rotor disk. The wind speed variation with height can be described by models, and one such model is the theoretical logarithmic wind profile derived from turbulence theory (Stull, 1988; Emeis, 2018). The logarithmic wind profile assumes the the mean wind speed varies logarithmically with height in the surface layer and in neutral stability, and that the mean wind speed $\bar{u}$ at height z can be characterised as:

$$\bar{u}(z) = \frac{u_*}{\kappa} \ln\left(\frac{z-d}{z_0}\right) \tag{2.1}$$

where u_* is the friction velocity, $\kappa = 0.4$ is the von Karman constant, z_0 is the roughness length and d is the displacement length.

Another model of the vertical wind speed profile for the surface layer is the empirical power law, which assumes that wind speed varies exponentially with height (Emeis, 2018). For a given height z, the wind speed is characterised as:

$$u(z) = u(z_r)\left(\frac{z}{z_r}\right)^{\alpha} \tag{2.2}$$

where $u(z_r)$ is the wind speed at the reference height z_r and α is the wind

shear coefficient, also called the Hellmann exponent or the power law exponent. The wind shear coefficient α depends on the surface roughness and the stability of the atmosphere. For the FINO1 research platform in the German Bight, α has been shown to increase with increasing stability and also with increasing wind speed (Türk et al., 2008).

A third model is the empirical NORSOK wind profile, which is based on measurements from the island Frøya on the coast of Norway, as used by Furevik et al. (2012). The NORSOK wind profile relates the wind speed u_0 at the reference height $z_r = 10$ m asl to the wind speed u at height z, and is given by:

$$u(z) = u_0\Big[1 + C\ln\Big(\frac{z}{z_r}\Big)\Big] \tag{2.3}$$

where $C = 5.73 \times 10^{-2}\Big[1 + 0.15u_0\Big]^{1/2}$.

Most wind speed observations are measured at heights lower than hub height (often at 10 m asl), and a vertical wind speed profile is therefore used to extrapolate the wind speed from the measurement height to hub height. For wind energy purposes, it has been common to use the power law with a fixed, time and space independent α for each geography type. Under normal offshore conditions, $\alpha = 0.12$ has been commonly used (Det Norske Veritas, 2010).

2.5 Wind data sources

The wind characteristics at a site can be studied using measurements or model simulations. For onshore conditions and small wind turbines heights, measurements can be done using meteorological masts with mounted wind measurements devices. For offshore conditions and ever-increasing turbine heights, the construction of meteorological masts is no longer economically feasible. For these sites, the wind climate can be investigated using remote sensing devices (e.g. LiDARs) or models.

Numerical weather prediction (NWP) models predict the weather by resolving or parameterizing the governing equations and components of the atmosphere and ocean (Emeis, 2018; Spiridonov et al., 2021). The NWP models use the current weather conditions as a basis for the initial conditions. The number of observations used by the models increases continually, leading to more accurate estimations. Output from the models is provided at 3D grid points within the domain, and at discrete time steps. Reanalysis data is produced by NWP models using observations from various sources.

Unlike the NWP models used in weather forecasting, the reanalyses use unchanged model and observation setup throughout the period analysed. This makes the reanalysis data consistent in time. The reanalysis data is often more coarsely resolved than the data produced by weather forecast NWP models but can be downscaled to a finer resolution.

2.6 Wind power

The fundamental expression of the power available in a cross-section of a wind flow is given by (Letcher, 2017):

$$P = \frac{1}{2}\rho u^3 A \tag{2.4}$$

where ρ is the air density, u is the wind speed and $A = \pi R^2$ is the swept area for a horizontal axis wind turbine, where R is the rotor radius. A wind turbine is unable to convert all the power in the wind flow to mechanical power. The power is therefore reduced by the power coefficient C_p, resulting in the following equation for the turbine power:

$$P_T = \frac{1}{2}\rho u^3 C_p A \tag{2.5}$$

The theoretical maximum power a wind turbine can extract is defined by Betz' limit. Betz' limit is developed based on the assumption of an ideal (non-viscous and incompressible), one-dimensional flow, and considers the conservation of mass, momentum and energy. The result is that a maximum of 59 % of the wind power can be extracted by a wind turbine, resulting in a maximum power coefficient of $C_p = \frac{16}{27}$. The power coefficients of actual wind turbines are lower than the theoretical maximum of $\frac{16}{27}$.

The power output of a wind turbine varies for different wind speeds and can be described by a power curve that characterizes the power output at each wind speed. Figure 2.3 shows a typical power curve, and it can be divided into four regions. In region 1, the power output is zero until the turbine starts at the cut-in wind speed. In region 2, the power increases according to equation 2.5 until the turbine reaches rated power at rated wind speed. The power output is held constant in region 3 at rated power until the wind speed reaches the cut-out wind speed. The power output is held constant by turning the blades and reducing the power the turbine can extract. Above cut-out wind speed in region 4, the wind turbine is shut-off to prevent damage to the turbine, and the power output of the wind turbine is zero.

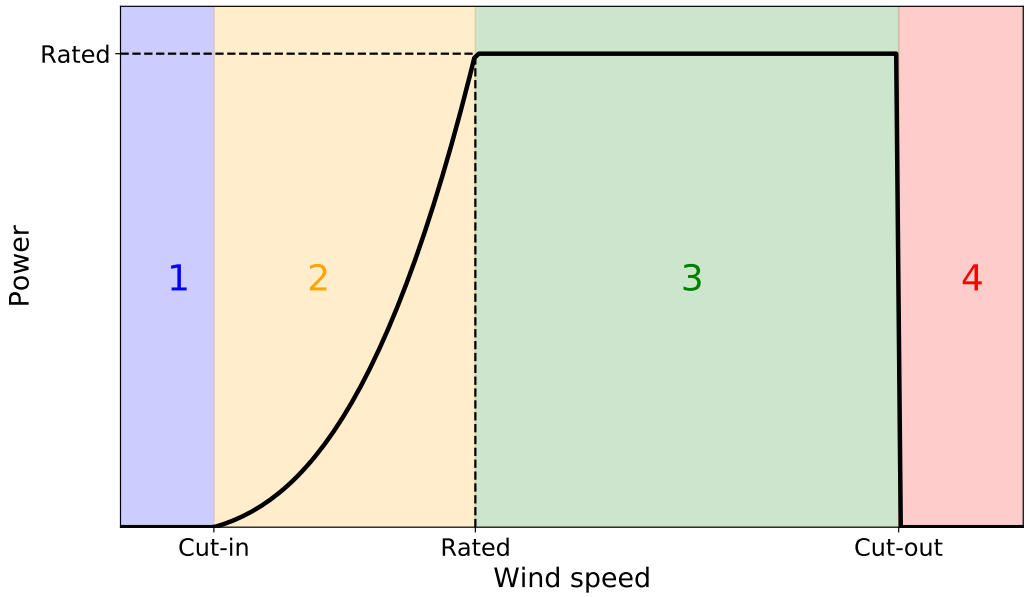

Figure 2.3: Power curve of a horizontal axis wind turbine. Power is measured on the y-axis and wind speed is measured on the x-axis.

The power curve can be altered by changing the properties of the turbine. By extending the rotor blades, the area of the rotor disk increases and the power output of the turbine increases. By increasing the hub height, the turbine reaches higher wind speeds, resulting in increased power output. Increasing the hub height can also shift the rated wind speed downwards if the capacity of the generator is held fixed because the generator will reach full power at a lower wind speed.

2.7 Rotor equivalent wind speed

According to the IEC 61400-12-1 standard (International Electrotechnical Commission, 2017), the power curve for a wind turbine is defined using the wind speed at hub height. For small rotor diameters, the wind speed at hub height has been considered representative of the whole rotor disk. However, for larger rotor diameters, the wind speed may change considerably over the disk, and the wind shear coefficient may not be constant. The rotor equivalent wind speed (REWS) has been developed to take into account the difference in wind speed over the rotor disk, and in the second edition of the IEC 61400-12-1 standard, it is recommended to use the REWS instead of the wind speed at the hub height.

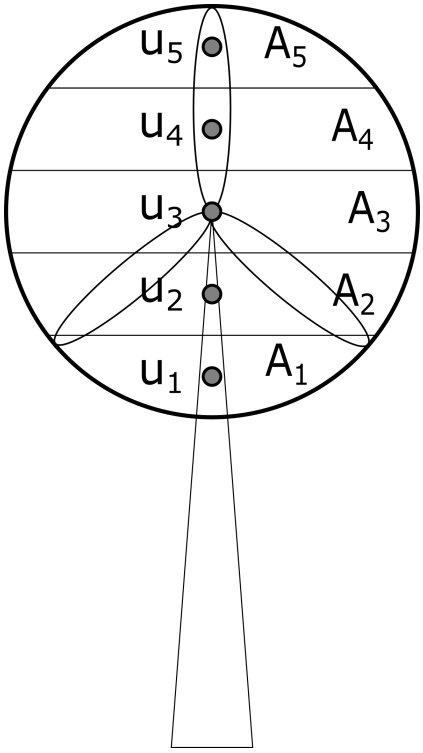

Figure 2.4: Illustration of the rotor equivalent wind speed method. A_1-A_5 are the section areas, and u_1-u_5 are the wind speeds in the center of each section. Adapted from (Wagner et al., 2011; Van Sark et al., 2019).

The rotor disk area is divided into horizontal segments as shown in figure 2.4, with the separation lines in the middle between the measurement points $u_1 - u_5$. The wind speed at each measurement point is weighted by the area in the section $A_1 - A_5$, and the REWS u_{eq} is given by:

$$u_{eq} = \sqrt[3]{\sum_{i=1}^{n_h} \frac{A_i}{A} u_i^3} \tag{2.6}$$

where n_h is the number of sections ($n_h \geq 3$), A is the area swept by the rotor, A_i is the area of section i and u_i is the wind speed in the middle of section i.

The segments are given by:

$$A_i = \int_{z_i}^{z_{i+1}} c(z)dz \tag{2.7}$$

where $c(z) = 2\sqrt{R^2 - (z-H)^2}$, R is the rotor radius and H is the hub

height.

Van Sark et al. (2019) investigated the difference between REWS and the wind speed at hub height and found that for $\frac{D}{H} \leq 1.8$ and $-0.05 \leq \alpha \leq 0.4$ the difference between the wind speeds is less than 1 % and concluded that it is not necessary to use REWS. D is the rotor diameter and H is the hub height.

2.8 Variable power output

Sudden changes in wind speed may lead to sudden, big changes in power output, called ramps or ramp events (Cutululis et al., 2012; Emeis, 2018). The ramps are often associated with storm events, where the wind speed exceeds the cut-out limit. These events occur more frequently offshore, where the wind speeds are stronger than onshore. With the development of offshore wind parks with increasing hub heights and with increasing distance from shore, the ramps are expected to increase (Emeis, 2018). By locating wind farms in clusters, the risk of ramps occurring at approximately the same time for individual wind turbines or wind farms increase.

The generation and consumption of electricity must be equal in magnitude at all times, and ramps lead to rapid variations in the electricity generation that can be difficult to balance. Options for balancing the variable wind power are e.g. large scale energy storage such as pumped hydropower (Graabak et al., 2016), interconnection between power plants (Solbrekke, Kvamstø, et al., 2020), or flexible power plants.

2.9 Storm control

The ramps described in section 2.8 can be reduced by implementing a storm control. A storm control is a control strategy that reduces the power output of the wind turbine when the wind speed exceeds the cut-out wind speed.

One type of storm control is the hysteresis strategy (Cutululis et al., 2012), illustrated in figure 2.5 A. When the wind speed exceeds the cut-out wind speed, the average wind speed must drop below a hysteresis limit (Cut-in 2) before the turbine can be turned on again at rated power. The hysteresis strategy is used to prevent frequent stops and startups of the wind turbine when the wind speed fluctuates around the cut-out wind speed.

Another type of storm control is the soft cut-out strategy (Markou et al., 2009; Bossanyi et al., 2012), illustrated in figure 2.5 B. When the wind speed exceeds the cut-out wind speed (Cut-out 1), the power output of the turbine

is gradually reduced from rated power to zero power at a higher wind speed (Cut-out 2). When the wind speed decreases the power follows the ramp back up to rated power. The soft cut-out strategy will lead to increased predictability and reduced variability of the power output (Bossanyi et al., 2012).

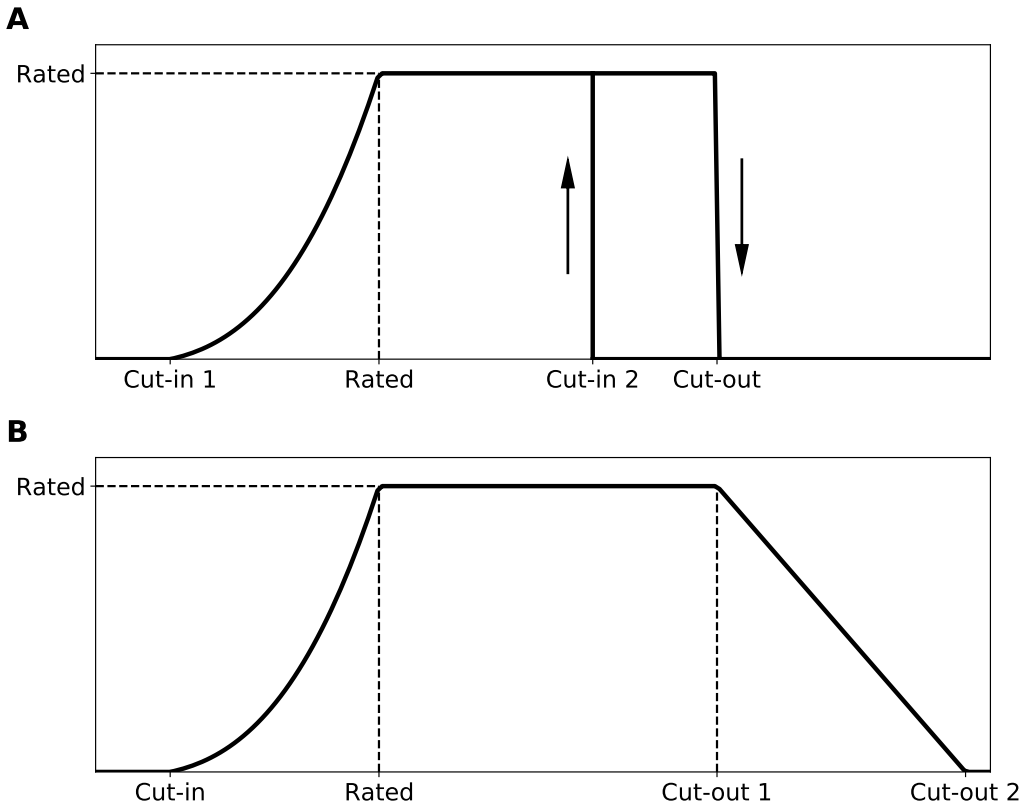

Figure 2.5: A: power curve with a hysteresis strategy. B: power curve with a soft cut-out strategy. Power is mesaured on the y-axis and wind speed is measured on the x-axis.

3 | Data and methods

3.1 Data

The data used in this thesis are the hindcast data sets NORA10 and NORA3. The data sets are produced by The Norwegian Meteorological Institute, and are downscalings of reanalysis data sets from The European Centre for Medium-Range Weather Forecasts (ECMWF). Table 3.1 lists some of the important features of NORA10 and NORA3. In the analysis, I will use the time period between 2004 and 2015 due to overlapping data in NORA10 and NORA3.

3.1.1 NORA10

The Norwegian 10 km Reanalysis Archive (NORA10) wind and wave hindcast is produced by Reistad et al. (2011) from a downscaling of the ERA-40 reanalysis from ECMWF using the High Resolution Limited Area Model (HIRLAM). The ERA-40 is a reanalysis data set covering the 45 year period from September 1957 to August 2002 (Uppala et al., 2005). ERA-40 has a spatial resolution of 125 km and a temporal resolution of 6 hours. The hydrostatic numerical weather prediction model (NWP) HIRLAM (version 6.4.2) is used to downscale the data to a spatial resolution of 10-11 km and a temporal resolution of 3 hours (Undén et al., 2002). The original NORA10 data set covered the period from September 1957 to August 2002, and after 2002 it has been extended using the operational analyses from ECMWF as boundary and initial conditions (Aarnes et al., 2012; Furevik et al., 2012). NORA10 covers the Norwegian Sea, the North Sea and the Barents Sea. The wind speed data is provided at the heights 10 m, 50 m, 80 m, 100 m, and 150 m above sea level (asl).

The 3h-output from NORA10 used in this thesis are the mean[1] wind speed at 10 m and 100 m asl. 10 m asl is the usual meteorological measurement

[1]Mean of the wind speeds 5 min before and 5 min after the hour.

height and 100 m asl is a common hub height for an offshore wind turbine.

3.1.2 NORA3

The Norwegian 3 km Reanalysis Archive (NORA3) data set is produced by Haakenstad, Breivik, Furevik, et al. (2021) from a downscaling of the ERA-5 reanalysis using the non-hydrostatic NWP HARMONIE-AROME (Cycle 40h1.2) (Bengtsson et al., 2017; Seity et al., 2011). The ERA-5 is made by ECMWF and is a state-of-the-art reanalysis data set (Hersbach et al., 2020). ERA-5 has a spatial resolution of 31 km and a temporal resolution of 1 hour. NORA3 covers the period from 1979 to today and will be extended backwards to 1950. The model covers the Norwegian Sea, the Barents Sea, and the North Sea, and it provides wind speed data at various heights.

In this thesis, I will use hourly, instantaneous wind speeds at the heights 10 m, 100 m, and 250 m asl. 10 m asl is the usual meteorological measurement height, 100 m asl is a common hub height for an offshore wind turbine, and 250 m asl is close to the upper height of a future, offshore wind turbine. I will also use 3-hourly, instantaneous temperature at the sea surface (SST) and at 100 m asl.

	NORA10	NORA3
Spatial resolution [km]	10-11	3
Temporal resolution [h]	3	1
Initial and boundary conditions		ERA40 ERA5
Downscaling model	HIRLAM	HARMONIE-AROME
Time period	1957-2002 + 2002-2021	1979-2021

Table 3.1: Key parameters of the data sets NORA10 and NORA3

.

The use of instantaneous values in NORA3 allows the wind speed to take on any value in the range $\bar{u} \pm u'$, where $\bar{u}$ is the mean wind speed and u' is the turbulent deviation. The range of possible wind speeds is therefore much larger for NORA3 than for NORA10, for which the wind speed is the 10 min mean wind speed[1]. This introduces uncertainty to the comparison of the wind speeds from the two models. By analysing mean values of the wind speeds based on a long time period, the uncertainty is reduced.

3.1.3 Sites

The different sites used in this thesis are listed in table 3.2 and shown in figure 3.1. Ekofisk, Sleipner A, Gullfaks C, Draugen and Norne are chosen due to the proximity to petroleum platforms with wind measurement devices, and hence the possibility of comparing model data with measurements. The coordinates for these sites were chosen as the nearest grid points in NORA10 and NORA3 to the petroleum platforms, and the distance between the grid positions arise due to the different spatial resolution of the models. Sørlige Nordsjø II and Utsira Nord are chosen because they are part of the areas opened for offshore wind energy in Norway on the 1st of January 2021 (Olje- og energidepartementet, 2020). The grid positions of the sites are unequal in NORA10 and NORA3 due to the spacing of the grids and resolution used.

Site	NORA10		NORA3		Distance [km]
	Lat	Lon	Lat	Lon	
Ekofisk	56.52	3.24	56.51	3.21	2.14
Sørlige Nordsjø II	56.74	5.01	56.80	5.00	7.13
Sleipner A	58.36	1.96	58.35	1.90	3.43
Utsira Nord	59.34	4.52	59.27	4.50	7.74
Gullfaks C	61.16	2.31	61.22	2.27	6.97
Draugen	64.38	7.87	64.36	7.79	4.48
Norne	66.01	7.96	66.01	8.07	5.05

Table 3.2: Grid position (lat, lon) and the distance (km) between the sites used in NORA3 and NORA10.

Figure 3.1: Position and name of the sites analysed.

3.2 Vertical wind speed profile

The model used to describe the vertical wind speed profile in this thesis is the empirical power law, described in section 2.4. By rearranging equation 2.2, we can obtain α for each time step (i) using the wind speeds at two known heights (z_1 and z_2):

$$\alpha_i = \frac{\ln\left(\frac{u(z_2)_i}{u(z_1)_i}\right)}{\ln\left(\frac{z_2}{z_1}\right)} \tag{3.1}$$

The wind speed can then be interpolated or extrapolated using equation 2.2 from the observation height to a higher height, such as the hub height.

In a review study, Gualtieri (2019) found that the power law is the most widely used model in the wind industry and the most accurate model when α is calculated for each time step between two heights and then extrapolated to hub height. The least accurate model is the power law with a fixed α for all wind speeds and stability conditions. Gualtieri concludes that the logarithmic model is unsuitable for modern wind turbines because of the inability to extrapolate the wind speed over a large enough distance.

In this thesis I will estimate the wind speed at a certain height by computing α at each time step using two heights and interpolate the wind speed to the desired height. I will investigate the validity of the assumption that a fixed $\alpha = 0.12$ can be used for all sites and all conditions.

3.3 Power curves

In this section equations will be presented for the power curves shown in section 2.3 and section 2.5.

3.3.1 Normalized wind power

In order to compare the power output at different sites and between different turbines, the power output can be normalized. If I assume that the air density, the swept area and C_p (for wind speeds below rated wind speed) are constant, the normalized power for each wind speed region shown in figure 2.3 can be simplified and characterized by:

$$P_N = \begin{cases} 0 & u < u_{ci} \\ \frac{u^3 - u_{ci}^3}{u_r^3 - u_{ci}^3} & u_{ci} \leq u < u_r \\ 1 & u_r \leq u \leq u_{co} \\ 0 & u > u_{co} \end{cases} \tag{3.2}$$

where u is the wind speed, u_{ci} is the cut-in wind speed, u_r is the rated wind speed, and u_{co} is the cut-out wind speed.

3.3.2 Storm control 1

The power curve with a hysteresis strategy described in section 2.9 will be referred to as Storm control 1 (SC1) in this thesis. The normalized power output of the turbine is described by equation 3.2 for wind speeds below the cut-out wind speed. When the wind speed exceeds the cut-out wind speed, the power output is zero until the wind speed drops below the hysteresis limit, where the turbine is started at rated power.

According to Cutululis et al. (2012), the typical value of the cut-out wind speed using SC1 is 25 m/s. The common value for the hysteresis limit is 20 m/s. In the analysis, I will use 25 m/s as the cut-out wind speed and 20 m/s and the hysteresis limit for SC1.

3.3.3 Storm control 2

The power curve with a soft cut-out strategy described in section 2.9 will be referred to as storm control 2 (SC2). The normalized power output is described by:

$$P_N = \begin{cases} 0 & u < u_{ci} \\ \frac{u^3 - u_{ci}^3}{u_r^3 - u_{ci}^3} & u_{ci} \leq u < u_r \\ 1 & u_r \leq u \leq u_{co,1} \\ \frac{u_{co,2} - u}{u_{co,2} - u_{co,1}} & u_{co,1} < u \leq u_{co,2} \\ 0 & u > u_{co,2} \end{cases} \tag{3.3}$$

Where $u_{co,1}$ is the wind speed at which the power is reduced, and $u_{co,2}$ is the wind speed where the turbine is shut off. The power output decreases linearly from rated power at $u_{co,1}$ to zero power at $u_{co,2}$. The wind speed values used are $u_{co,1} = 25m/s$ and $u_{co,2} = 35m/s$.

3.4 NREL 5 MW and NREL 15 MW

In the analysis of the wind resources and different power curves I will compare two theoretical wind turbines for offshore conditions developed by the National Renewable Energy Laboratory (NREL); the NREL 5 MW and the NREL 15 MW (Jonkman et al., 2009; Gaertner et al., 2020). Key parameters of the turbines can be found in table 3.3. The turbines have been chosen because they are freely available and widely used in research. I have chosen to analyse two turbines to be able to look at the importance of a larger rotor disk and an increased hub height.

	NREL 5 MW	NREL 15 MW
Rated power	5 MW	15 MW
Cut-in wind speed	3 m/s	3 m/s
Rated wind speed	11.4 m/s	10.59 m/s
Cut-out wind speed	25 m/s	25 m/s
Rotor diameter	126 m	240 m
Hub height	90 m	150 m

Table 3.3: Key parameters of the wind turbines NREL 5 MW and NREL 15 MW developed by the National Renewable Energy Laboratory (Jonkman et al., 2009; Gaertner et al., 2020)

.

In figure 3.2 and 3.3, I have compared the power curve obtained by equation 3.2 with a constant C_p between the cut-in and rated wind speed with the power curves of NREL 5MW and NREL 15MW, respectively. Due to the almost identical power curves, I will assume a constant C_p for wind speeds between cut-in and rated throughout the thesis. I will also assume that C_P is constant between cut-in and rated for SC1 and SC2.

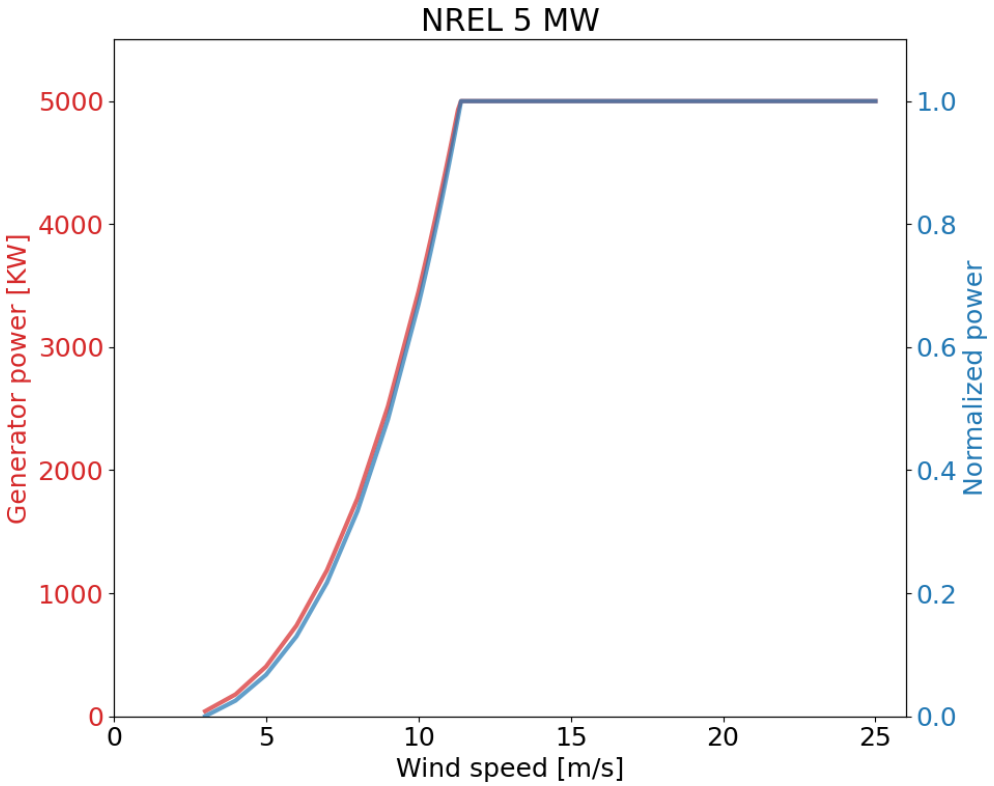

Figure 3.2: The left axis shows the power curve in KW using NREL 5 MW (red curve) (Jonkman, 2010). The right axis shows the normalized power curve with constant C_P between cut-in and rated wind speed (blue curve) calculated using equation 3.2.

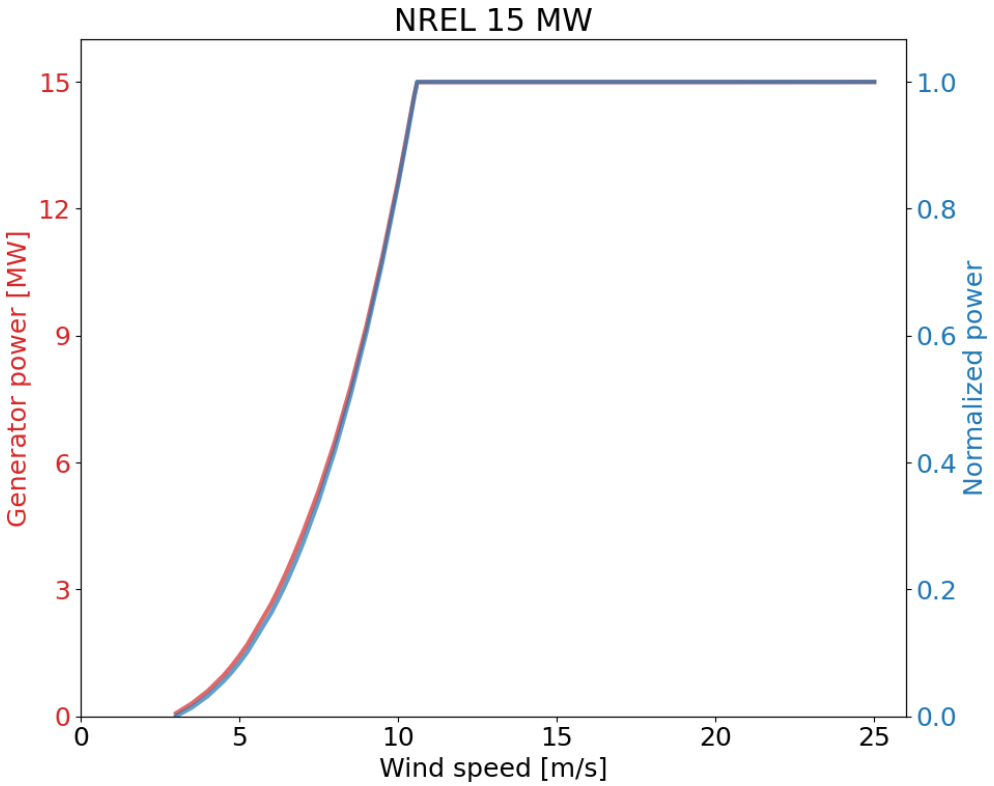

Figure 3.3: The left axis shows the power curve in MW using NREL 15 MW (red curve) (Barter et al., 2020). The right axis shows the normalized power curve with constant C_P between cut-in and rated wind speed (blue curve) calculated using equation 3.2.

3.5 Rotor equivalent wind speed

The rotor equivalent wind speed method (REWS) described in section 2.7 is presented in this section for the NREL 5 MW and NREL 15 MW turbines.

The NREL 5 MW reference wind turbine has a hub height of 90 m and rotor diameter of 126 m and the NREL 15 MW reference wind turbine has a hub height of 150 m and rotor diameter of 240 m. Dividing the area swept by the rotor into five equal height segments gives the measurement heights, segment separation lines, and segment area ratios for NREL 5 MW in table 3.4 and for NREL 15 MW in table 3.5.

i	Measurement height [m]	Segment separation line [m]	Segment area ratio
1	39.6	27.0	0.1424
2	64.8	52.2	0.2312
3	90	77.4	0.2529
4	115.2	102.6	0.2312
5	140.4	127.8	0.1424
6	-	153.0	-

Table 3.4: Details from the calculation of the rotor equivalent wind speed (REWS) u_{eq} for NREL 5 MW.

To calculate the wind speed at the measurement heights for NREL 5 MW, α computed between 10 m and 100 m asl is used to interpolate the wind speed from 10 m asl to the three measurement heights below 100 m asl (39.6 m, 64.8 m, and 90 m asl), and α computed between 100 m and 250 m asl is used to extrapolate the wind speed from 100 m to the two measurement levels above 100 m asl (115.2 m and 140.4 m asl).

i	Measurement height [m]	Segment separation line [m]	Segment area ratio
1	54	30.0	0.1424
2	102	78.0	0.2312
3	150	126.0	0.2529
4	198	174.0	0.2312
5	246	222.0	0.1424
6	-	270.0	-

Table 3.5: Details from the calculation of the rotor equivalent wind speed (REWS) u_{eq} for NREL 15 MW.

To calculate the wind speed at the measurement heights for NREL 15 MW, α computed between 10 m and 100 m asl is used to extrapolate the wind speed from 10 m asl to the measurement height below 100 m asl (54 m asl), and α computed between 100 m and 250 m asl is used to extrapolate the wind speed from 100 m asl to the four measurement levels above 100 m asl (102 m, 150 m, 198 m, and 246 m asl).

The equivalent wind speed at hub height u_{eq} will be computed using equation 2.6 with the segment area ratios and wind speeds at the measurement heights described in this section.

3.6 Statistics

This section presents the long term statistics of wind speed and energy production, and short term power variability used in this thesis.

3.6.1 Weibull distribution

The long term distribution of the wind speed at any site is assumed to follow a 2-parameter Weibull distribution. The probability density function (pdf) of the 2-parameter Weibull distribution is defined as (Jaffe et al., 2018):

$$f(u,k,\lambda) = \frac{k}{\lambda}\left(\frac{u}{\lambda}\right)^{k-1} e^{-(u/\lambda)^k} \qquad u \geq 0 \tag{3.4}$$

where u is the wind speed, λ (>0) is the scale parameter and k (>0) is the shape parameter. The value of λ is decided by the strength of the wind speeds at the site, with λ increasing for a windier site. k is determined by the variability of wind, with k decreasing for a more variable site.

The arithmetic mean and standard deviation are used to present the centre and spread of the distribution due to the small difference between the arithmetic and Weibull mean and standard deviation, respectively.

3.6.2 Capacity factor

An important efficiency statistic for wind energy is the capacity factor (CF), which describes the ratio of the energy generated during a period to the maximum energy that could be generated in the same period. It is defined as (Letcher, 2017):

$$CF = \frac{E_{actual}}{E_{installed}} = \frac{T\bar{P}}{TP_r} = \frac{\bar{P}}{P_r} \tag{3.5}$$

where E_{actual} is the energy generated, $E_{installed}$ is the maximum energy that could be generated in the same time period T, $\bar{P}$ is the arithmetic mean power generated in the time period, and P_r is the rated power.

For normalized power, the rated power is equal to 1 and the CF is equal to the mean normalized power, $CF = \bar{P_N}$.

3.6.3 Ramp rate

A variability measure for wind power is the ramp rate, which is the change in power for a time step i, given by:

$$\frac{\Delta P}{\Delta t} = \frac{P_{i+1} - P_i}{t_{i+1} - t_i} \tag{3.6}$$

where P_i is the power output of a wind turbine at time step t_i and P_{i+1} is the power output at the next time step t_{i+1}.

The ramps described in section 2.8 can be measured by the ramp rate. There is not a single definition of a ramp, but it is often defined as the events when either ΔP (magnitude) or Δt (duration) exceeds a threshold. According to Gallego et al. (2014), there is no consensus on the value of the magnitude and the duration, but they are mostly in the range 10-75% of rated power and 30 min - 4 h respectively.

In this thesis, I will evaluate ramp rates for wind speeds exceeding 20 m/s with a duration of 1 h using data from NORA3.

4 | Results and discussion

4.1 Comparison of NORA3 and NORA10

In this section I will compare the wind speeds at 10 m and 100 m above sea level (asl) modelled by NORA10[1] and NORA3[2] and the resulting power output from the NREL 5 MW turbine using the two models in the time period 2004-2015. This comparison is made to see if the new data set NORA3 will improve the power estimates.

I have chosen to look at the heights 10 m and 100 m asl to give a picture of the wind speeds close to the sea surface and close to a typical hub height. In addition, 10 m asl is the usual reference height for meteorological measurements. NORA10 provides wind speeds at 50 m, 80 m, and 150 m asl, but these heights will not be investigated further. NORA3 provides wind speeds at 50 m and 250 m asl, and the latter will be used in section 4.2.

4.1.1 Wind speed distribution

The wind speed distribution indicates the prevailing winds and the variability of the wind at a site. Figure 4.1 shows the wind speed distributions at 10 m and 100 m asl for NORA3 and NORA10 for Ekofisk. The wind speed distribution at 10 m asl from NORA3 is narrower and shifted towards lower wind speeds than NORA10. The distributions at 100 m asl for the two models are almost similar and are wider and moved towards higher wind speeds than the distributions at 10 m asl. The distributions in figure 4.1 seems to follow a Weibull distribution, with a tail reaching higher wind speeds. The wind speeds that a wind turbine can utilize are located between the cut-in wind speed and the cut-out wind speed. The ideal wind speeds are located between the rated wind speed and the cut-out wind speed where the turbine generates at rated capacity. For the NREL 5 MW turbine, the cut-in wind

[1] 3-hourly, 10 min mean values.
[2] Hourly, instantaneous values.

speed, rated wind speed, and cut-out wind speed are 3 m/s, 11.4 m/s, and 25 m/s, respectively. The wind speed distributions at 100 m asl in figure 4.1 cover the range between cut-in and cut-out, with the maximum close to the rated wind speed, making the site ideal for wind power purposes. The distributions for the other sites show a similar pattern, but the maximum of the distribution in 100 m asl is shifted towards lower wind speeds towards the north. The distributions for the other sites can be seen in appendix A, and the fitted Weibull parameters for all sites are listed in appendix B.

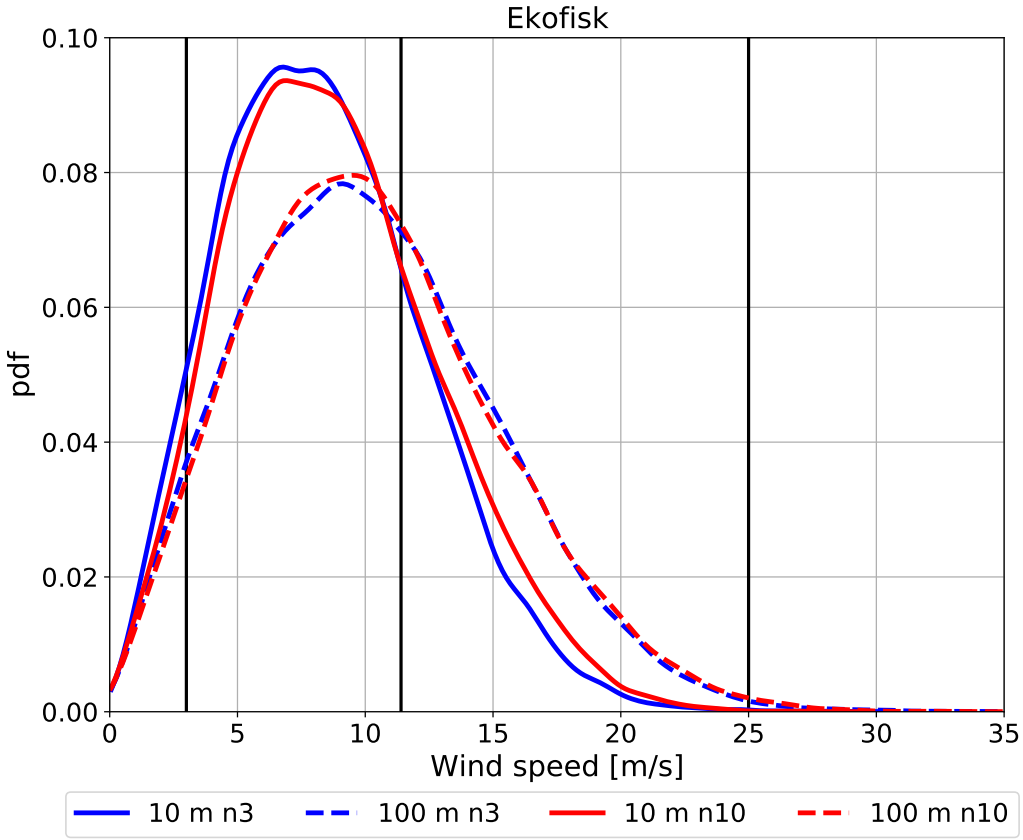

Figure 4.1: Probability density function (pdf) for the wind speed at 10 m and 100 m asl for NORA3 and NORA10 for Ekofisk. The black, vertical lines are located at 3 m/s, 11.4 m/s, and 25 m/s, which are the cut-in, rated, and cut-out wind speeds of the NREL 5 MW wind turbine. Time period: 2004-2015.

Table 4.1 shows that the arithmetic mean wind speeds for the whole time period at 10 m and 100 m asl for NORA3 and NORA10 are in close agreement. The mean wind speed at 10 m asl is lower for NORA3 than for

NORA10 for all the sites, consistent with the difference between NORA3 and NORA10 seen in figure 4.1 and in appendix A. The mean wind speed at 100 m asl is higher than at 10 m asl, with NORA3 giving a lower estimate than NORA10 for all sites except Utsira Nord and Gullfaks C. Table 4.1 also shows that in both heights, the mean wind speed varies between the different sites, with maximums at Sleipner A and Gullfaks C. In both layers, the difference between NORA10 and NORA3 decreases with increasing latitude. The difference in mean wind speed between the two heights also decreases with increasing latitude for both models. The mean wind speed difference between the heights will be further investigated in section 4.1.2. Table 4.1 shows that the arithmetic standard deviation of the mean wind speed is higher at 100 m asl than at 10 m asl. This is consistent with the wider distribution of wind speed seen in figure 4.1. The standard deviation of the wind speed at 10 m asl is lower for NORA3 than for NORA10. At 100 m asl, the standard deviation is approximately similar for the four southernmost sites and higher for NORA3 for the others.

Site	μ 10 m asl		μ 100 m asl		σ 10 m asl		σ 100 m asl	
	n10	n3	n10	n3	n10	n3	n10	n3
Ekofisk	8.77	8.36	10.26	10.18	4.11	3.95	4.93	4.92
Sørlige Nordsjø II	8.95	8.57	10.46	10.4	4.03	3.89	4.8	4.8
Sleipner A	9.1	8.74	10.55	10.47	4.38	4.23	5.23	5.22
Utsira Nord	8.61	8.46	10.0	10.11	4.5	4.32	5.33	5.29
Gullfaks C	9.11	8.95	10.46	10.52	4.53	4.46	5.39	5.46
Draugen	8.45	8.27	9.65	9.62	4.32	4.25	5.12	5.19
Norne	8.72	8.54	9.89	9.87	4.19	4.15	4.96	5.4
Average	8.82	8.56	10.18	10.17	4.29	4.18	5.11	5.13

Table 4.1: Arithmetic mean (μ) and standard deviation (σ) of wind speed at 10 m and 100 m above sea level (asl) for NORA10 (n10) and NORA3 (n3). Time period considered: 2004-2015.

In a comparison between NORA10, NORA3, and observational data from six maritime measurement stations, Haakenstad, Breivik, Furevik, et al. (2021) found that both models give a lower estimate of the mean wind speed at 10 m asl than observations, with NORA3 giving the lowest estimate for most months. The model Haakenstad, Breivik, Furevik, et al. use to extrapolate the observed wind speeds from measurement height down to 10 m asl is the NORSOK profile (Haakenstad, Breivik, Reistad, et al., 2019), which has been found to overestimate the wind shear (Furevik et al., 2012). The NOR-

SOK profile will be further discussed in section 4.2.3. The lower estimate of NORA10 was also found in a comparison with rawinsonde measurement at 100 m asl at the Ekofisk site by (Furevik et al., 2012). (Furevik et al., 2012) also found that NORA10 were unable to represent inverse wind profile, which might be connected to the underestimation of the wind speed. (Solbrekke, Sorteberg, et al., 2021) found in a comparison between NORA3 and six maritime stations (heights 68-140 m asl), that the lower estimate of the mean wind speed in NORA3 is due to more frequent events of low wind speed events and a less frequent events of high wind speed than the observations.

If the wind speeds modelled by NORA10 and NORA3 are lower than the actual wind speeds, the wind power estimates calculated using NORA10 and NORA3 will be too low. Furthermore, the underestimation of the wind speeds by the models may lead to a lower estimate of wind speeds above cut-out resulting in too few events where the turbine is shut off due to too high wind speeds.

The wind speed characteristics investigated in this section make the sites ideal for wind power generation. This is consistent with the grade 7 (of 7) classification of the offshore wind energy resources in the North Sea and the Norwegian Sea (Zheng et al., 2014).

4.1.2 The wind shear coefficient α

As described in section 3.2, the wind shear coefficient α gives the relation between the wind speeds at two different heights and can be used to interpolate or extrapolate the wind speed from a reference height to another height. α increases with increasing difference in wind speed between the two heights. This section aims to investigate the variation of α using NORA10 and NORA3 and whether the assumption of a fixed $\alpha = 0.12$ could be used, independent of the weather situation.

Figure 4.2 shows the distribution of α computed between 10 m and 100 m asl for NORA3 and NORA10 for Ekofisk for all wind speeds and wind speeds above 3 m/s. A common feature for NORA3 and NORA10 for all wind speeds is the majority of $\alpha > 0$, with a maximum of the distribution around 0.05. The α-distribution for NORA10 is focused around the maximum, while the distribution for NORA3 has two maximums, one at 0.05 and one at 0.14. The other sites have a similar distribution of α, but the first maximum for NORA3 increases and shifts towards lower values of α towards the north, while the second maximum in α for NORA3 decreases towards the north and is not present for the two northernmost sites. The distributions for the other sites can be found in appendix C.

An inspection of the α values showed that wind speeds below 3 m/s (at

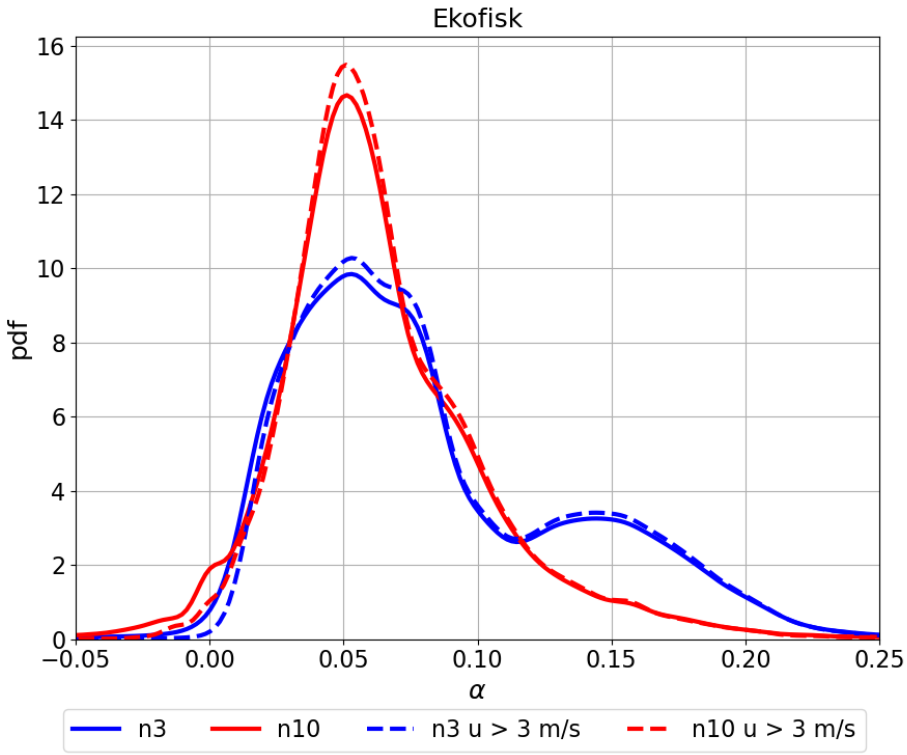

Figure 4.2: Distribution of α for NORA10 (n10) and NORA3 (n3) computed between 10 m and 100 m above sea level (asl) for all wind speeds and for wind speeds (at 90 m asl) above 3 m/s (cut-in wind speed for NREL 5 MW). Time period: 2004-2015

90 m asl), the cut-in wind speed for the NREL 5 MW turbine, lead to many α outliers. I choose to investigate the α-distribution excluding wind speeds below cut-in, since these low wind speeds are not contributing to wind power production. seen as the stapled lines in figure 4.2. The distribution of α excluding the wind speeds below cut-in result in fewer values of $\alpha < 0$ for both NORA3 and NORA10 compared to the distribution for all wind speeds. The maximums of the distributions are also higher. This means that utilizing the distribution of α for all wind speeds will give an erroneous impression of the values of α that affect the power estimate.

Table 4.2 shows that the mean α for all wind speeds is higher for NORA3 than for NORA10 at all sites. This is because the difference in mean wind speed between 10 m and 100 m asl is higher for NORA3 than for NORA10, as seen in table 4.1. For both NORA10 and NORA3, there is a decrease in

Site	Mean α			Mean α for u > 3 m/s		
	NORA10	NORA3	$\Delta\alpha$	NORA10	NORA3	$\Delta\alpha$
Ekofisk	0.064	0.081	0.017	0.066	0.084	0.018
Sørlige Nordsjø II	0.064	0.081	0.017	0.066	0.083	0.017
Sleipner	0.059	0.073	0.014	0.062	0.076	0.014
Utsira Nord	0.062	0.073	0.011	0.064	0.077	0.013
Gullfaks C	0.055	0.063	0.008	0.057	0.066	0.009
Draugen	0.052	0.06	0.008	0.055	0.063	0.008
Norne	0.049	0.057	0.008	0.051	0.059	0.008
Average	0.058	0.070	0.012	0.060	0.073	0.012

Table 4.2: Arithmetic mean α calculated for the sites using NORA10 and NORA3 computed between 10 m and 100 m above sea level (asl) and the difference ($\Delta\alpha$) (NORA3-NORA10) for all wind speeds and for wind speeds (at 90 m asl) above 3 m/s (cut-in wind speed for NREL 5 MW). Time period: 2004-2015.

mean α from south to north. Table 4.2 also shows that the mean αs for wind speeds above 3 m/s are higher than the mean αs for all wind speeds. This is expected due to the shift towards higher values of α seen in figure 4.2 for wind speeds above 3 m/s. The increase in the mean α for all wind speeds to mean α for wind speeds above 3 m/s is approximately the same for NORA10 and NORA3. The increase in the mean α implies that using mean α for all wind speeds will give a too low α for the higher wind speeds, which will lead to a lower extrapolated wind speed at hub height, which again will give a too low power output. In the following part of section 4.1.2, I will analyse α for the events of wind speeds above 3 m/s only.

Figure 4.3 A shows the diurnal variation of mean[3] α for NORA10 and NORA3 for Ekofisk. NORA3 show a larger diurnal variation than NORA10. The diurnal variations are smaller than the difference between the two models. For onshore sites, α varies on a diurnal scale due to the rapid warming and cooling of the landmasses and the resulting stability changes. For offshore sites, the diurnal variation is expected to be small due to the large heat capacity of the ocean, and therefore the small stability changes. The diurnal variation of α for offshore and onshore sites can be seen in e.g. Pena Diaz et al. (2012).

Figure 4.3 B shows the diurnal variation of mean[3] α for NORA3 and NORA10 in January and July. As expected, the diurnal variation is larger in

[3]Mean of all values of α at each hour using NORA3 and every third hour using NORA10.

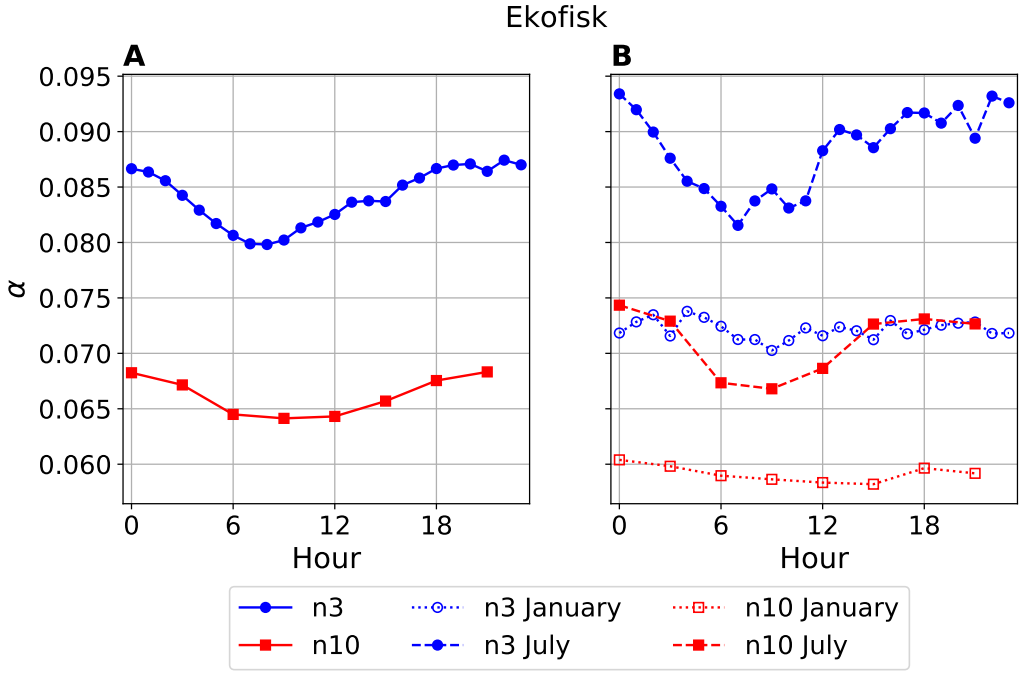

Figure 4.3: Diurnal variation of mean α for Ekofisk computed between 10 m and 100 m above sea level (asl) for NORA3 (n3) and NORA10 (n10) for wind speeds (at 90 m asl) above 3 m/s (cut-in wind speed for NREL 5 MW). A: Mean α for all days. B: Mean α for all days in January and July. Time period: 2004-2015.

July than in January and larger than the diurnal variation seen in figure 4.3 A for the whole time period. For the northernmost sites, α is larger in July than in January, but it does not vary as much throughout the day as for the southernmost sites. The plots for the other sites can be found in appendix D.

Figure 4.4 shows the diurnal variation of α for Utsira Nord. This is the site which differs the most from the other sites by having a maximum at 15 hours in July for both models. An investigation of the diurnal variation of wind speed in July for all the sites showed an increase in wind speed during the afternoon for Utsira Nord for both models, but it was more evident in NORA3. This might be a sea breeze effect, which is more apparent in NORA3 due to the improved resolution of the coast. At the latitudes investigated, the hours of sunlight in winter are few, and the warming and cooling of the ocean surface are negligible, with resulting negligible changes in stability and α. In summer, the sun shines both during the day and the night, and the heating

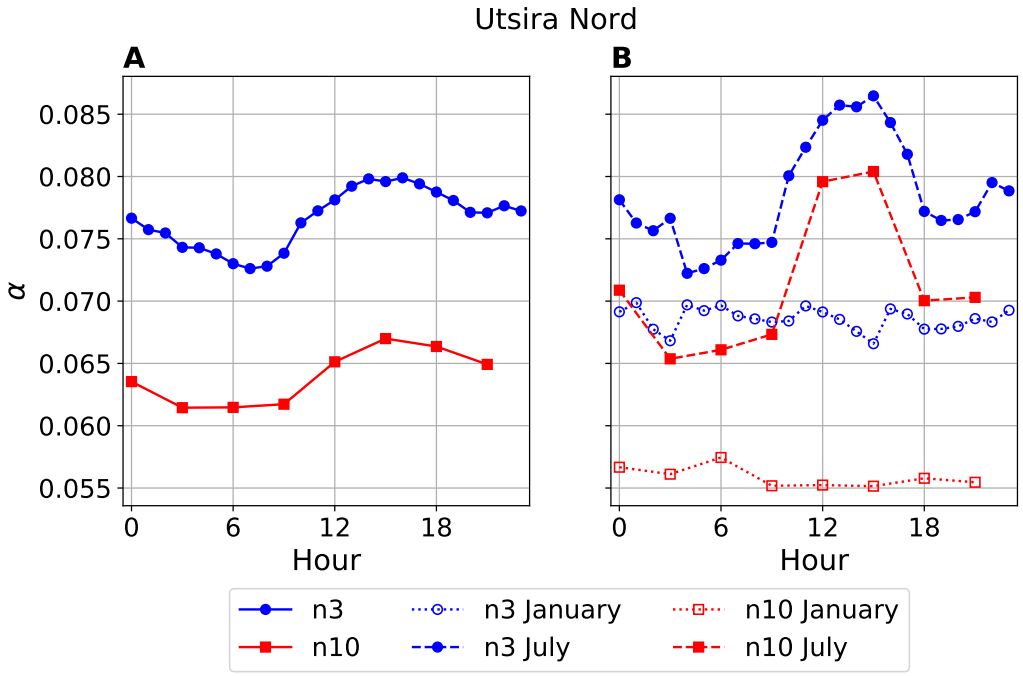

Figure 4.4: Diurnal variation of mean α for Utsira Nord computed between 10 m and 100 m above sea level (asl) for NORA3 (n3) and NORA10 (n10) for wind speeds (at 90 m asl) above 3 m/s (cut-in wind speed for NREL 5 MW). A: Mean α for all days. B: Mean α for all days in January and July. Time period: 2004-2015.

of the ocean surface leads to stability and α changes. For the northernmost sites close to the Arctic circle, there are almost 24 hours of sun, and the sun is lower on the horizon. This leads to the smaller variation of α for these sites. The difference seen between the mean value for the whole year, for July, and for January underlines the importance of investigating the seasonal variation of α.

The seasonal variation of mean[4] α is shown in figure 4.5, accompanied by the mean[4] temperature difference (ΔT) between 100 m asl and the sea surface from NORA3. The figure shows that the mean α for NORA3 and NORA10 varies throughout the year, with a maximum in spring (April) and a minimum in winter(December/January). The figure also shows a close relation between mean α and the mean temperature difference between the atmosphere and the sea surface. As described in section 2.3, ΔT is a rough measure of the atmospheric stability. For a dry atmosphere, $\Delta T > -0.6K$

[4]Mean of all values of α of each month.

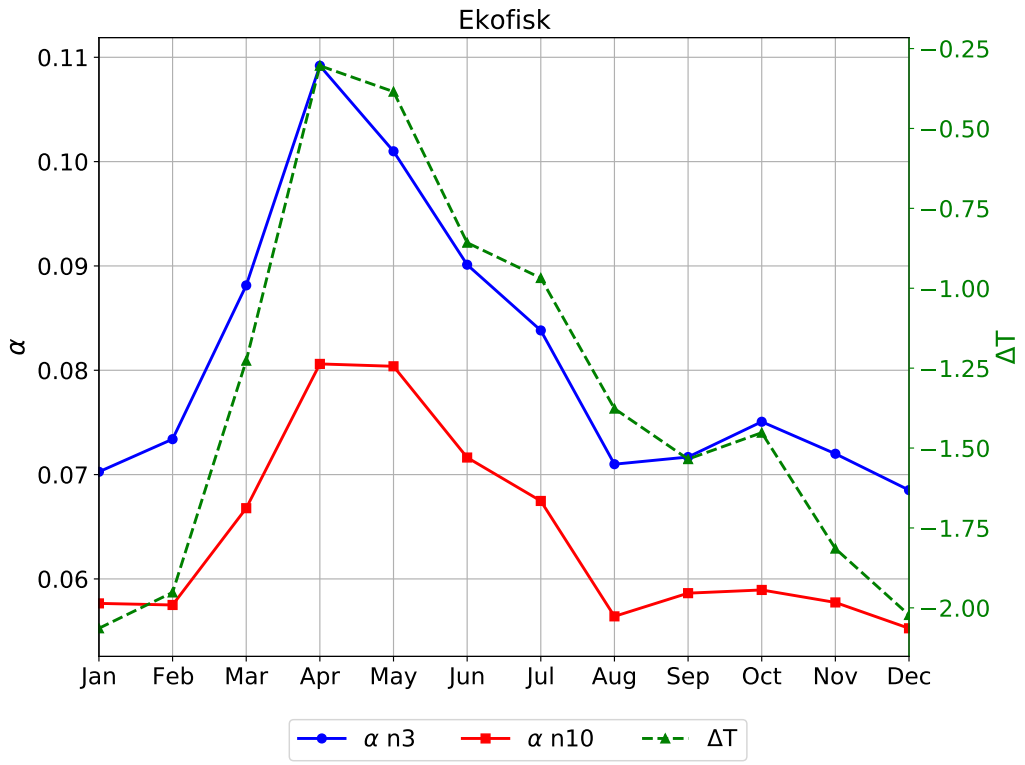

Figure 4.5: Left axis: monthly mean α for wind speeds (at 90 m above sea level (asl)) above 3 m/s (Cut-in wind speed for the NREL 5 MW turbine) for NORA3 (n3) and NORA10 (n10) computed between 10 m and 100 m asl for Ekofisk. Right axis: temperature difference in K between 100 m asl and sea surface (SST) computed from NORA3. Time period: 2004-2015.

characterizes stable conditions, $\Delta T < -1K$ characterizes unstable conditions, and $-1 \leq \Delta T \leq -0.6K$ characterizes neutral or conditionally unstable conditions. In spring, the ocean is cold, and the atmosphere is getting warmer due to the increased insolation. This gives a neutral or stable atmosphere with high α values. In winter, the temperature difference between the ocean and the atmosphere results in an unstable atmosphere with low α values. α is higher for NORA3 than for NORA10, consistent with the previous figures and tables. As previously seen in table 4.2, α decreases with increasing latitude. The same can be seen in the plots in appendix E. The decrease of α with increasing latitude is probably related to the smaller temperature difference between the atmosphere and the ocean towards the north, which results in more unstable conditions and more mixing of the atmosphere. The plots in appendix E also show that the maximum value of mean α occurs

later in the year towards the north.

In a study of the vertical wind shear released from the former meteorological station at the weather ship Polarfront in the Norwegian Sea the use of three stability dependent values of α categorized using the temperature difference between the atmosphere (at 20 m asl) and the sea surface were used. The use of the power law with the three values of α were found to give a got fit to the measured wind shear using rawinsonde measurements (Furevik et al., 2012). The values of α used were 0.04, 0.05, and 0.09 for unstable, neutral, and stable stability, respectively. The mean value of α for all conditions was found to be 0.06.

An investigation of mean α for different wind speeds can be seen in figure 4.6, which shows that mean α increases with increasing wind speed for all months and both models. The plots for the other sites show a similar relation, and they can be found in appendix F. As the wind speed increases, the waves grow, resulting in a higher surface roughness. The surface roughness increases the roughness length (the height where $u = 0$), and the wind speed at the reference height will therefore be lower.

Site	Ratio of $\alpha \geq 0.12$ [%] NORA3	NORA10
Ekofisk	23.5	8.3
Sørlige Nordsjø II	22.9	8.7
Sleipner A	17.2	5.8
Utsira Nord	18.1	8.9
Gullfaks C	10.6	4.6
Draugen	10.5	6.7
Norne	8.3	4.3
Average	15.9	6.7

Table 4.3: Ratio of αs equal to or higher than 0.12 for all sites for NORA3 and NORA10 computed between 10 m and 100 m. Time period: 2004-2015.

As described in chapter 2.4, the standardized wind shear coefficient used to extrapolate the wind speed from a reference height to hub height is $\alpha = 0.12$ for normal offshore conditions. The results from the present investigation does not support the use of a fixed $\alpha = 0.12$. The highest overall mean α for all wind speeds found is for Ekofisk from NORA3 and is 0.081. As seen in figure 4.3, 4.5, and 4.6, α varies throughout the day, the year, and for different wind speeds. The only occasion when mean α exceeds 0.12 is during spring for NORA3 for wind speeds above rated wind speed and only for the two

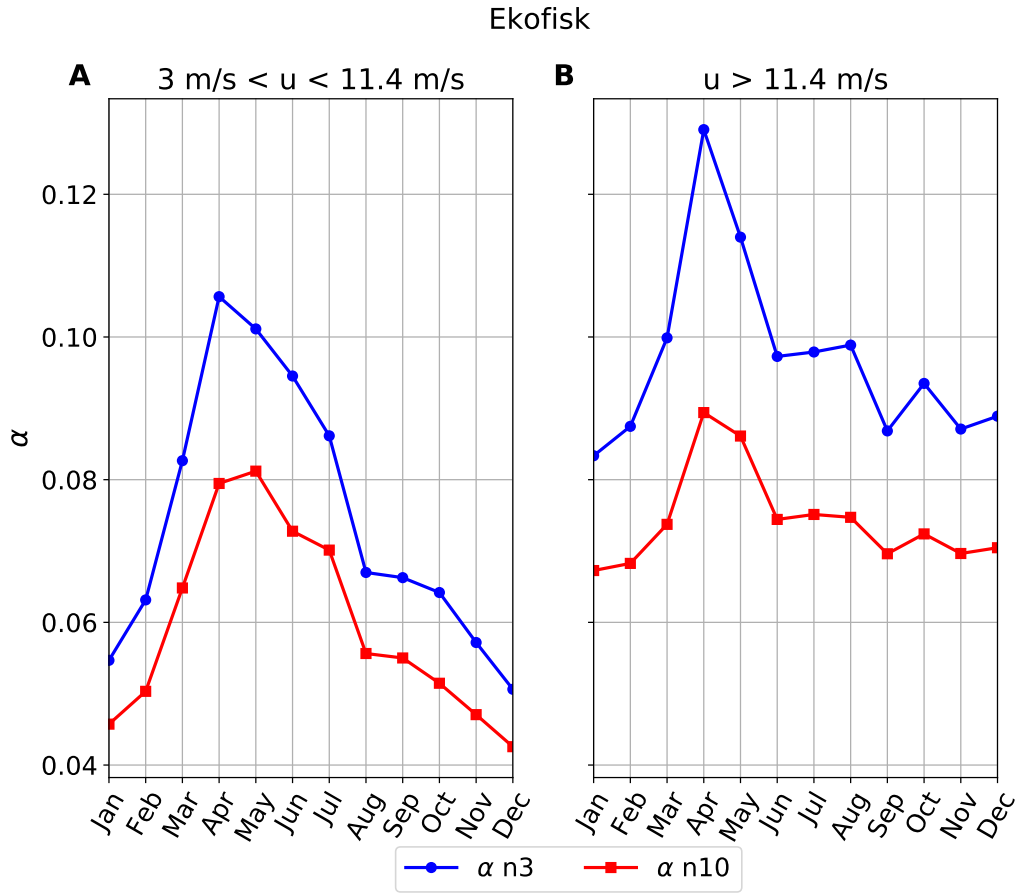

Figure 4.6: Monthly mean α at Ekofisk for NORA3 (n3) and NORA10 (n10) computed between 10 m and 100 m above sea level (asl). A: Mean α for wind speeds between 3 m/s (Cut-in wind speed for the NREL 5 MW turbine) and 11.4 m/s (Rated wind speed for the NREL 5 MW turbine). B: Mean α for wind speeds at hub height above 11.4 m/s (Rated wind speed for the NREL 5 MW turbine). Time period: 2004-2015.

southernmost sites. Table 4.3 lists the ratio of $\alpha > 0.12$, ranging from 8.3-23.5 % from north to south in NORA3 and 4.3-8.3 % in NORA10. Using a too high value of α when extrapolating the wind speed from a reference height to the higher hub height will lead to an overestimation of the wind speed. For the wind speeds below rated, this will lead to an overestimation of the power output of a wind turbine. For wind speeds close to the cut-out wind speed, an overestimation of the wind speed will lead to an overestimation of the events where the wind turbine is shut down to prevent damage, which will contribute to an underestimation of the power output. The power output of

a wind turbine using $\alpha = 0.12$ will be further investigated in section 4.2.3.

If NORA3 and NORA10 represented the atmosphere equally, I would expect them to give the same value of α. In the previous figures and tables, α calculated with NORA3 have been consistently higher than for NORA10. This might be due to the increased resolution of NORA3, more vertical layers, different parametrizations, or because NORA3 uses an improved ocean model, resolving the sea surface more accurately. Despite the increased α calculated using NORA3, the two models are in close agreement, and they show similar diurnal and seasonal variations and similar variations with increased wind speed. A further investigation of the differences between NORA3 and NORA10 is outside the scope of this thesis.

4.1.3 Capacity factor

This section will present the capacity factor (CF) for the NREL 5 MW turbine using wind speeds and α from NORA10 and NORA3. The normalized power for the NREL 5 MW turbine is calculated using equation 3.2, with the wind speed interpolated from 10 m asl to hub height (at 90 m asl) using α computed between 10 m and 100 m asl (as in section 4.1.2). CF is calculated using equation 3.5. An investigation of CF calculated using wind speeds interpolated from 50 m asl using α computed between 50 m and 100 m asl (not shown) resulted in minor difference (0.1 percentage points) compared to using α computed between 10 m and 100 m asl for both NORA3 and NORA10.

Table 4.4 shows CF calculated for the whole time period for NREL 5 MW using NORA10 and NORA3 for all the sites. Gullfaks C is the site with the highest mean wind speed, but the CF obtained is not the highest. This means that using the mean wind speed calculated at a site to estimate the CF will give an erroneous result, and that ranging sites based on the mean wind speed for wind energy purposes will give a wrong impression. Sørlige Nordsjø II obtains the highest CF in both models, and Draugen obtains the lowest CF in both models. The CFs calculated using NORA10 and NORA3 are in close agreement, with an average difference (ΔCF) of 0.001. NORA3 gives the lowest CF for all sites except Utsira Nord, and Gullfaks C. Utsira Nord is the site closest to shore, and the improved resolution of the coast in NORA3 might be the reason of the difference. There is a decrease in CF with increasing latitude, consistent with the previously seen decrease in wind speed and α with increasing latitude. The two sites closest to shore, Utsira Nord and Draugen are also two of the three sites with the lowest CF. This is because the wind speed at these sites is the most affected by land.

The CFs listed in table 4.4 are higher than the CFs calculated by Solbrekke, Sorteberg, et al. (2021) for four of the same sites. The difference might be due to the usage of a different turbine (Siemens 6MW), leading to a higher cut-in and rated wind speed used by Solbrekke, Sorteberg, et al.

If the CFs calculated in this thesis are realistic, they will be comparable to the CF of the first floating offshore wind farm in Europe, Hywind Scotland. During the first two years of operation, Hywind Scotland achieved a CF of 0.54, while the average in the UK was around 0.4 (Equinor, 2021). CF from the NREL 5 MW turbine is calculated using all time steps, assuming that the wind speed is the only factor affecting the power output. Therefore, the availability is assumed to be 100 %, while the availability for modern offshore wind farms can be lower than 95 % (Cevasco et al., 2021).

Figure 4.7 shows monthly CF for Ekofisk for NORA10 and NORA3. As

Site	CF NORA 10	CF NORA 3	ΔCF
Ekofisk	0.579	0.575	0.004
Sørlige Nordsjø II	0.601	0.599	0.002
Sleipner	0.588	0.582	0.006
Utsira Nord	0.544	0.555	-0.011
Gullfaks C	0.575	0.575	0
Draugen	0.52	0.515	0.005
Norne	0.549	0.543	0.006
Average	0.565	0.564	0.001

Table 4.4: Capacity factor(CF) calculated for NREL 5 MW using NORA10 and NORA3, and difference (ΔCF) between the models (NORA10-NORA3). The wind speed is extrapolated from 10 m above sea level (asl) to hub height at 90 m asl using α computed between 10 m and 100 m asl. Time period: 2004-2015.

expected, CF is higher in winter than in summer, with a difference of almost 0.35 between July and January. The two models give approximately the same estimate of CF. The difference ΔCF between NORA3 and NORA10 is small for all months but is biggest during the autumn and winter. The other sites show the same pattern, with NORA3 giving a lower CF than NORA10 in winter and the opposite in summer. The figures for the other sites can be found in appendix G. Utsira Nord shows a bigger difference during the summer months and a lower difference during the winter months than the other sites. This is also seen in table 4.4 where the CF is higher for NORA3 than for NORA10 for Utsira Nord.

Figure 4.8 shows the interannual variation of CF for NORA3 and NORA10 and the difference between the models. In the time period analysed, CF ranges from 0.51-0.63. A change in CF of 0.1 is large and underlines the importance of evaluating a long enough time period when planning a wind farm. The other sites show a similar interannual variation. As with the monthly CF, NORA3 and NORA10 are in close agreement. For all the sites, there is a trend of NORA3 giving a lower estimate than NORA10 at the end of the period. The plots can be found in appendix H. The difference between NORA3 and NORA10 might be due to changes in the operational analysis from ECMWF, which gives the initial and boundary conditions to NORA10 in the time period chosen (H. Haakenstad, personal communication, April 4th, 2021).

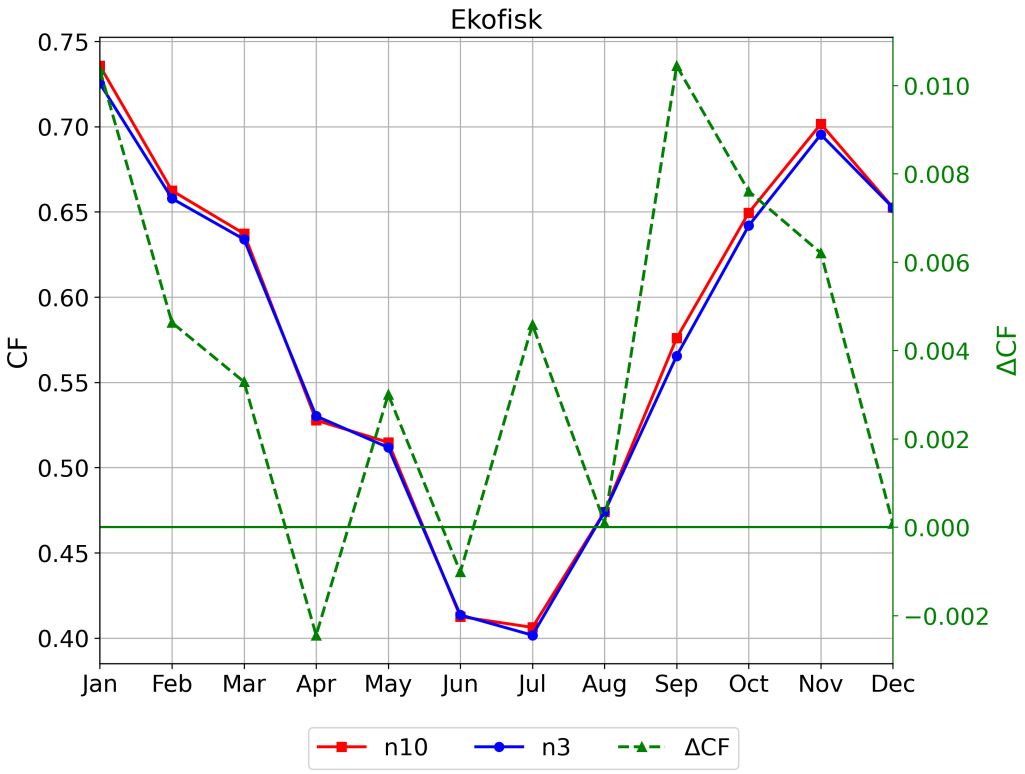

Figure 4.7: Capacity factor (CF) for each month using NORA10 (n10) and NORA3 (n3) for Ekofisk, with ΔCF on the right axis (NORA10-NORA3). CF is calculated using the NREL 5 MW turbine. The wind speed is extrapolated from 10 m above sea level (asl) to hub height at 90 m asl using α computed between 10 m and 100 m asl. Time period: 2004-2015

This chapter shows that the wind speeds in 10 m and 100 m asl modelled by NORA3 and NORA10 are in close agreement. The wind shear coefficient α computed between 10 m and 100 m asl is higher using NORA3 than NORA10, but the resulting difference in CF using NORA3 or NORA10 is negligible. Furthermore, the sites analysed have ideal wind speed characteristics, and placing the wind turbine NREL 5 MW at the sites would lead to high CFs.

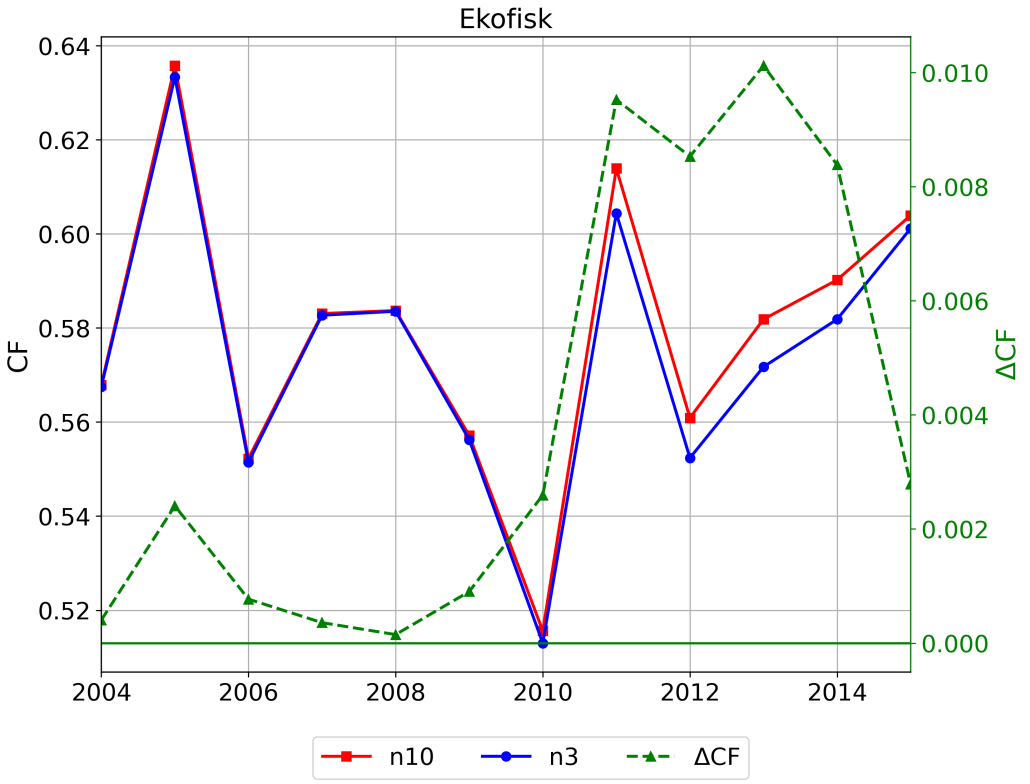

Figure 4.8: Yearly capacity factor (CF) using NORA10 (n10) and NORA3 (n3) for Ekofisk, with ΔCF on the right axis (NORA10-NORA3). CF is calculated using the NREL 5 MW turbine. The wind speed is extrapolated from 10 m above sea level (asl) to hub height at 90 m asl using α computed between 10 m and 100 m asl. Time period: 2004-2015.

4.2 Sensitivity analysis of the capacity factor

This section will compare the capacity factor (CF) of various wind turbines to investigate differences and possible improvements to the power output.

In the further work, I will use the wind speeds from NORA3. This is due to the expected improvement in NORA3 compared to NORA10. I also want to focus on the differences between the turbines and not on the difference between NORA3 and NORA3.

4.2.1 NREL 5 MW and NREL 15 MW

The power output of the NREL 5 MW turbine has already been shown in section 4.1.3 and is calculated using equation 3.2. The wind speed used in equation 3.2 is interpolated from 10 m to 90 m asl (hub height) using hourly α-values computed between 10 m and 100 m asl. CF is calculated using equation 3.5 using all time steps, assuming 100 % availability. The normalized power output and CF of the NREL 15 MW turbine are calculated in the same way, but the wind speed is interpolated from 100 m to 150 m asl (hub height) using hourly α-values computed between 100 m and 250 m asl. The heights used were chosen to give the most accurate value of the wind speed at hub height, and therefore the most accurate power output. An investigation of α computed between 10 m and 250 m asl (not shown) resulted in a lower value than α computed between 10 m and 100 m asl and a higher value than α computed between 100 m and 250 m asl. The resulting CFs for the NREL 5 MW and NREL 15 MW calculated using the wind speed at hub height interpolated from 10 m asl using α computed between 10 m and 250 m asl were lower than the CFs presented in this section by 0.011 and 0.006 in average for all sites for NREL 5 MW and NREL 15 MW, respectively.

Table 4.5 shows that NREL 15 MW has a higher CF than NREL 5 MW, with an average difference for all sites of 0.051 (approximately 10 %). This increase in CF is expected, as the lower cut-in wind speed and rated wind speed for the NREL 15 MW turbine enables the turbine to extract more of the energy embedded in the wind. In addition, the increased hub height exposes the rotor disk to higher wind speeds further up in the atmosphere. For both turbines there is a trend towards lower CFs towards the north. There is also a decrease in the difference between the turbines towards the north.

The monthly CF for the two turbines with the corresponding ΔCF can be seen in figure 4.9 for Ekofisk. NREL 15 MW gives a higher CF than the

Site	CF NREL 5 MW	CF NREL 15 MW	ΔCF
Ekofisk	0.575	0.633	0.058
Sørlige Nordsjø II	0.599	0.658	0.059
Sleipner A	0.582	0.636	0.054
Utsira Nord	0.555	0.605	0.05
Gullfaks C	0.575	0.622	0.047
Draugen	0.515	0.562	0.047
Norne	0.543	0.593	0.05
Average	0.564	0.615	0.051

Table 4.5: Capacity factor (CF) calculated for NREL 5 MW and NREL 15 MW for each site and difference (ΔCF) between the turbines (NREL 15 MW - NREL 5 MW). For NREL 5 MW, the wind speed is extrapolated from 10 m above sea level (asl) to hub height at 90 m asl using α computed between 10 m and 100 m asl. For NREL 15 MW, the wind speed is extrapolated from 100 m asl to hub height at 150 m asl using α computed between 100 m and 250 m asl. Time period: 2004-2015.

NREL 5 MW for all months, but the difference is largest during late spring and summer. The big difference is caused by the NREL 15 MW's improved utilization of the lower wind speeds. The figures for the other sites can be found in appendix I, and they have similar pattern as Ekofisk.

The comparison between the two turbines shows that changing from NREL 5 MW to NREL 15 MW will not only give a higher maximum power output; it will also increase the time the turbine generates power, i.e. it has shorter duration of the zero production events.

The power output and CF for NREL 5 MW and NREL 15 MW calculated as described in this section will be used as references in the analyses of the other key parameters in the following sections, and they will be referred to as *Standard*.

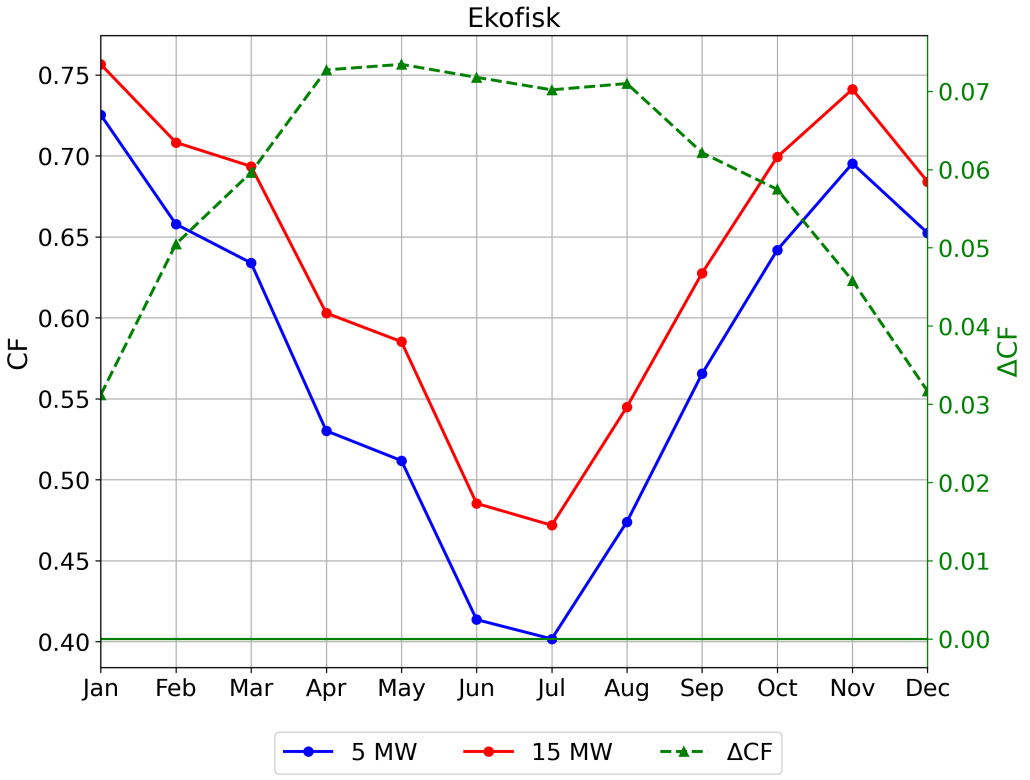

Figure 4.9: Monthly capacity factor (CF) for NREL 5 MW and NREL 15 MW, with difference between the turbines (ΔCF) on the right axis. For NREL 5 MW, the wind speed is extrapolated from 10 m above sea level (asl) to hub height at 90 m asl using α computed between 10 m and 100 m asl. For NREL 15 MW, the wind speed is extrapolated from 100 m asl to hub height at 150 m asl using α computed between 100 m and 250 m asl. Time period: 2004-2015.

4.2.2 Rotor equivalent wind speed

In section 4.2.1, the normalized power was calculated using the wind speed at hub height. In this section, the normalized power is calculated using the rotor equivalent wind speed (REWS), as described in section 2.7 and 3.5. In the REWS-method, the equivalent wind speed over the rotor disk is calculated by weighting the wind speeds at different heights to account for the wind shear over the rotor disk.

Table 4.6 shows CF for all the sites using REWS and using wind speed at hub height (Standard). For both turbines, CF is marginally lower using REWS than using wind speeds at hub height, with an average difference for all sites of 0.004 (<1 %) for NREL 5 MW and 0.001 for NREL 15 MW (<1 %). This means that using the wind speed at hub height to estimate CF will give a small overestimation of the power production compared to using REWS.

Site	NREL 5 MW: CF			NREL 15 MW: CF		
	Standard	REWS	ΔCF	Standard	REWS	ΔCF
Ekofisk	0.575	0.570	-0.003	0.633	0.63	-0.003
Sørlige Nordsjø II	0.599	0.594	-0.005	0.658	0.655	-0.003
Sleipner A	0.582	0.579	-0.003	0.636	0.634	-0.002
Utsira Nord	0.555	0.552	-0.003	0.605	0.603	-0.002
Gullfaks C	0.575	0.573	-0.002	0.622	0.62	-0.002
Draugen	0.515	0.512	-0.003	0.562	0.561	-0.001
Norne	0.543	0.540	-0.003	0.593	0.591	-0.002
Mean	0.564	0.560	-0.004	0.615	0.614	-0.001

Table 4.6: Capacity factor (CF) calculated for NREL 5 MW and NREL 15 MW for all sites using wind speed at hub height (Standard) and Rotor Equivalent Wind Speed (REWS) with ΔCF (REWS-Standard). Standard is computed as in 4.2. See section 4.2.2 for REWS. Time period: 2004-2015.

Figure 4.10 shows monthly CF for NREL 5 MW and NREL 15 MW using REWS and using wind speed at hub height (Standard) for Ekofisk. The difference between the two methods is small for both turbines. The biggest difference between the turbines occur in spring/early summer, and this corresponds in time with the largest α-values, as seen in figure 4.5. When the wind shear is higher, the difference in wind speed over the rotor disk is higher, and therefore, the difference between using REWS and using wind speed at hub height increases. Still, the difference between the curves is

small, hence it is not necessary to use REWS for these turbines. This is consistent with the conclusion by Van Sark et al. (2019).

The difference found between NREL 5 MW and NREL 15 MW can be due to the large portion of rotor disk of the NREL 15 MW covering the part of the vertical wind speed profile where the wind shear is small.

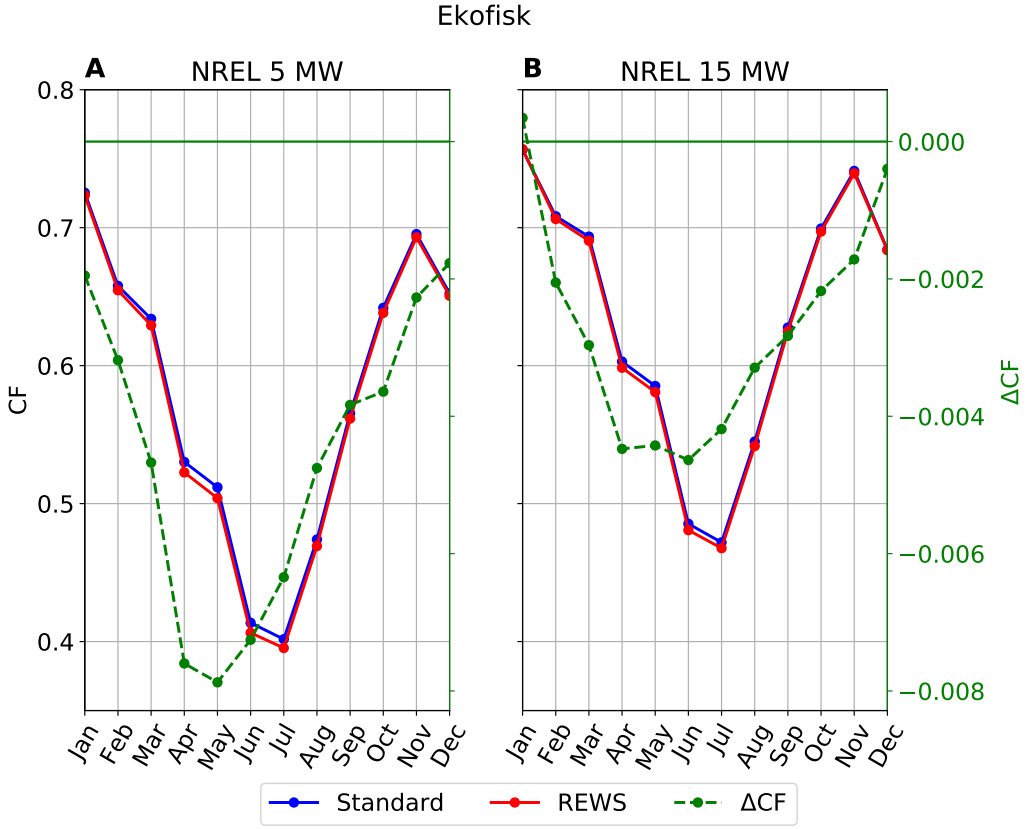

Figure 4.10: Monthly capacity factor (CF) calculated for NREL 5 MW (A) and NREL 15 MW (B) for Ekofisk using wind speed at hub height (Standard) and Rotor Equivalent Wind Speed (REWS). The right axis shows the difference (ΔCF) between the curves (Standard-REWS). Standard is computed as in 4.2. See section 4.2.2 for REWS. Time period: 2004-2015.

4.2.3 NREL 5 MW and NREL 15 MW with fixed $\alpha = 0.12$

The power law with a fixed $\alpha = 0.12$ is commonly used to extrapolate the wind speed from a reference height, usually 10 m asl, to hub height as described in section 2.4. However, as seen in section 4.1.2, α computed between 10 m and 100 m is asl rarely close to 0.12 and is for the sites analysed on average 0.070 (NORA3). In this section, the impact on the capacity factor of using $\alpha = 0.12$ will be investigated for NREL 5 MW and NREL 15 MW.

Table 4.7 lists CF for NREL 5 MW and NREL 15 MW using $\alpha = 0.12$ and using Standard. As expected, CF calculated using fixed $\alpha = 0.12$ to extrapolate the wind speed from 10 m asl to hub height results in a higher CF. ΔCF increases with increasing extrapolation distance, seen as the larger ΔCF for NREL 15 MW than for NREL 5 MW. The extrapolation distances are 80 m for NREL 5 MW and 140 m for NREL 15. The monthly ΔCF is approximately constant throughout the year (not shown). Table 4.7 also shows that the difference between using Standard and using $\alpha = 0.12$ increases with increasing latitude for both turbines. This is consistent with the decrease in α with increasing latitude seen in section 4.1.2.

When a too high value of α is used to extrapolate the wind speed to hub height, the gradient of the wind profile will be overestimated, resulting in a too high wind speed at hub height. The larger the extrapolation distance, the larger the overestimation of the extrapolated wind speed. Since the power of a wind turbine is proportional to the cube of the wind speed, an overestimation of the wind speed will affect the power output and the resulting CF greatly. The overestimated wind speed will lead to an overestimation of the power output for wind speeds below rated wind speed and also an overestimation of the events of wind speeds above cut-out. The resulting increase in CF (seen in table 4.7) means that using a fixed and too large α and a large extrapolation distance can give a severe overestimation of the power potential of the turbine.

The power law is one of many models used to extrapolate or interpolate the wind speed from one height to another. Other models are e.g. the theoretical logarithmic law or the NORSOK profile described in section 2.4. The validity of the power law has not been investigated in this thesis. It was chosen based on the conclusion in the review study by Gualtieri (2019) (mentioned in section 3.2) that the power law with α calculated between two heights results in the most accurate extrapolated wind speed. Gualtieri also concludes that the logarithmic law is unsuitable for modern wind turbines and that the power law with a fixed α is the least accurate model. Furevik et al. (2012) found that the NORSOK profile overestimates the gradient of the

vertical wind profile more than the power law using three stability dependent values of α and more than using the mean $\alpha = 0.06$ (Furevik et al., 2012).

Site	NREL 5 MW: CF			NREL 15 MW: CF		
	Standard	$\alpha = 0.12$	ΔCF	Standard	$\alpha = 0.12$	ΔCF
Ekofisk	0.575	0.621	0.046	0.633	0.691	0.058
Sørlige Nordsjø II	0.599	0.646	0.047	0.658	0.716	0.058
Sleipner A	0.582	0.635	0.053	0.636	0.698	0.062
Utsira Nord	0.555	0.605	0.05	0.605	0.665	0.06
Gullfaks C	0.575	0.636	0.061	0.622	0.691	0.069
Draugen	0.515	0.587	0.072	0.562	0.65	0.088
Norne	0.543	0.623	0.08	0.593	0.688	0.095
Average	0.564	0.622	0.058	0.615	0.685	0.07

Table 4.7: Capacity factor (CF) calculated for NREL 5 MW and NREL 15 MW for all sites using Standard and extrapolating the wind speed from 10 m above sea level (asl). The wind speeds are extrapolated from 10 m asl to 90 m and 150 m asl for NREL 5 MW and NREL 15 MW, respectively. ΔCF is the difference between the methods (Fixed α - Standard). Time period: 2004-2015.

4.2.4 Storm control 1

As described in section 3.3.2, storm control 1 (SC1) is a controller strategy for high wind speeds. The strategy prevents frequent stops and startups of the turbine, by keeping the turbine turned off after a shut down due to high wind speeds until the wind speed falls below a limit (20 m/s) below the cut-out wind speed (25 m/s), where it is started again at full power.

Table 4.8 shows CF calculated using the standard power curve and using SC1 for NREL 5 MW and NREL 15 MW. SC1 leads to a lower power output for both NREL 5 MW and NREL 15 MW for all sites. This is because SC1 leads to events of zero power where the standard turbine would produce at rated power. There is a slight increase in the difference between the methods towards the north, with Gullfaks C giving the biggest difference. This is due to the higher wind speeds towards the north, and the maximum at Gullfaks C seen in section 4.1.1 and the higher wind speed distribution seen in appendix A.

Site	NREL 5 MW CF			NREL 15 MW CF		
	Standard	SC1	ΔCF	Standard	SC1	ΔCF
Ekofisk	0.575	0.572	-0.003	0.633	0.628	-0.005
Sørlige Nordsjø II	0.599	0.595	-0.004	0.658	0.653	-0.005
Sleipner A	0.582	0.577	-0.005	0.636	0.628	-0.008
Utsira Nord	0.555	0.55	-0.005	0.605	0.598	-0.007
Gullfaks C	0.575	0.569	-0.008	0.622	0.613	-0.009
Draugen	0.515	0.51	-0.005	0.562	0.554	-0.008
Norne	0.543	0.539	-0.004	0.593	0.587	-0.006
Average	0.564	0.559	-0.005	0.615	0.609	-0.006

Table 4.8: Capacity factor (CF) calculated using a Standard and using Storm control 1 (SC1) for NREL 5 MW and NREL 15 MW. ΔCF is the difference between the strategies (SC1-Standard). Time period: 2004-2015.

Figure 4.11 shows the monthly CF for both strategies, and it shows that the largest difference between the two strategies is found during the winter months (Dec-Jan-Feb). This is due to more frequent events of wind speeds around cut-out wind speed during the winter. For NREL 15 MW, the difference is bigger than for NREL 5 MW during winter, and this is because the NREL 15 MW experiences higher wind, and thus more frequent events of wind speeds around cut-out. The plots for the other sites can be found in appendix K, and they show the same pattern.

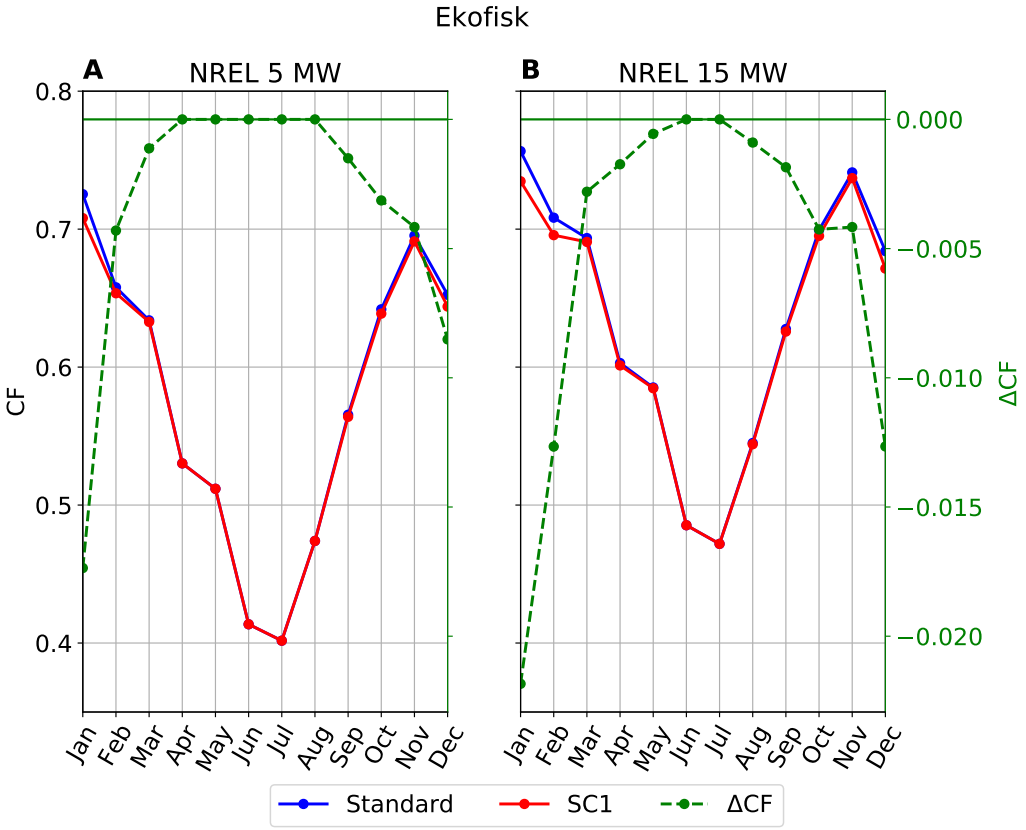

Figure 4.11: Monthly capacity factor (CF) calculated for NREL 5 MW (A) and NREL 15 MW (B) for Ekofisk using Standard and storm control 1 (SC1). The right axis shows the difference (ΔCF) between the curves (Standard-SC1). Time period: 2004-2015

4.2.5 Storm control 2

As described in section 3.3.3, storm control 2 (SC2) is a controller strategy that gradually reduces the wind turbine's power output when the wind speed exceeds the cut-out wind speed (25 m/s) to zero power (35 m/s). In this section, I will compare the power output using SC2 with the power output calculated in section 4.2, which uses an abrupt shutoff strategy.

Table 4.9 shows CF for NREL 5 MW and NREL 15 MW using a standard power curve with an abrupt shut down when u reaches the cut-off limit and SC2. According to our expectation, SC2 gives an increased power output for both NREL 5 MW and for NREL 15 MW due to the utilization of wind speeds above cut-out. The increase is larger for NREL 15 MW, due to the increased hub height and larger rotor diameter, and it will therefore be more affected by winds above the cut-out wind speed. Similarly as for SC1, the difference between Standard and SC2 increases slightly towards the north, and is largest for Gullfaks C for both turbines.

Site	NREL 5 MW CF			NREL 15 MW CF		
	Standard	SC2	ΔCF	Standard	SC2	ΔCF
Ekofisk	0.575	0.577	0.002	0.633	0.638	0.005
Sørlige Nordsjø II	0.599	0.601	0.002	0.658	0.662	0.004
Sleipner A	0.582	0.587	0.005	0.636	0.643	0.007
Utsira Nord	0.555	0.56	0.005	0.605	0.611	0.006
Gullfaks C	0.575	0.582	0.007	0.622	0.631	0.009
Draugen	0.515	0.519	0.004	0.562	0.568	0.006
Norne	0.543	0.547	0.004	0.593	0.598	0.005
Average	0.564	0.568	0.004	0.615	0.622	0.007

Table 4.9: Capacity factor (CF) calculated using Standard and using storm control 2 (SC2) for NREL 5 MW and NREL 15 MW. ΔCF is the difference between the methods (SC2 - Standard). Time period: 2004-2015.

Figure 4.12 shows that CF calculated with SC2 gives almost no increase in CF in summer, but the largest increase in winter. This is because there are more events of wind speeds above 25 m/s in winter than during the summer. The figures for the other sites can be found in appendix L, and they show the same pattern as Ekofisk.

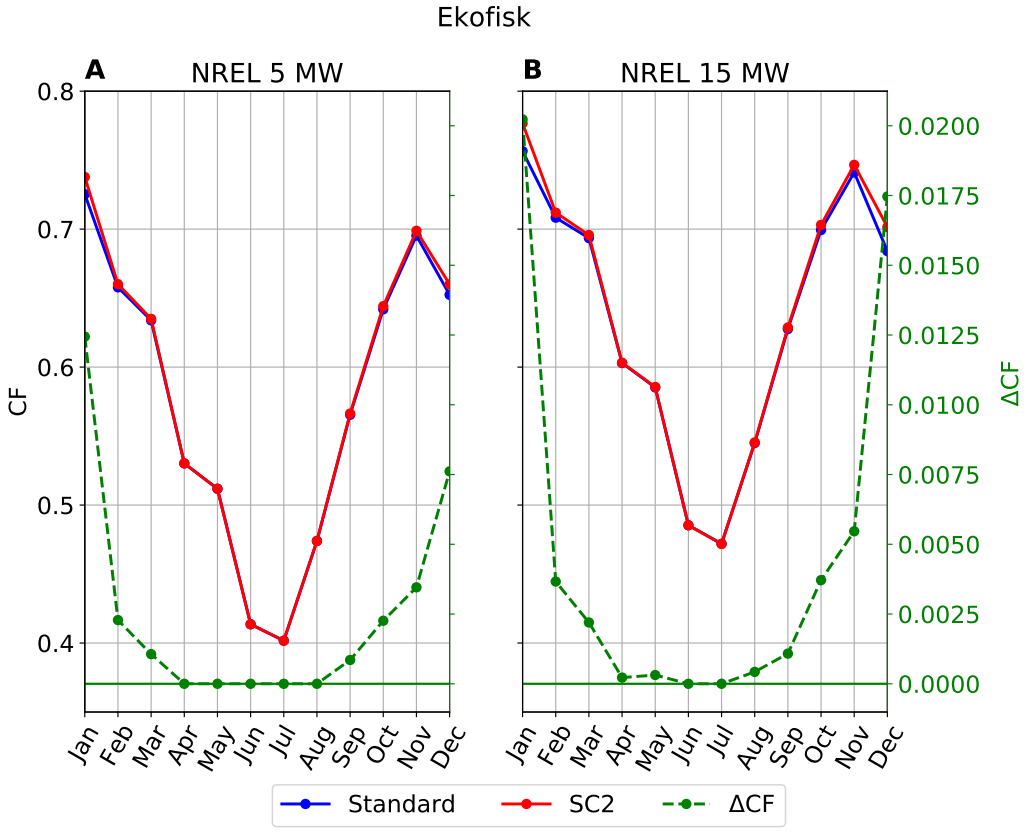

Figure 4.12: Monthly capacity factor (CF) calculated for NREL 5 MW (A) and NREL 15 MW (B) for Ekofisk using Standard and storm control 2 (SC2). The right axis shows the difference (ΔCF) between the curves (SC2-Standard). Time period: 2004-2015.

4.3 Sensitivity analysis of the temporal power variability

The ramp rate, described in section 3.6.3, is a measure of the short term variability of the wind power and gives in this study the power difference between two subsequent hours. The ramp rates for all wind speeds show that the vast majority are either zero or centred around zero, with very few events at -1 and 1. The events with ramp rates of -1 (full production to zero production) and 1 (zero production to full production) occur almost exclusively at large wind speeds when the turbine is either shut down to prevent damage or started up at full power when the wind speed has decreased below cut-out. In order to investigate the difference between the turbines and between the different power curves (Standard, SC1, SC2), the ramp rates shown in this section are limited at wind speeds above 20 m/s. These events can be difficult to forecast due to the sensitivity of the power curve, and they are important because they destabilize the electricity generation.

4.3.1 NREL 5 MW and NREL 15 MW

Figure 4.13 shows that the number of events with ramp rates of -1 and 1 is larger for the NREL 15 MW than for the NREL 5 MW. This is expected, as the NREL 15 MW experiences higher wind speeds than the NREL 5 MW, and thus more events of wind speeds above cut-out wind speed. The ratio of wind speeds above 20 m/s is 2.3 % and 4.6 % for NREL 5 MW and NREL 15 MW, respectively. Changing from a NREL 5 MW turbine to a NREL 15 MW turbine will result in an increase of events of zero production at high wind speeds which again will lead to a less stable electricity generation. The plots for the other sites can be seen in appendix M, accompanied by the ratio of wind speeds above 20 m/s for the sites.

4.3.2 SC1 and SC2

Figure 4.14 shows the normalized ramp rate for the NREL 5 MW turbine using Standard, storm control 1 (SC1) and storm control 2 (SC2). As expected, SC1 does not show ramp rates of 1 (from zero to full production) when the ramp rates are limited for wind speeds above 20 m/s because the turbine starts production again at wind speeds below 20 m/s. The events of -1 are reduced compared to the standard power curve because the turbine is prevented from frequent stops and start around the cut-out wind speed. SC2 has no events of -1 or 1 since the linear soft cut-out between 25 and 35 m/s

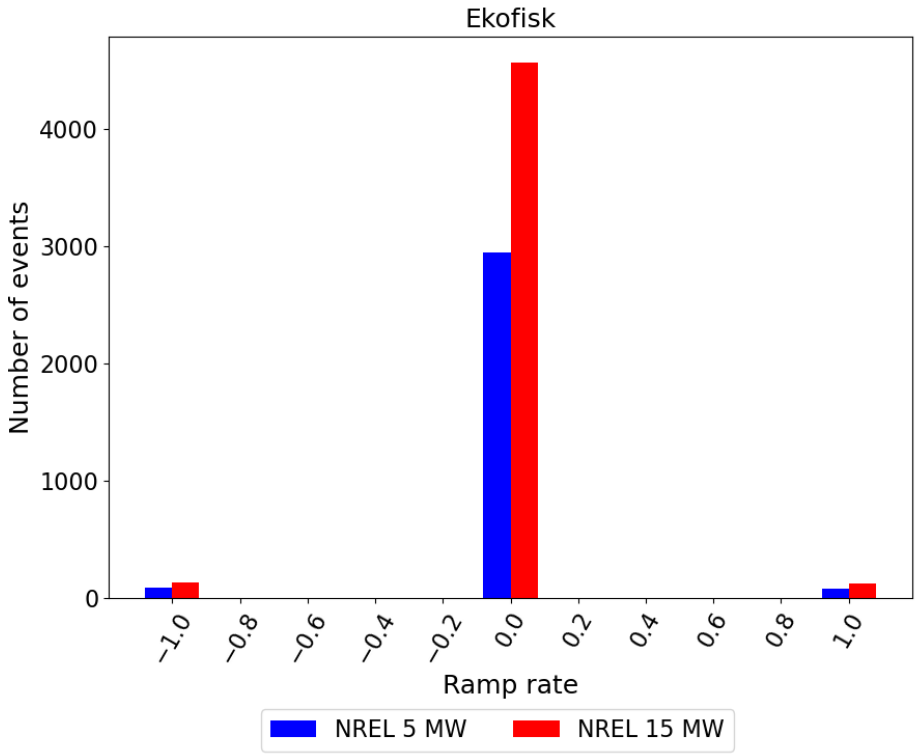

Figure 4.13: Ramp rate for wind speeds above 20 m/s using NREL 5 MW and NREL 15 MW for Ekofisk. Bin widths are 0.2, 0.1 on each side of ticks. Unit: $h^{-}1$. Time period: 2004-2015.

prevent abrupt shut down and start up of the power production (-1 and 1 in ramp rate). Figure 4.14 shows that changing from a standard power curve to SC1 or SC2 will lead to a more stable electricity generation. The figures for the other sites show a similar pattern, adn can be found in appendix N.

The number of ramp rates for the NREL 15 MW turbine using a standard power curve, storm control 1 and storm control 2 are approximately equal to the ramp rates for the NREL 5 MW turbine (not shown). By changing from the NREL 5 MW turbine to the NREL 15 MW turbine the number of ramp rate events of -1 and 1 will increase, as seen in section 4.3.1. By utilizing SC1 or SC2 for the NREL 15 MW turbine, the number of event of ramp rates of -1 or 1 will be lower than for the standard power curve using NREL 5 MW.

An investigation (not shown) of the ramp rates for NREL 5 MW and NREL 15 MW using the wind speeds extrapolated from 10 m asl to hub height using the fixed $\alpha = 0.12$ as in section 4.2.3 showed larger values of

-1 and 1 than using Standard shown in figure 4.13. By repeating figure 4.14 using the wind speed extrapolated to hub height using fixed $\alpha = 0.12$, the decrease in ramp rates of -1 and 1 by implementing SC1 or SC2 is much larger than seen in 4.14. This means that using the extrapolated wind speed from 10 m to hub height will give an erroneous impression of the advantage of implementing a storm control, and the storm control may not reduce the power variability as much as estimated.

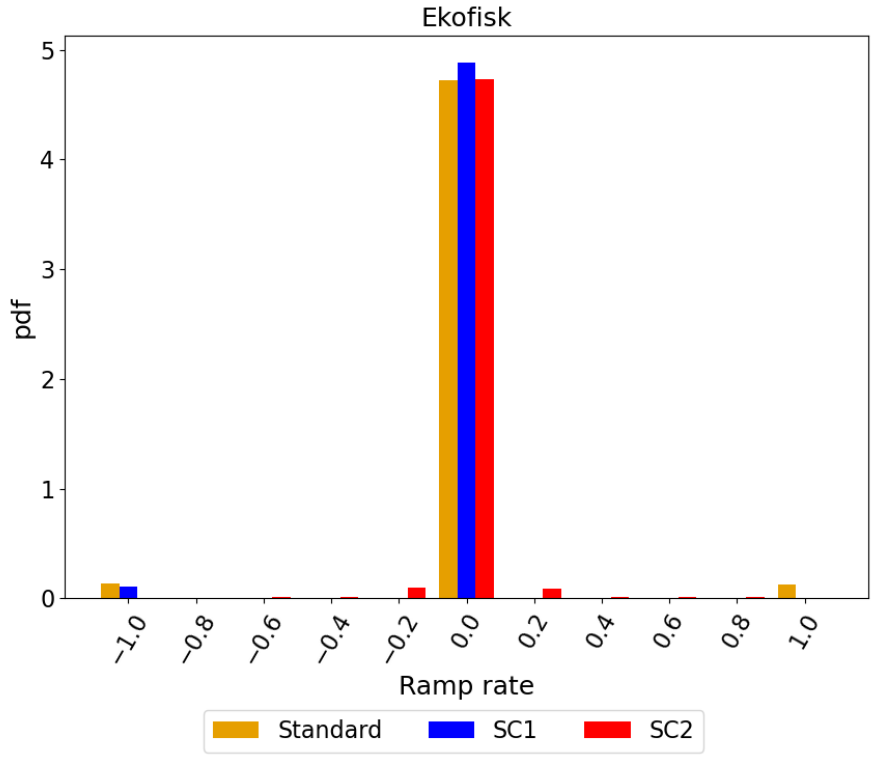

Figure 4.14: Normalized ramp rate for wind speeds above 20 m/s for the standard power curve, storm control 1 (SC1) and storm control 2 (SC2) for Ekofisk. Bin widths are 0.2, 0.1 on each side of ticks. Unit: $h^{-}1$. Time period: 2004-2015.

4.4 Final discussion

In this section I will summarize how the key parameters affect the power generation of the NREL 5 MW and NREL 15 MW turbines and discuss the relation between the findings.

Table 4.10 summarizes the average CFs for all sites found in the previous sections. A large increase in CF (0.051) comes from changing from the NREL 5 MW turbine to the NREL 15 MW turbine using Standard power curve (as described in section 4.2.1. CF for the NREL 5 MW turbine calculated using NORA3 is marginally smaller than CF calculated using NORA10 (-0.001) (section 4.1). CF calculated using REWS gives a decrease in CF compared to the standard power curve for both turbines (-0.004 for NREL 5 MW and -0.001 for NREL 15 MW) (section 4.2.2). The largest increase in CF (0.058 and 0.07 for NREL 5 MW and NREL 15 MW, respectively) comes from using a fixed $\alpha = 0.12$ to extrapolate the wind speed from 10 m to hub height (section 4.2.3). A decrease (-0.003) for both turbines comes from CF calculated using SC1 compared to CF using Standard (section 4.2.4). CF calculated using SC2 gives higher CF than using Standard, and the absolute difference is larger than for REWS and SC1, and larger for NREL 15 MW (0.007) than for NREL 5 MW (0.004) (see section 4.2.5).

	Average CF	
Method	NREL 5 MW	NREL 15 MW
Standard NORA10	0.565	-
Standard NORA3	0.564	0.615
REWS	0.561	0.612
$\alpha = 0.12$ from 10 m	0.622	0.685
SC1	0.561	0.612
SC2	0.568	0.622

Table 4.10: Summary of average capacity factor (CF) for all sites for the parameters analysed. Time period: 2004-2015.

The difference of CF between the turbines and between the methods varies throughout the year for all the sites. The difference between NORA3 and NORA10 fluctuates throughout the year in an unordered manner for the various sites, but the general trend for all the sites is that NORA10 gives a higher CF than NORA3 in winter and the opposite in summer (section 4.1). The difference in CF between NREL 5 MW and NREL 15 MW using Standard is largest during late spring and summer (April-August) for

all the sites due to the better utilisation of the wind speeds below and close to rated wind speed of NREL 15 MW (section 4.2.1). The difference between REWS and Standard is also largest during the summer season, but the largest difference varies from April at the southernmost site to August at the northernmost site due to the varying stability of the atmosphere (section 4.2.2). The difference in CF is approximately equal throughout the year between Standard and the method of using a fixed $\alpha = 0.12$ (section 4.2.3). For SC1 and SC2 compared to Standard, the difference in CF is largest during winter (December-January) due to the higher wind speeds (see section 4.2.4 and 4.2.5).

The ramp rates investigated in section 4.3 show that the number of events where the turbine goes from full power to zero power (-1) and from zero power to full power (1) is larger for the NREL 15 MW wind turbine than for the NREL 5 MW wind turbine. Section 4.3 also showed that the ratio of ramp rates equal to -1 or 1 is lower for storm control 1 than for the standard power curve, and eliminated for storm control 2. This means that a wind turbine's short-term variability will increase by going from NREL 5 MW to NREL 15 MW, and will decrease by utilizing a storm control. Therefore, the importance of implementing a storm control increases as the hub height of the wind turbine increases.

In reality, wind turbines use a hysteresis strategy (SC1) to prevent damage to the wind turbine and not the standard power curve with an abrupt shutdown. This means that the real difference will be between SC2 and SC1, and not between the standard power curve and SC1 or SC2 as investigated in section 4.2.4 and 4.2.5. By changing from SC1 to SC2, CF will on average increase by 0.007 and 0.01 for the NREL 5 MW and NREL 15 MW, respectively. CF will increase by 0.061 by going from the NREL 5 MW with SC1 to NREL 15 MW with SC2. A commercial turbine that uses a soft cut-out strategy (SC2) is the SG 8.0-167 DD from Siemens Gamesa (Siemens Gamesa, 2021), which was the turbine that was connected the most to the grid in Europe in 2020 (WindEurope, 2021). Siemens Gamesa calls the strategy High Wind Ride Through (Siemens AG, 2012).

The power law with a fixed $\alpha = 0.12$ is often used to extrapolate the wind speed to a desired height when information about the surface roughness or the stability is unavailable. The large ΔCF found in this analysis between using fixed $\alpha = 0.12$ compared to Standard (average for all sites are 0.058 for NREL 5 MW and 0.07 for NREL 15 MW) shows that using a fixed $\alpha = 0.12$ will give a severe overestimation of CF. Using $\alpha = 0.12$ should be avoided, but if it is still used, it is important to know that it will give a wrong estimate for the sites investigated in this study and that the difference in CF will increase with increasing extrapolation distance. By choosing to

use the power law with a fixed $\alpha = 0.12$, the effect of using REWS, SC1, SC2, or choice of model will be marginal compared to the overestimation due to the wrong choice of α. A wind resource assessment will therefore not give a correct impression of the various parameters when they are dominated by the effect of the wind shear.

In the calculation of CF there are several aspects that introduce uncertainty. As discussed in section 4.1.1, the wind speeds modelled by NORA3 and NORA10 may underestimate the actual wind speed (Haakenstad, Breivik, Furevik, et al., 2021). The use of 10 min mean wind speed in NORA10 and instantaneous wind speed in NORA3 will also lead to a difference in the range of the estimates which has not been investigated. Due to the yearly differences in the wind speed seen as the interannual variation in CF in figure 4.8 suggests that the use of a finite time series will introduce uncertainty to the estimates. By assuming an availability of 100 %, the CFs calculated will overestimate the CFs of actual wind turbines.

5 | Conclusion

In this master thesis, I have investigated how the increasing size of an offshore wind turbine affects the capacity factor (CF) and the temporal power variability, and how they change when a storm control is used. I also aimed to investigate how the increased size affects the importance of modelling the vertical wind shear over the rotor disk and how the choice of numerical wind speed model affects CF. Wind speeds from the hindcast data sets NORA3 and NORA10 were compared for seven sites in the North Sea and the Norwegian Sea for the time period 2004-2015, and a sensitivity analysis in key parameters related to offshore wind power production was performed using the reference turbines NREL 5 MW and NREL 15 MW. The parameters in the analysis were the hub height, the rotor diameter, the shape and wind speed limits of the power curve, and the wind shear over the rotor disk.

In the comparison between NORA3 and NORA10 in section 4.1 I found that the mean wind speed at 10 m asl was lower for NORA3 than for NORA10 (in average 3 % for all the sites), while the mean wind speed at 100 m above sea level (asl) was in a close agreement between the models (in average $<$0.1 % for all the sites). Due to the difference in wind speed at 10 m asl, the mean wind shear coefficient α computed between 10 m and 100 m asl was higher for NORA3 (on average 0.070 for all sites) than for NORA10 (on average 0.058 for all sites). α was found to vary throughout the day, throughout the year, and with wind speed. α was also found to decrease with increasing latitude. A close relation was found between the monthly mean α and the mean temperature difference between 100 m asl and the sea surface temperature (SST), which is a simple stability measure. The widely used fixed $\alpha = 0.12$ (Det Norske Veritas, 2010) was not representative of the sites analysed. CF calculated for the whole time period for the NREL 5 MW turbine using NORA3 (0.564 on average for all sites) and NORA10 (0.565 on average for all sites) were found to be in close agreement. CF was found to vary on an annual and interannual scale, and the difference in CF between NORA10 and NORA3 increases towards the end of the time period due to changes in NORA10 (H. Haakenstad, personal communication, April

4th, 2021). The site closest to shore, Utsira Nord, was found to be the most sensitive to the choice of the numerical model, which probably is due to the improved representation of the coast in NORA3.

Power output from NREL 5 MW and NREL 15 MW was calculated using the standard power curve, and using wind speed at hub height (90 m and 150 m) interpolated using α calculated at each time step using wind speed data from NORA3 were compared, and later referred to as *Standard*. The NREL 15 MW was found to give a higher CF (0.615 on average for all sites) than NREL 5 MW (0.564 on average for all sites). The difference in CF between the turbines was found to be largest during summer due to the improved utilization of the lower wind speeds for the NREL 15 MW (rated wind speed of 10.59 m/s compared to 11.4 m/s for NREL 5 MW).

I found that using the rotor equivalent wind speed (REWS) resulted in a slightly lower CF (-0.003 on average for all the sites) for both NREL 5 MW and NREL 15 MW than using Standard. The largest difference was found to be during Spring/Summer, corresponding in time with the maximum mean α due to a highly stratified atmosphere caused by the large temperature difference between the relatively cold ocean and the overlaying warm atmosphere. The monthly difference was larger for NREL 5 MW than NREL 15 MW due to the lower value of α between 100 m and 250 m asl.

CF calculated using a fixed $\alpha = 0.12$ to extrapolate the wind speed from 10 m asl to hub height gave a large overestimation for NREL 5 MW (increase on average 0.058 for all sites), and a larger overestimation for NREL 15 MW (increases on average 0.070 for all sites) due to the larger extrapolation distance. The extrapolation distance was 80 m and 140 m for NREL 5 MW and NREL 15 MW, respectively. The overestimation was approximately equal for all months.

A decrease in CF was found using a power curve with a hysteresis strategy, here called storm control 1 (SC1) (see section 3.3.2 for explanation), compared to Standard for the NREL 5 MW turbine (-0.005 in average for all the sites) and NREL 15 MW turbine (-0.006 in average for all the sites). The largest difference was found during the winter months (December/January) due to higher wind speeds in winter, with the largest difference during winter for NREL 15 MW.

The use of a power curve with a soft cut-out strategy, here called storm control 2 (SC2) (explained in section 3.3.3), resulted in a higher CF than Standard for NREL 5 MW (0.004 in average for all sites) and NREL 15 MW (0.007 in average for all sites). The difference was found to be largest during winter (December-January) due to higher wind speeds, and the effect was largest for NREL 15 MW.

The short term temporal power variability measured by the hourly ramp

rate (power difference between two hours) was larger for NREL 15 MW than for NREL 5 MW. The ramp rate was smaller for SC1 than for Standard and smaller still for SC2. This means that by implementing a storm control, the short term power variability can be reduced, especially for sites frequently experiencing strong winds. NREL 15 MW with SC2 results in the largest CF and only a marginally larger ramp rate than NREL 5 MW with SC2, and is therefore the best combination in terms of CF and power variability.

The use of a fixed $\alpha = 0.12$ with a large extrapolation distance dominates the effect of all the other parameters for the sites used in this study. Hence, there is little point in choosing a better model, REWS instead of wind speed at hub height, SC1, or SC2 if $\alpha = 0.12$ is used.

Based on the conclusions in this thesis I recommend that the power law with a fixed $\alpha = 0.12$ should be avoided for the extrapolation distances and the sites used here, and that α should be computed at each time step between two heights as close to the usage height as possible. Furthermore, it does not seem necessary to use REWS due to the small difference between using the wind speed at hub height for these sites and wind turbines. A storm control should be used to reduce the temporal variability of the power output, and SC2 should rather be used than SC1. Lastly, I recommend to evaluate a time period of several years when doing a wind resource assessment due to the large interannual variations.

Recommendations for future work

Based on the findings of how the wind shear coefficient α computed between 10 m and 100 m asl varies throughout the year, with wind speed, with latitude, and with numerical model (NORA3 or NORA10), I propose to further investigate the wind shear of the entire height range available in NORA10 and NORA3, and to investigate further the relation between the atmospheric stability, the wave conditions and the wind shear. Secondly I propose to investigate whether the decrease of α seen for increasing latitude continues towards the North, and how it is affected by distance from shore. Taking into the account the wind shear over the rotor disk using REWS was found to affect the power output of the wind turbines to a very little extent, but I also propose to look at the power output if the vertical wind direction profile also was taken into account. Lastly, I propose to evaluate how the cost of the energy generated, the levelized cost of energy (LCOE), changes by varying the parameters studied in this thesis.

Bibliography

Aarnes, O. J. et al. (2012). "Wave Extremes in the Northeast Atlantic". In: 25.5, pp. 1529–1543. DOI: 10.1175/JCLI-D-11-00132.1.

Barter, G. et al. (2020). *IEA-15-240-RWT_tabular, Rotor performance*. URL: https://github.com/IEAWindTask37/IEA-15-240-RWT/blob/master/Documentation/IEA-15-240-RWT_tabular.xlsx (visited on Oct. 20, 2020).

Bengtsson, L. et al. (2017). "The HARMONIE-AROME Model Configuration in the ALADIN-HIRLAM NWP System". In: *Monthly Weather Review* 145.5, pp. 1919–1935. DOI: 10.1175/MWR-D-16-0417.1.

Bossanyi, E. et al. (2012). "Improving wind farm output predictability by means of a soft cut-out strategy". In: *European Wind Energy Conference and Exhibition EWEC 2012*.

CarbonBrief (2020). *Wind and solar are 30-50% cheaper than thought, admits UK government*. URL: https://www.carbonbrief.org/wind-and-solar-are-30-50-cheaper-than-thought-admits-uk-government (visited on May 12, 2021).

Cevasco, D. et al. (2021). "Reliability, availability, maintainability data review for the identification of trends in offshore wind energy applications". In: *Renewable and Sustainable Energy Reviews* 136, p. 110414. DOI: https://doi.org/10.1016/j.rser.2020.110414.

Cutululis, N. A. et al. (2012). "Offshore Wind Power Production in Critical Weather Conditions". In: *Proceedings of EWEA 2012 - European Wind Energy Conference & Exhibition*. European Wind Energy Association (EWEA).

Det Norske Veritas (2010). *ENVIRONMENTAL CONDITIONS AND ENVIRONMENTAL LOADS; DNV-RP-C205;* tech. rep. Høvik, Norway.

Emeis, S. (2018). *Wind Energy Meteorology - Atmospheric Physics for Wind Power Generation*. Second. Garmisch-Partenkirchen, Germany: Springer International Publishing. DOI: 10.1007/978-3-319-72859-9.

Equinor (2021). *Hywind Scotland remains the UK's best performing offshore wind farm*. URL: https://www.equinor.com/en/news/20210323-hywind-scotland-uk-best-performing-offshore-wind-farm.html#:~:text=For%

20its%20third%20consecutive%20year,new%20record%20in%20the%20UK. (visited on Apr. 23, 2021).

European Commission (2019). *COMMUNICATION FROM THE COMMISSION: The European Green Deal, 11.12.2019, COM(2019) 640 final*. Tech. rep. Brussels, Belgium. URL: https://eur-lex.europa.eu/legal-content/EN/ALL/?uri=COM:2019:640:FIN.

— (2020a). *Clean Energy Transition - Technologies and Innovations, 14.10.2020, SWD(2020) 953 final*. Tech. rep. Brussels, Belgium. URL: https://eur-lex.europa.eu/legal-content/EN/TXT/?uri=CELEX%3A52020SC0953.

— (2020b). *COMMUNICATION FROM THE COMMISSION TO THE EUROPEAN PARLIAMENT, THE COUNCIL, THE EUROPEAN ECONOMIC AND SOCIAL COMMITTEE AND THE COMMITTEE OF THE REGIONS: An EU Strategy to harness the potential of offshore renewable energy for a climate neutral future, 19.1*. Tech. rep. Brussels, Belgium.

Furevik, B. R. et al. (2012). "Near-surface marine wind profiles from rawinsonde and NORA10 hindcast". In: *Journal of Geophysical Research: Atmospheres* 117.D23. DOI: 10.1029/2012JD018523.

Gaertner, E. et al. (2020). *Definition of the IEA Wind 15-Megawatt Offshore Reference Wind Turbine*. Tech. rep. Golden: National Renewable Energy Laboratory.

Gallego, C. et al. (2014). "Detecting and characterising ramp events in wind power time series". In: *Journal of Physics: Conference Series* 555, p. 12040. DOI: 10.1088/1742-6596/555/1/012040.

Graabak, I. et al. (2016). "Variability Characteristics of European Wind and Solar Power Resources-A Review". In: *Energies* 9.6, p. 449. DOI: 10.3390/en9060449.

Gualtieri, G. (2019). "A comprehensive review on wind resource extrapolation models applied in wind energy". In: *Renewable and Sustainable Energy Reviews* 102, pp. 215–233. DOI: 10.1016/j.rser.2018.12.015.

Haakenstad, H., Ø. Breivik, B. R. Furevik, et al. (2021). "NORA3: A non-hydrostatic high-resolution hindcast for the North Sea, the Norwegian Sea and the Barents Sea". In: *Journal of Applied Meteorology and Climatology*. Preprint available from: https://folk.uib.no/iso056/Paper_NORA3_Haakenstad_etal.pdf.

Haakenstad, H., Ø. Breivik, M. Reistad, et al. (2019). "NORA10EI: A revised regional atmosphere-wave hindcast for the North Sea, the Norwegian Sea and the Barents Sea". In: *International Journal of Climatology*. DOI: 10.1002/joc.6458.

Hersbach, H. et al. (2020). "The ERA5 global reanalysis". In: *Quarterly Journal of the Royal Meteorological Society* 146.730, pp. 1999–2049. DOI: 10.1002/qj.3803.

International Electrotechnical Commission (2017). *IEC 64000-12-1, Wind turbines - Part 12-1: Power performance measurements of electricity producing wind turbines, 2nd edition.* Tech. rep.

Jaffe, R. L. et al. (2018). *The Physics of Energy.* Cambridge: Cambridge University Press. DOI: DOI:10.1017/9781139061292.

Jonkman, J. (2010). *NREL 5-MW reference turbine.* URL: https://wind.nrel.gov/forum/wind/viewtopic.php?t=363 (visited on Oct. 20, 2020).

Jonkman, J. et al. (2009). *Definition of a 5-MW Reference Wind Turbine for Offshore System Development.* Tech. rep. Springfield: National Renewable Energy Laboratory (NREL).

Letcher, T. M. (2017). *Wind Energy Engineering: A Handbook for Onshore and Offshore Wind Turbines.* San Diego: Elsevier Science & Technology.

Markou, H. et al. (2009). "Control strategies for operation of pitch regulated turbines above cut-out wind speeds". In: *EWEC 2009 Proceedings online.* EWEC. URL: http://proceedings.ewea.org/ewec2009/proceedings/.

Olje- og energidepartementet (2020). *Kongelig resolusjon: opning av havvind.* URL: https://www.regjeringen.no/no/aktuelt/opner-omrader/id2705986/ (visited on Aug. 20, 2020).

Pena Diaz, A. et al. (2012). *Offshore vertical wind shear: Final report on NORSEWInD's work task 3.1.* Tech. rep. DTU Wind Energy E; No. 0005, p. 116.

Reistad, M. et al. (2011). "A high-resolution hindcast of wind and waves for The North Sea, The Norwegian Sea and The Barents Sea". In: *Journal of Geophysical Research* 116. DOI: 10.1029/2010JC006402.

Seity, Y. et al. (2011). "The AROME-France convective-scale operational model". In: *Monthly Weather Review* 139.3, pp. 976–991. DOI: 10.1175/2010MWR3425.1.

Siemens AG (2012). *High Wind Ride Through.* URL: https://pdf.archiexpo.com/pdf/siemens-gamesa/high-wind-ride-through/88089-134501.html (visited on Feb. 16, 2021).

Siemens Gamesa (2021). *SG 8.0-167 DD: Offshore wind turbine.* URL: https://www.siemensgamesa.com/en-int/products-and-services/offshore/wind-turbine-sg-8-0-167-dd (visited on Feb. 16, 2021).

Solbrekke, I. M., A. Sorteberg, et al. (2021). "Norwegian hindcast archive (NORA3) - A validation of offshore wind resources in the North Sea and Norwegian Sea". In: *Wind Energ. Sci. Discuss.* 2021, pp. 1–31. DOI: 10.5194/wes-2021-22.

Solbrekke, I. M., N. G. Kvamstø, et al. (2020). "Mitigation of offshore wind power intermittency by interconnection of production sites". In: *Wind Energ. Sci.* 5.4, pp. 1663–1678. DOI: 10.5194/wes-5-1663-2020.

Spiridonov, V. et al. (2021). *Fundamentals of Meteorology*. First. Springer International Publishing. DOI: 10.1007/978-3-030-52655-9_9.

Stull, R. B. (1988). *An Introduction to Boundary Layer Meteorology*. First. Springer Netherlands. DOI: 10.1007/978-94-009-3027-8.

Türk, M. et al. (2008). "The Wind Profile Above the Sea-Investigations Basing on Four Years of FINO 1 Data". In: *DEWI Magazine* 33, pp. 12–16.

Undén, P. et al. (2002). *HIRLAM-5 Scientific Documentation*. Tech. rep. Norrköping, Sweden: SMHI.

Uppala, S. M. et al. (2005). "The ERA-40 re-analysis". In: *Quarterly Journal of the Royal Meteorological Society* 131.612, pp. 2961–3012. DOI: 10.1256/qj.04.176.

Van Sark, W. G. et al. (2019). "Do we really need rotor equivalent wind speed?" In: *Wind Energy* 22.6, pp. 745–763. DOI: 10.1002/we.2319.

Wagner, R. et al. (2011). "Accounting for the speed shear in wind turbine power performance measurement". In: *Wind Energy* 14.8, pp. 993–1004. DOI: 10.1002/we.509.

WindEurope (2021). *Offshore Wind in Europe: Key trends and statistics 2020*. Tech. rep. Brussels, Belgium. URL: https://windeurope.org/intelligence-platform/product/offshore-wind-in-europe-key-trends-and-statistics-2020/.

Wiser, R. et al. (2021). "Expert elicitation survey predicts 37% to 49% declines in wind energy costs by 2050". In: *Nature Energy*. DOI: 10.1038/s41560-021-00810-z.

Zheng, C. wei et al. (2014). "Assessment of the global ocean wind energy resource". In: *Renewable and Sustainable Energy Reviews* 33, pp. 382–391. DOI: 10.1016/j.rser.2014.01.065.

Appendices

Appendix A: Wind speed distribution

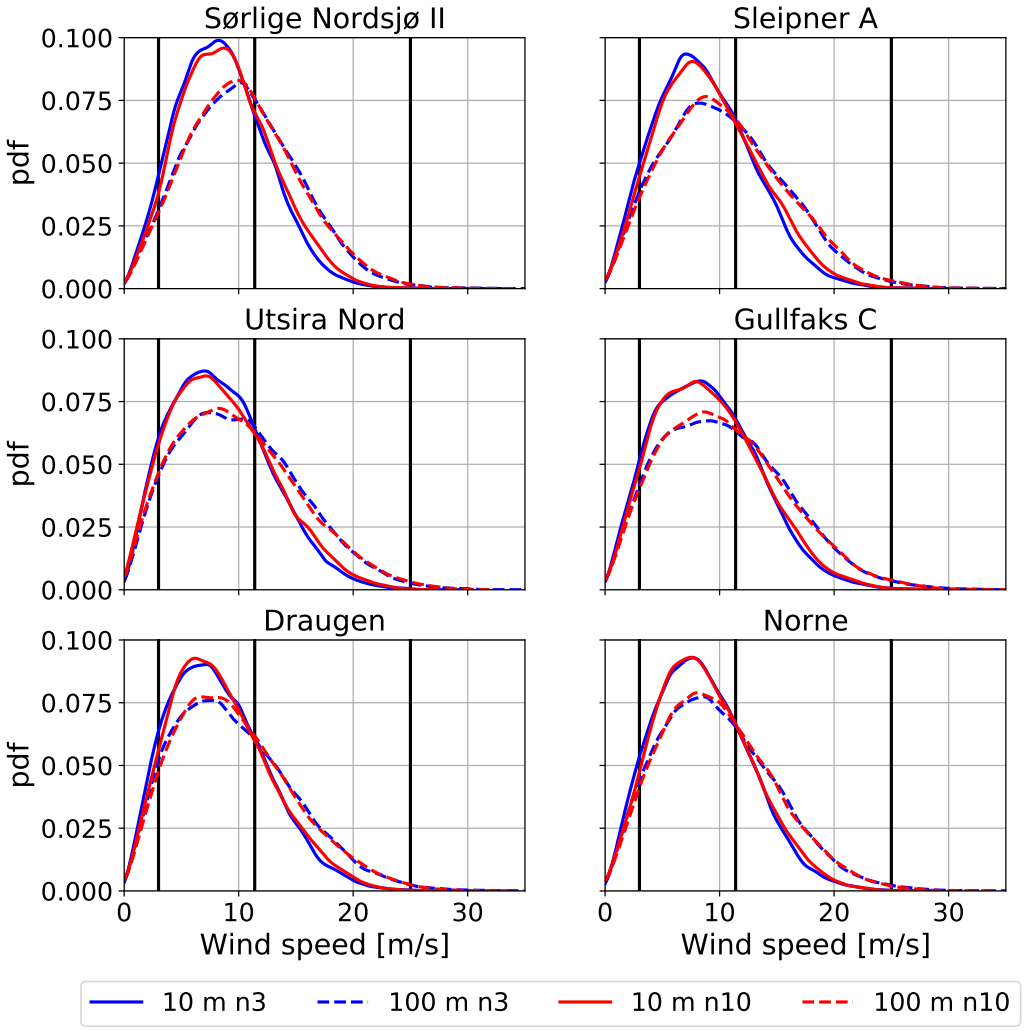

Figure A.1: Probability density function (pdf) for the wind speeds in 10 m and 100 m for NORA3 (n3) and NORA10 (n10) for the sites Sørlige Nordsjø II, Sleipner A, Utsira Nord, Gullfaks C, Draugen and Norne. The black, vertical lines are located at 3 m/s, 11.4 m/s, and 25 m/s, which are the cut-in, rated, and cut-out wind speeds of the NREL 5 MW. Time period: 2004-2015.

Appendix B: Weibull parameters

Site	Shape 10 m		Scale 10 m		Shape 100 m		Scale 100 m	
	n10	n3	n10	n3	n10	n3	n10	n3
Ekofisk	2.25	2.24	9.9	9.44	2.19	2.18	11.57	11.49
Sørlige Nordsjø II	2.36	2.33	10.1	9.66	2.3	2.28	11.79	11.72
Sleipner A	2.19	2.18	10.27	9.87	2.12	2.1	11.91	11.81
Utsira Nord	2.00	2.05	9.71	9.55	1.95	1.99	11.27	11.4
Gullfaks C	2.11	2.11	10.28	10.1	2.03	2.01	11.8	11.86
Draugen	2.05	2.04	9.54	9.33	1.97	1.93	10.89	10.85
Norne	2.19	2.17	9.84	9.64	2.09	2.05	11.17	11.14
Average	2.17	2.16	9.95	9.66	2.09	2.08	11.49	11.47

Table B.1: Fitted weibull parameters (shape and scale) in 10 m and 100 m height for NORA10 (n10) and NORA3 (n3) for all sites. Time period: 2004-2015.

Appendix C: Distribution of α

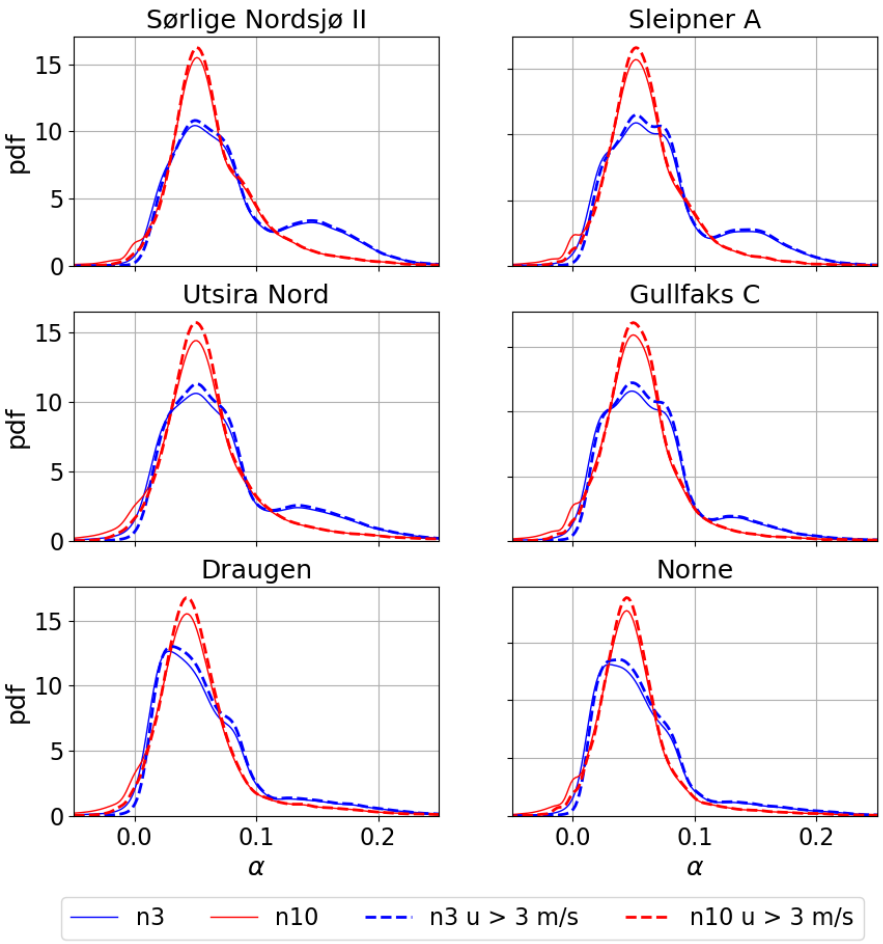

Figure C.1: Probability density function (pdf) of α computed between 10 m and 100 m for NORA3 (n3) and NORA10 (n10) for all wind speeds and wind speeds (at 90 m) above 3 m/s (Cut-in wind speed for the NREL 5 MW wind turbine). Sites: Sørlige Nordsjø II, Sleipner A, Utsira Nord, Gullfaks C, Draugen and Norne. Time period: 2004-2015.

Appendix D: Hourly mean α

Figures D.1-D.5 shows hourly mean α for the whole time period for NORA3 (n3) and NORA10 (n10) for the sites Sørlige Nordsjø II, Sleipner A, Gullfaks C, Draugen and Norne. A: mean for all days. B: mean for all days in January and July. Time period: 2004-2015.

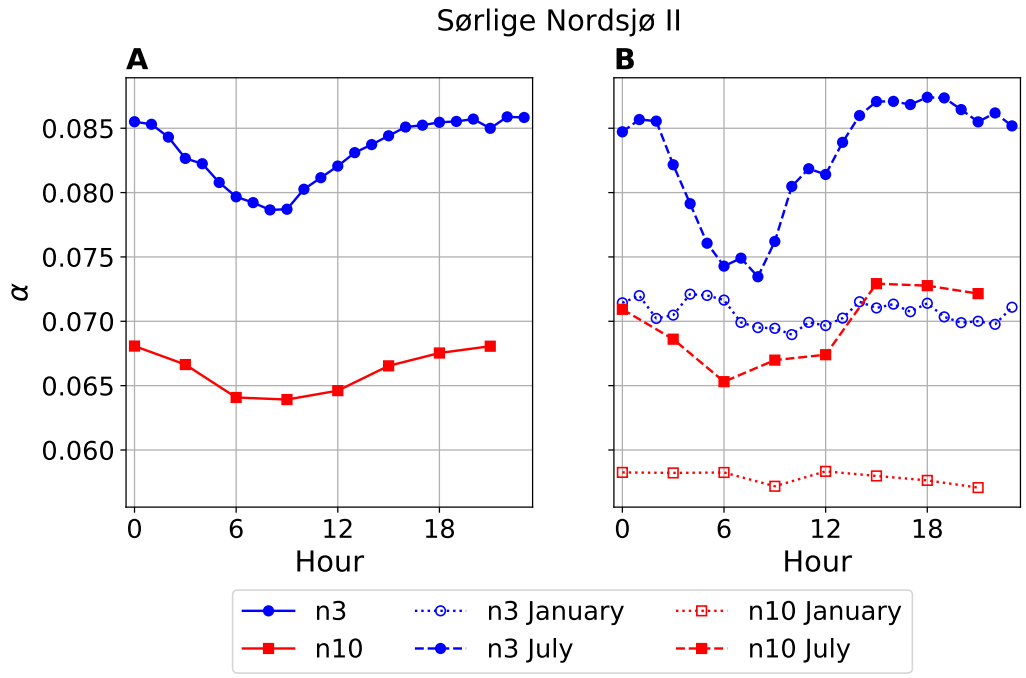

Figure D.1:

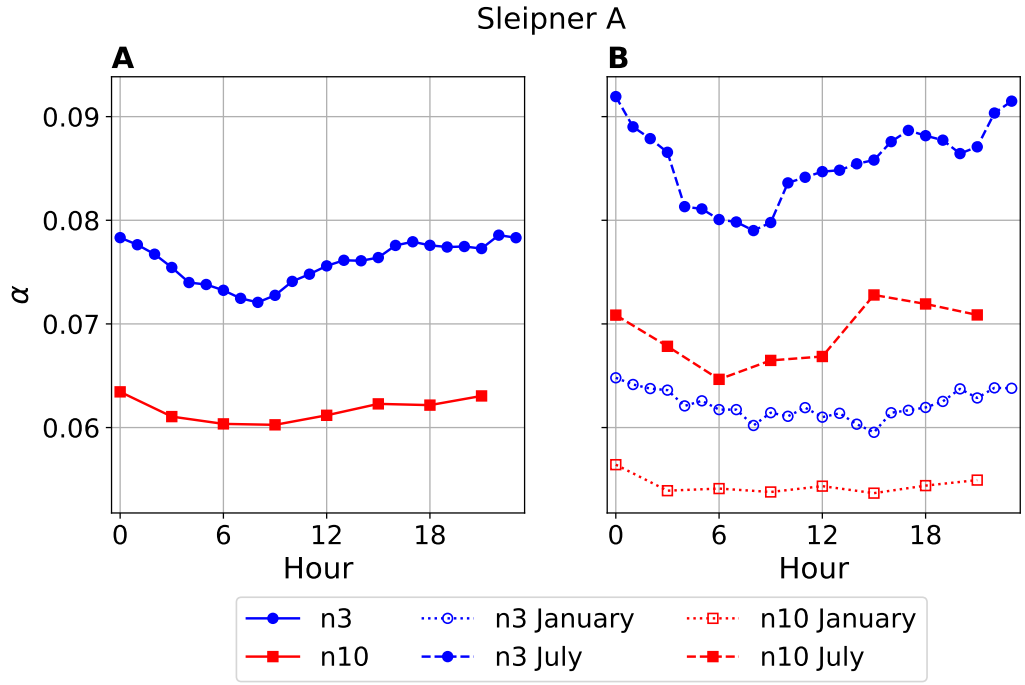

Figure D.2:

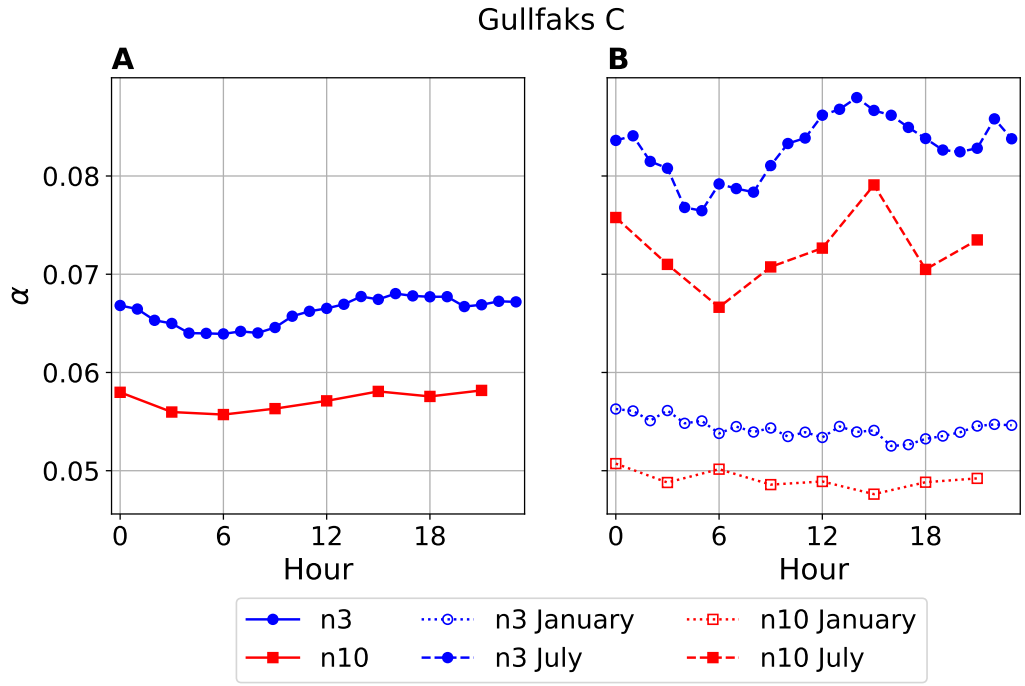

Figure D.3:

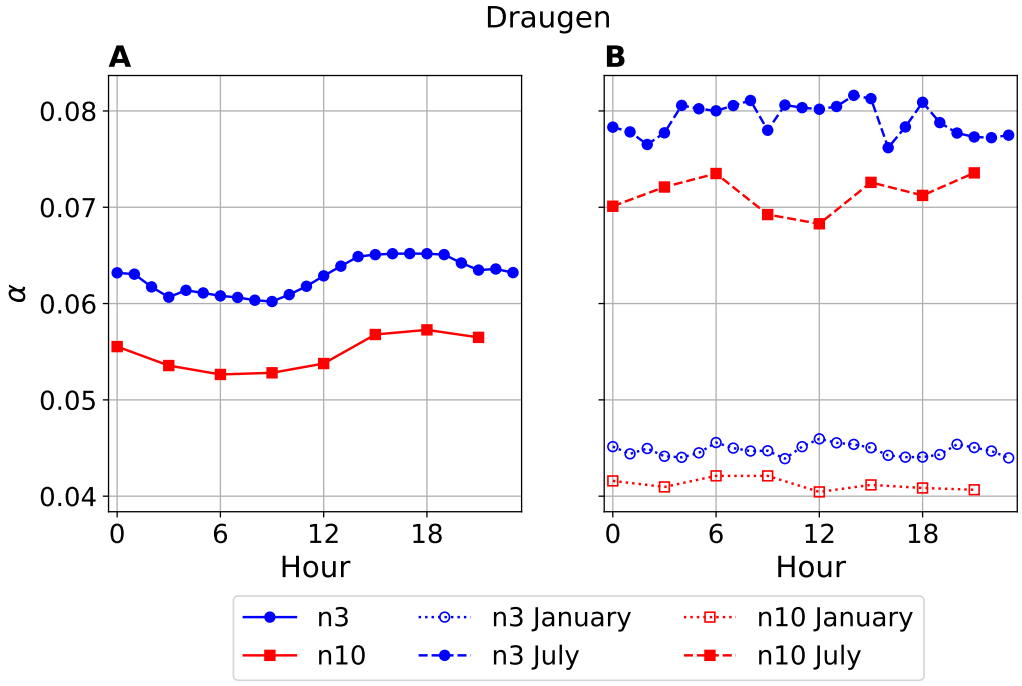

Figure D.4:

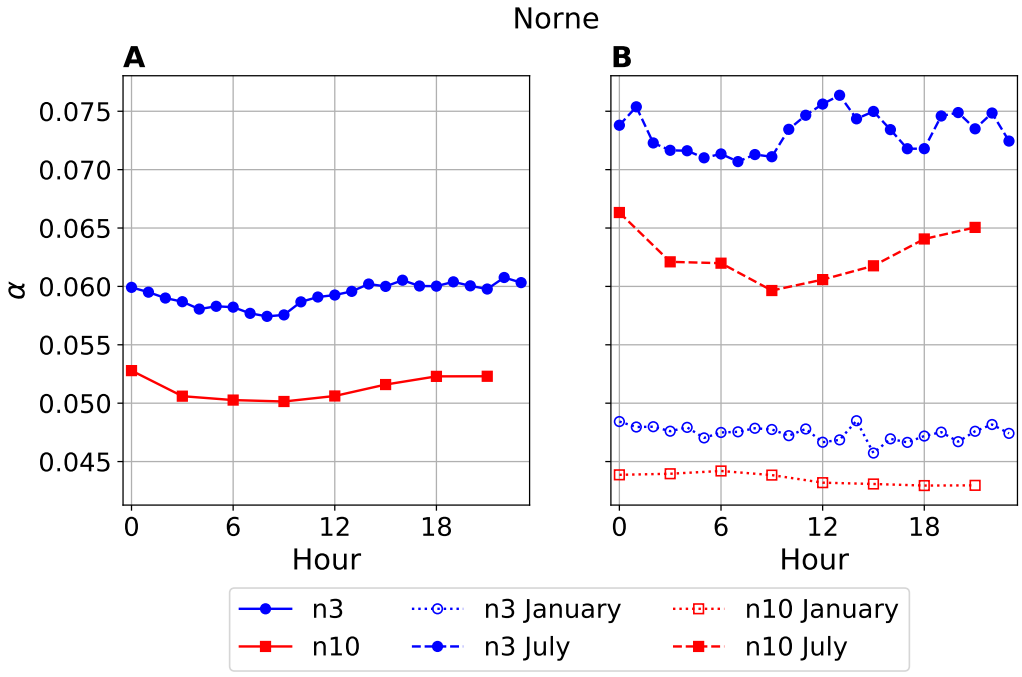

Figure D.5:

Appendix E: Monthly α variation for all sites

Figures E.1-E.6 show the monthly variation of mean α for wind speeds above 3 m/s (cut-in wind speed for NREL 5 MW) computed between 10 m and 100 m for NORA3 (n3) and NORA10 (n10) on the left axis and the temperature difference (ΔT) between 100 m and sea surface temperature (SST) computed from NORA3 on the right axis. Sites: Sørlige Nordsjø II, Sleipner A, Utsira Nord, Gullfaks C, Draugen and Norne. Time period: 2004-2015.

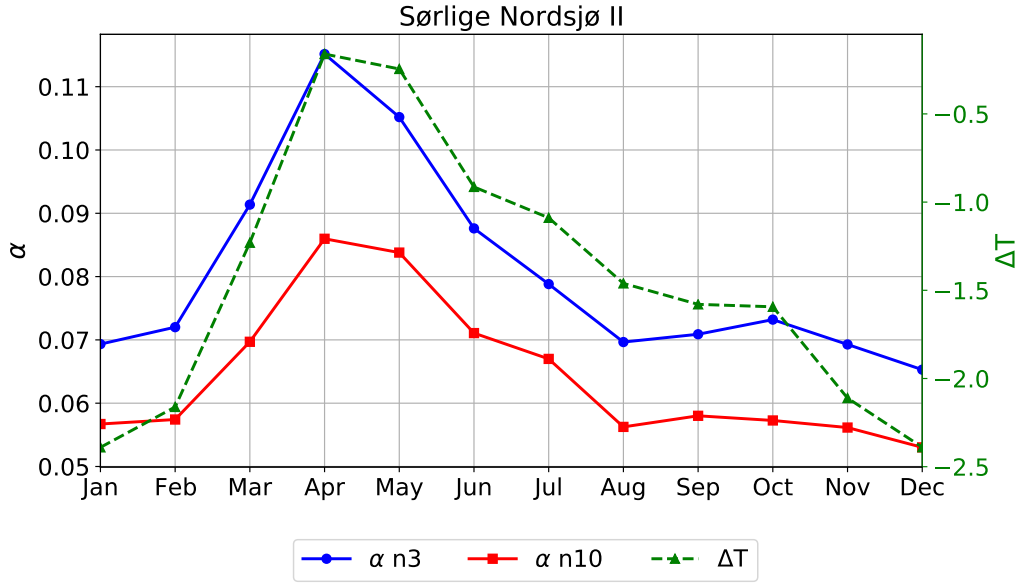

Figure E.1:

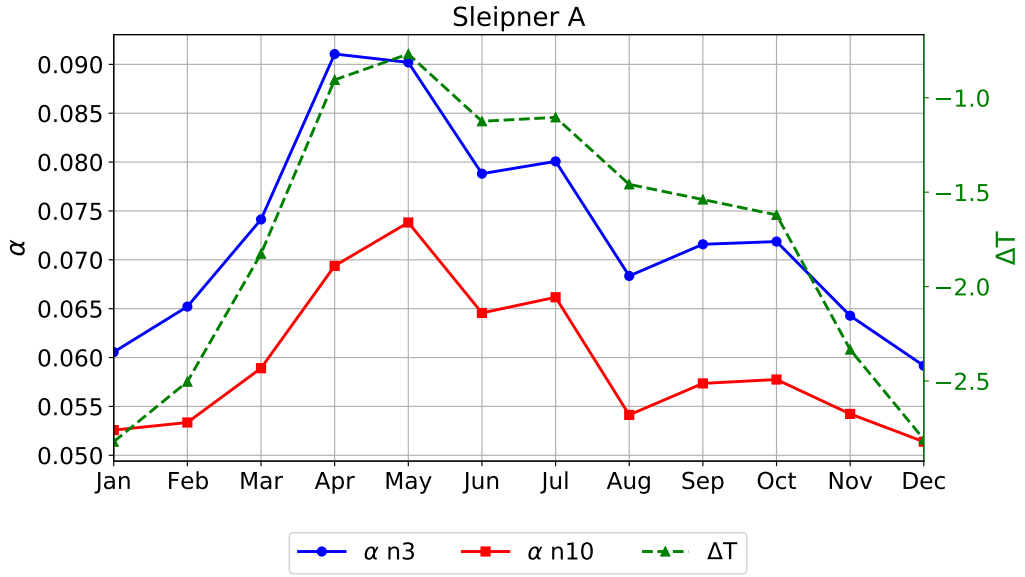

Figure E.2:

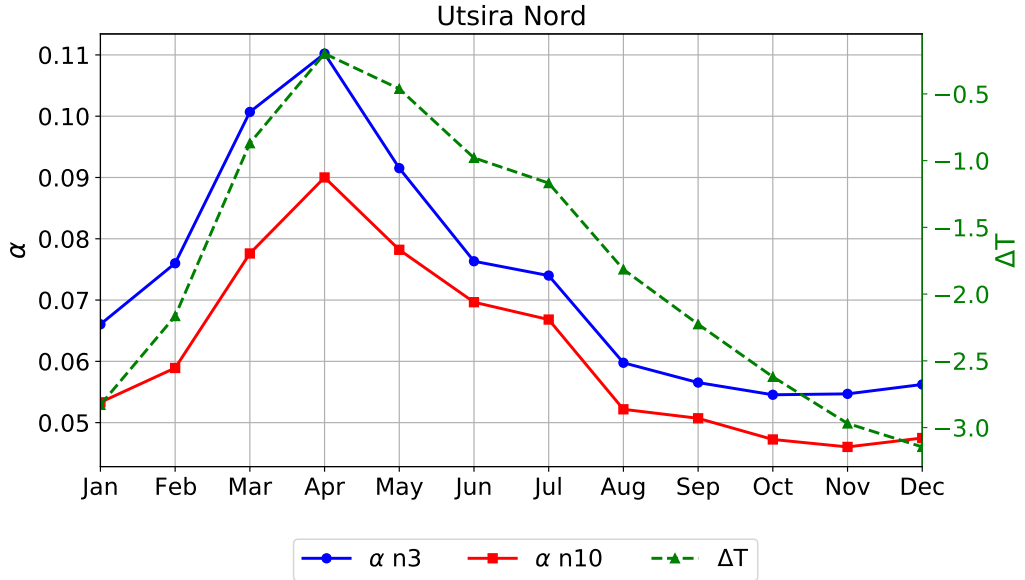

Figure E.3:

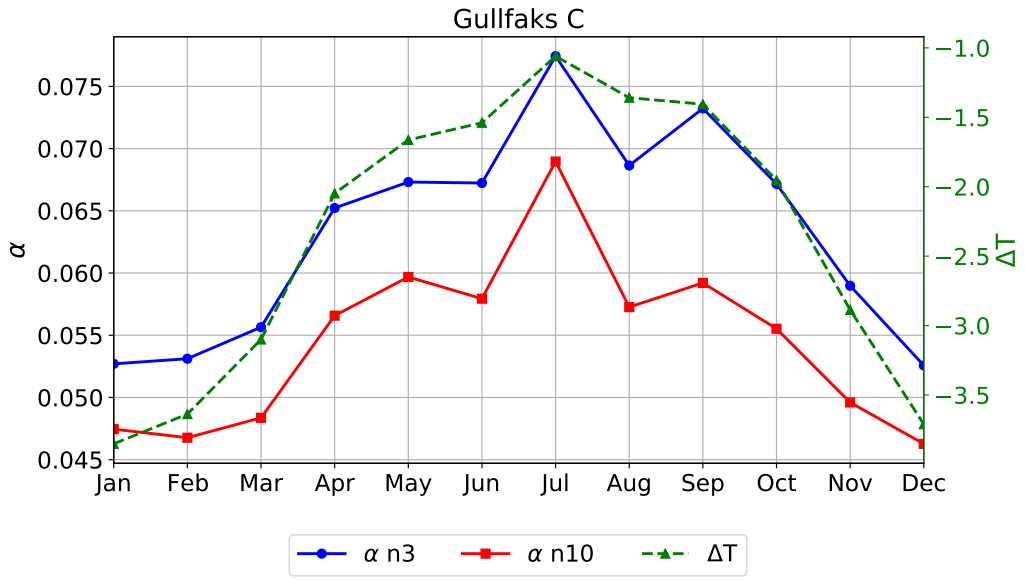

Figure E.4:

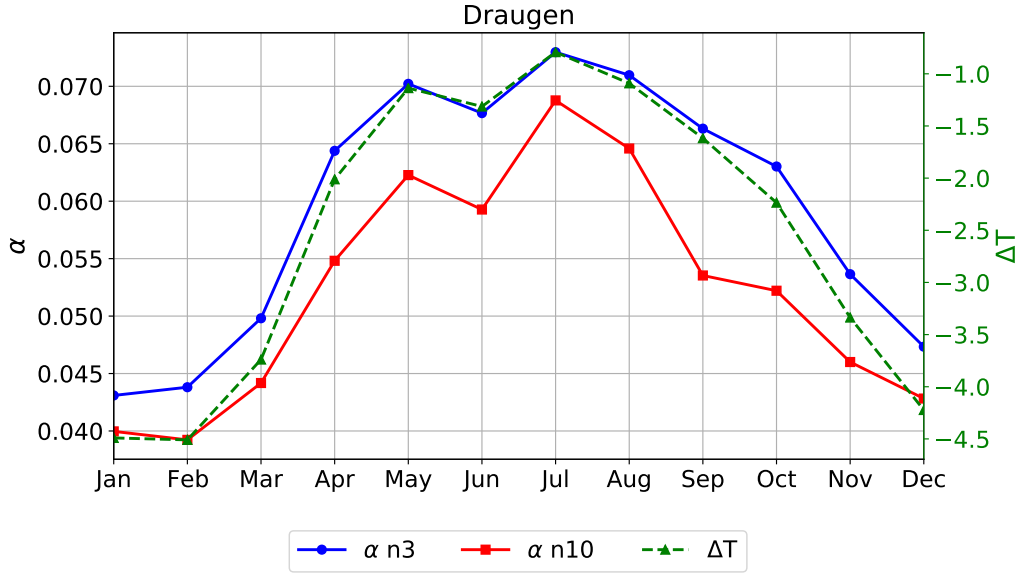

Figure E.5:

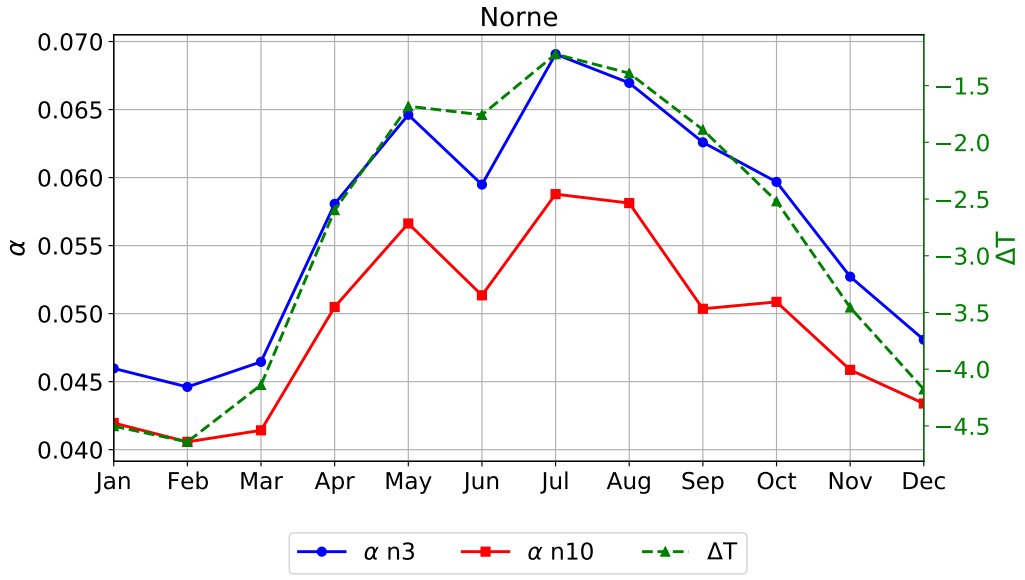
Norne
0.070
0.065
0.060
0.055
0.050
0.045
0.040
α
−1.5
−2.0
−2.5
−3.0
−3.5
−4.0
−4.5
ΔT
Jan
Feb
Mar
Apr
May
Jun
Jul
Aug
Sep
Oct
Nov
Dec
α n3
α n10
ΔT

Figure E.6:

Appendix F: Monthly α variation for all sites for high wind speeds

Figures F.1-F.6 show the monthly variation of mean α computed between 10 m and 100 m for NORA3 (n3) and NORA10 (n10). A: mean α for wind speeds between 3 m/s (cut-in wind speed for NREL 5 MW) and 11.4 m/s (rated wind speed for NREL 5 MW). B: mean α for wind speeds above 11.4 m/s (rated wind speed for NREL 5 MW). Sites: Sørlige Nordsjø II, Sleipner A, Utsira Nord, Gullfaks C, Draugen and Norne. Time period: 2004-2015.

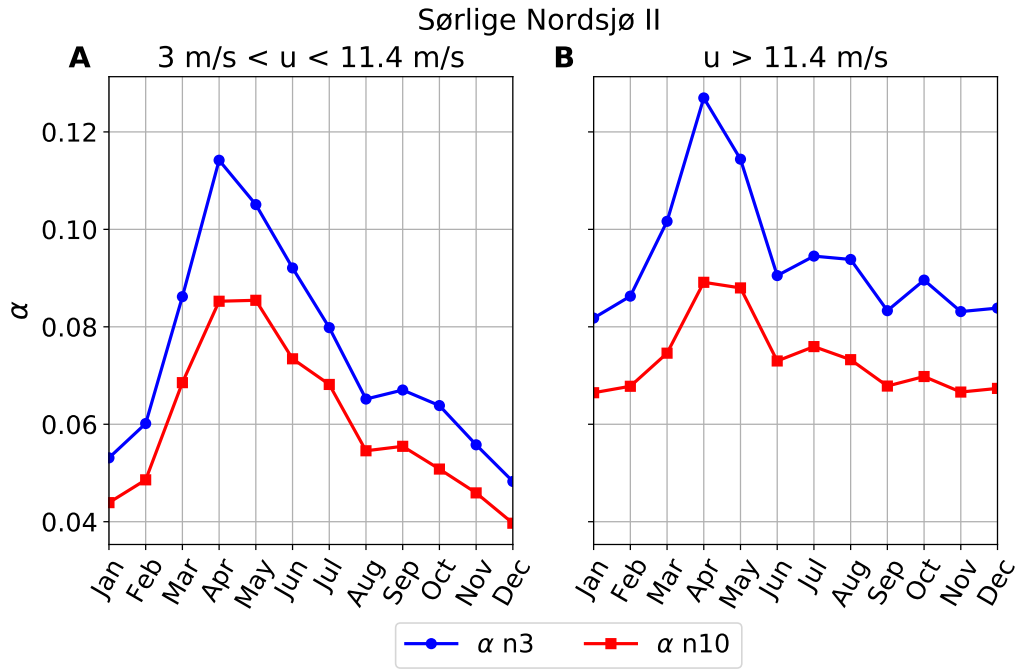

Figure F.1:

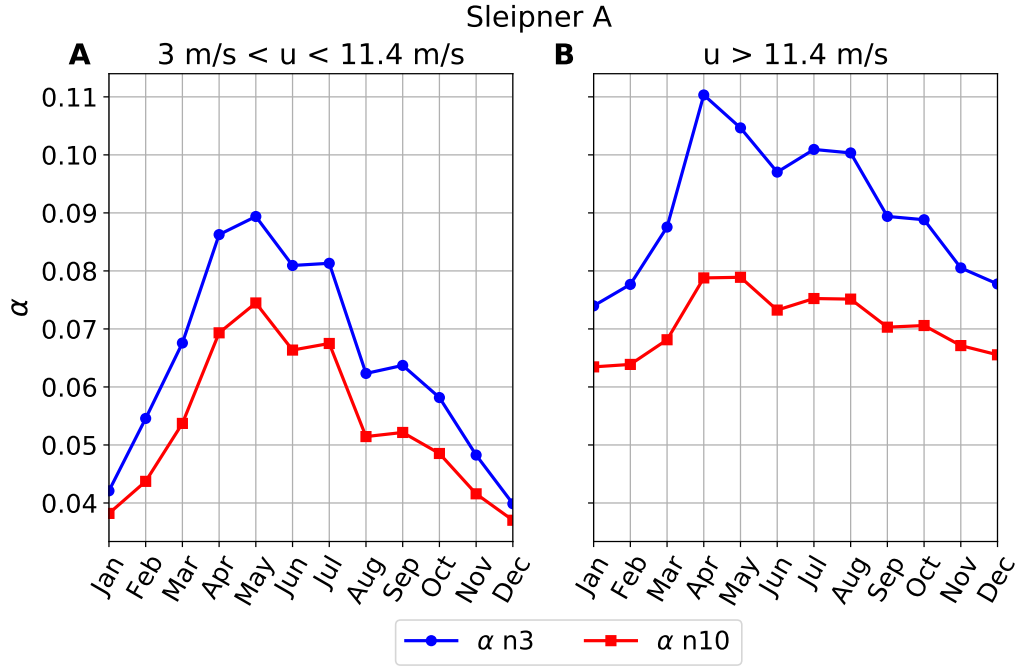

Figure F.2:

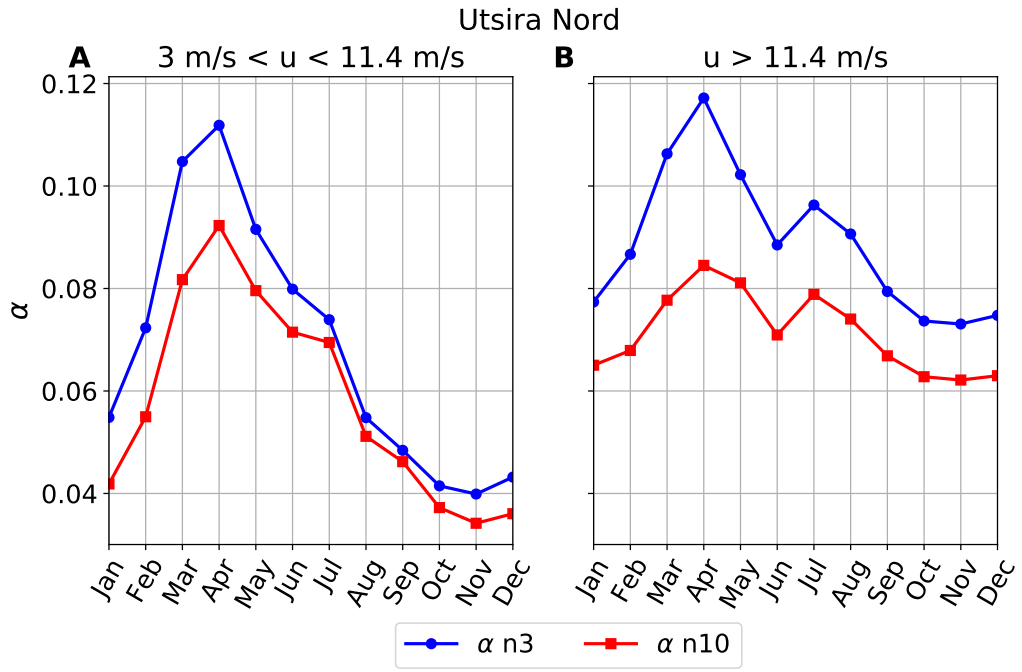

Figure F.3:

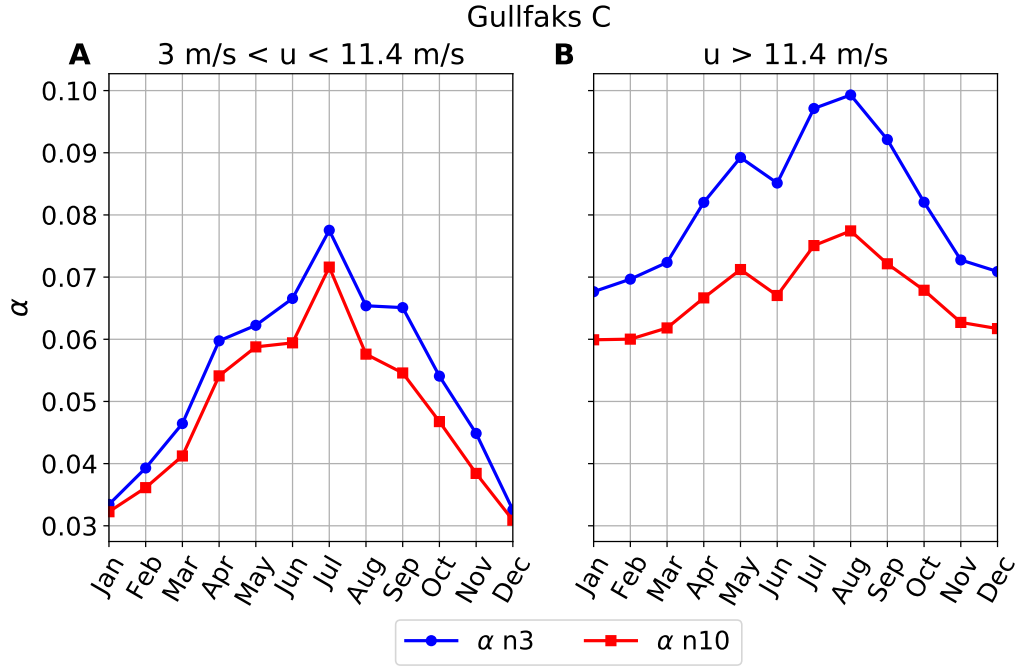

Figure F.4:

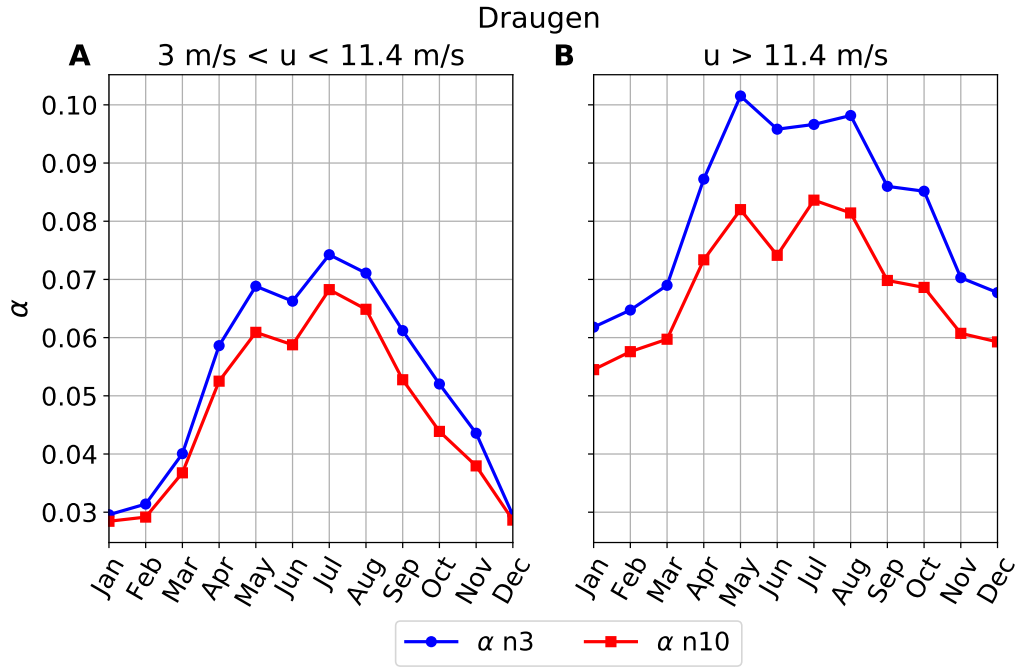

Figure F.5:

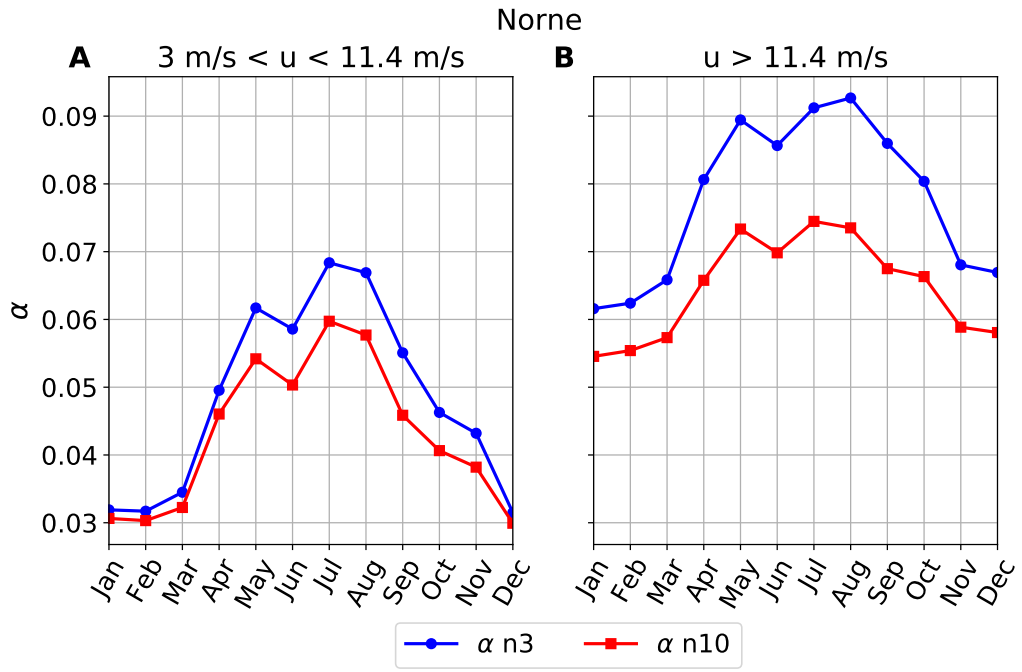
Norne
A
3 m/s < u < 11.4 m/s
B
u > 11.4 m/s
α
0.09
0.08
0.07
0.06
0.05
0.04
0.03
Jan
Feb
Mar
Apr
May
Jun
Jul
Aug
Sep
Oct
Nov
Dec
α n3
α n10

Figure F.6:

Appendix G: Monthly capacity factor

Figures G.1-G.6 show the monthly capacity factor (CF) computed for the NREL 5 MW turbine using NORA10 (n10) and NORA3 (n3) with the difference (ΔCF) between the curves (n10-n3) on the left axis. Sites: Sørlige Nordsjø II, Sleipner A, Utsira Nord, Gullfaks C, Draugen and Norne. Time period: 2004-2015.

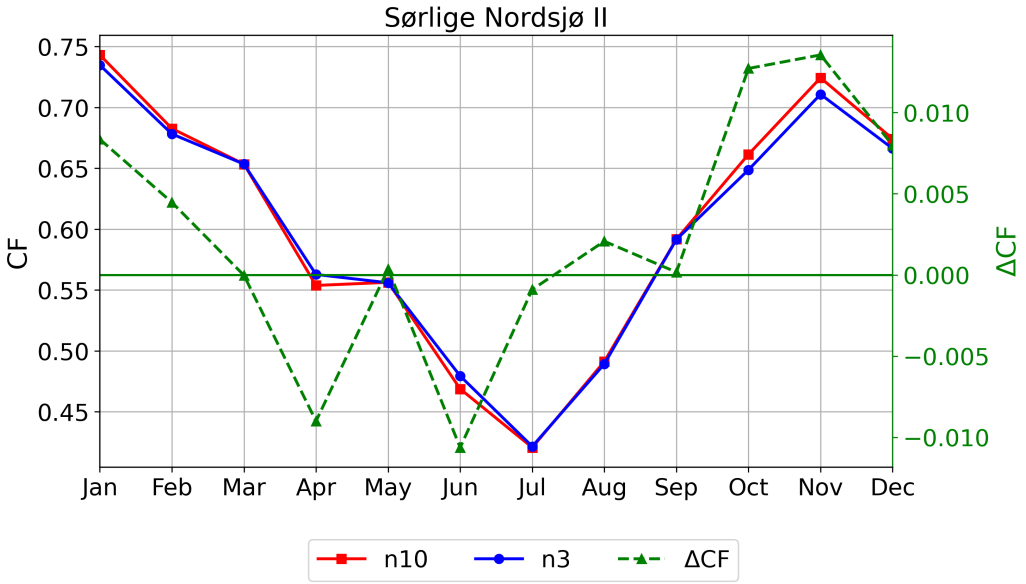

Figure G.1:

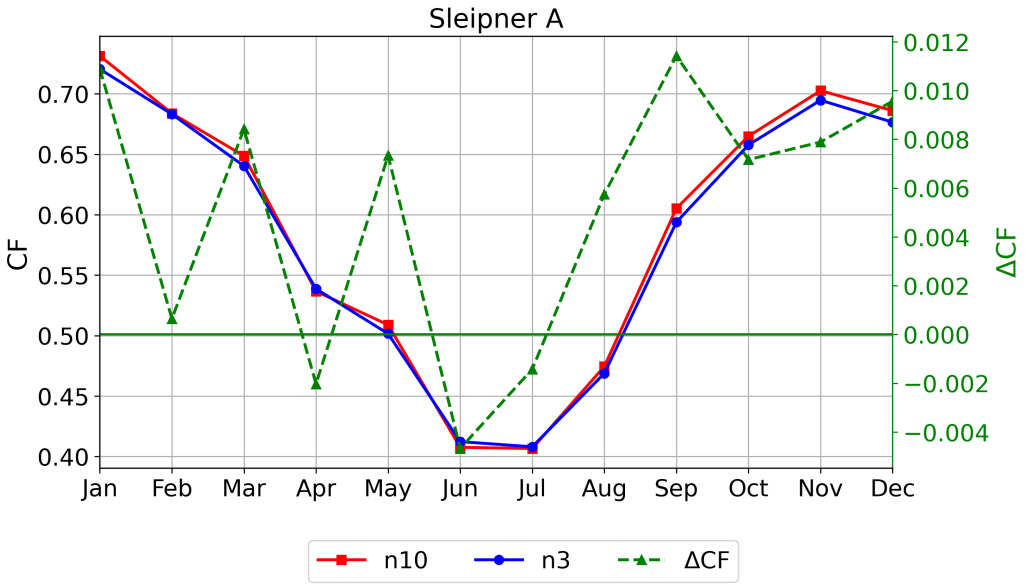

Figure G.2:

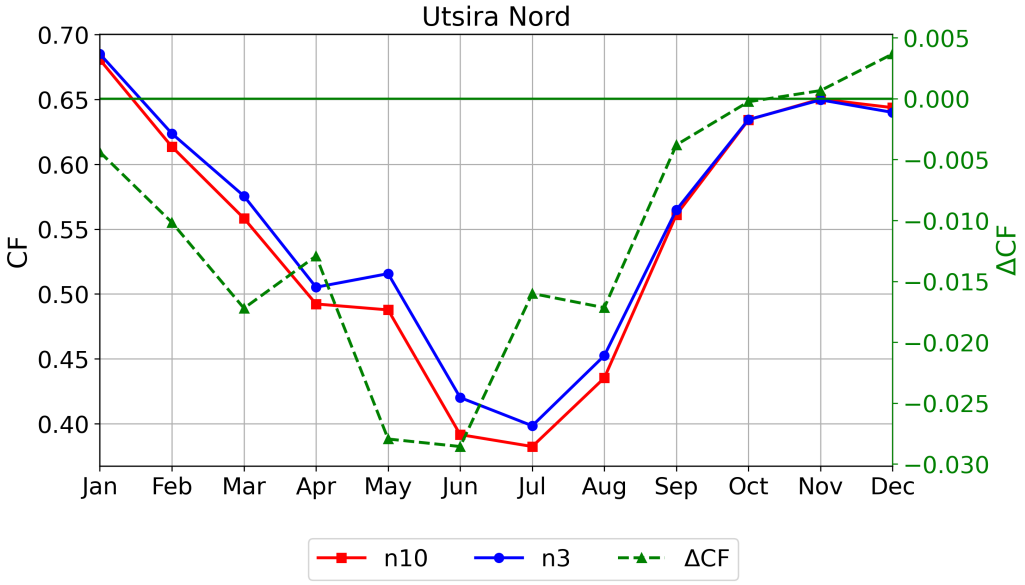

Figure G.3:

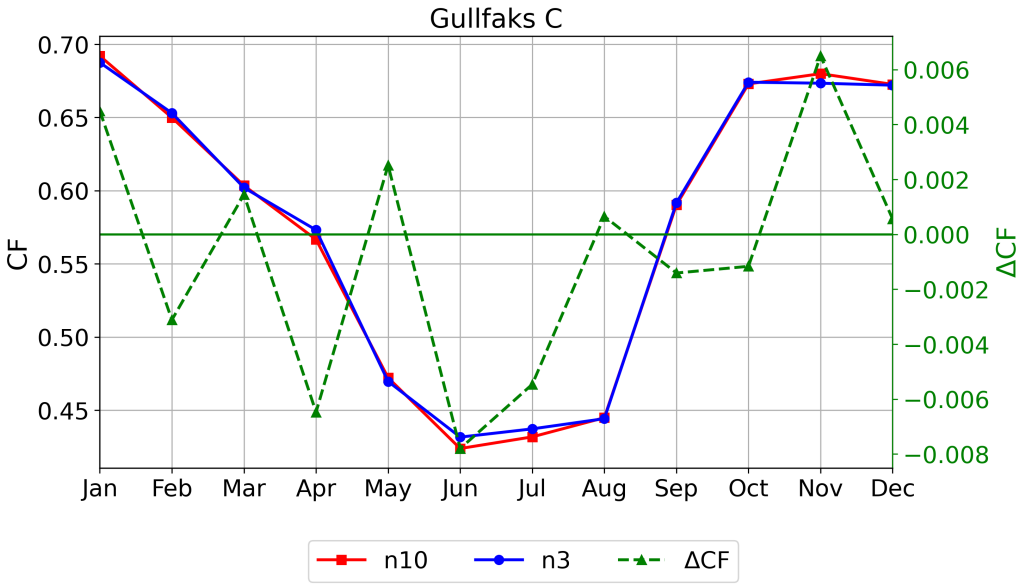

Figure G.4:

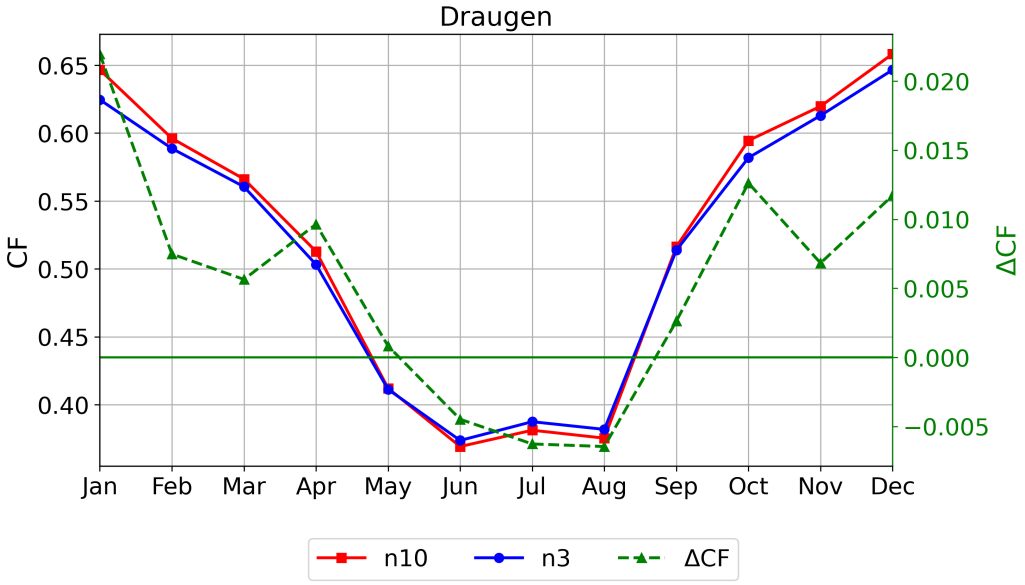

Figure G.5:

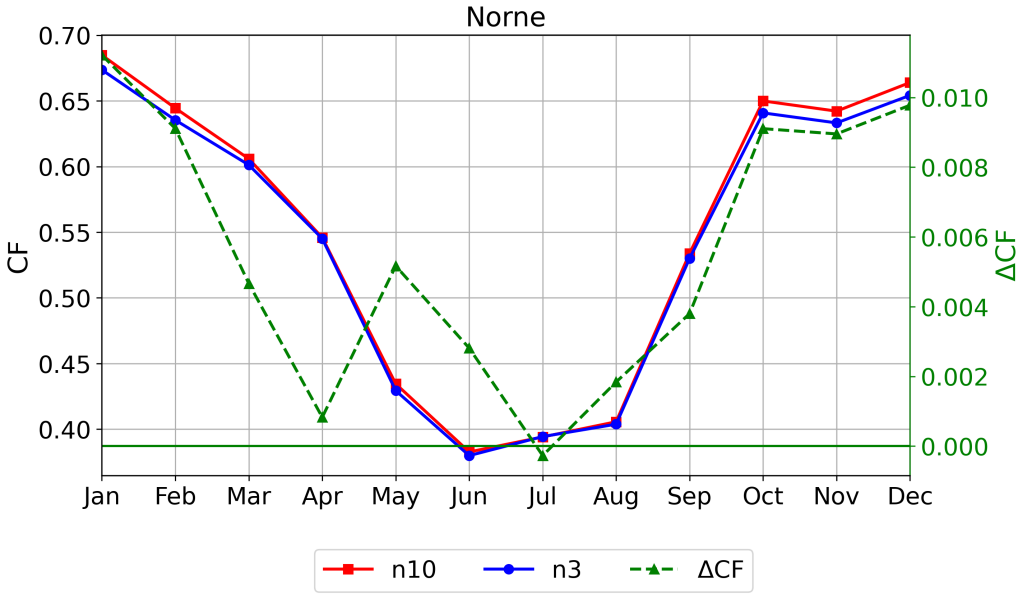
Norne
CF
ΔCF
0.70
0.65
0.60
0.55
0.50
0.45
0.40
0.010
0.008
0.006
0.004
0.002
0.000
Jan
Feb
Mar
Apr
May
Jun
Jul
Aug
Sep
Oct
Nov
Dec
n10
n3
ΔCF

Figure G.6:

Appendix H: Yearly capacity factor

Figures H.1-H.6 show the yearly capacity factor (CF) computed for the NREL 5 MW turbine using NORA10 (n10) and NORA3 (n3) with the difference (ΔCF) between the curves (n10-n3) on the left axis. Sites: Sørlige Nordsjø II, Sleipner A, Utsira Nord, Gullfaks C, Draugen and Norne. Time period: 2004-2015.

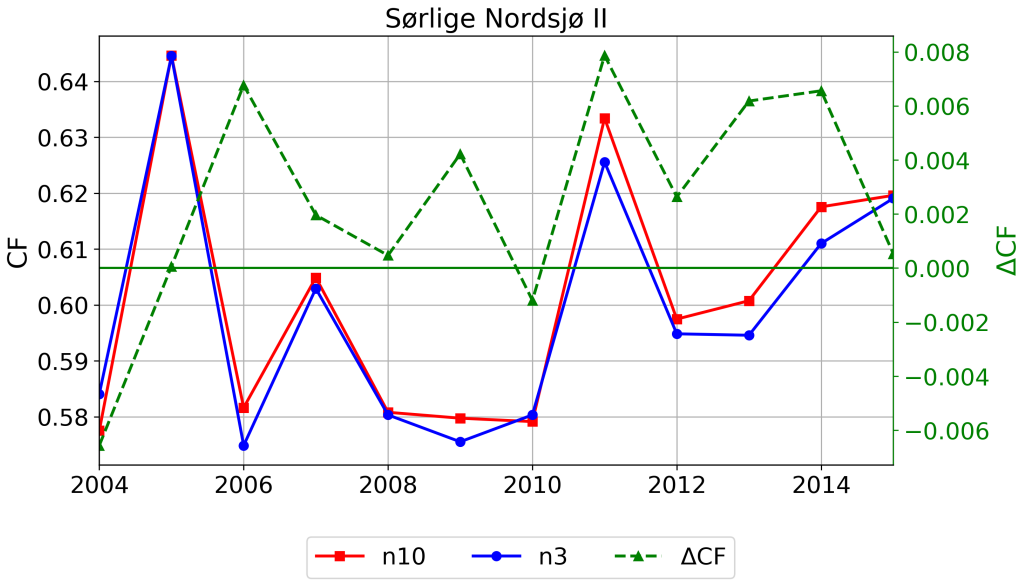

Figure H.1:

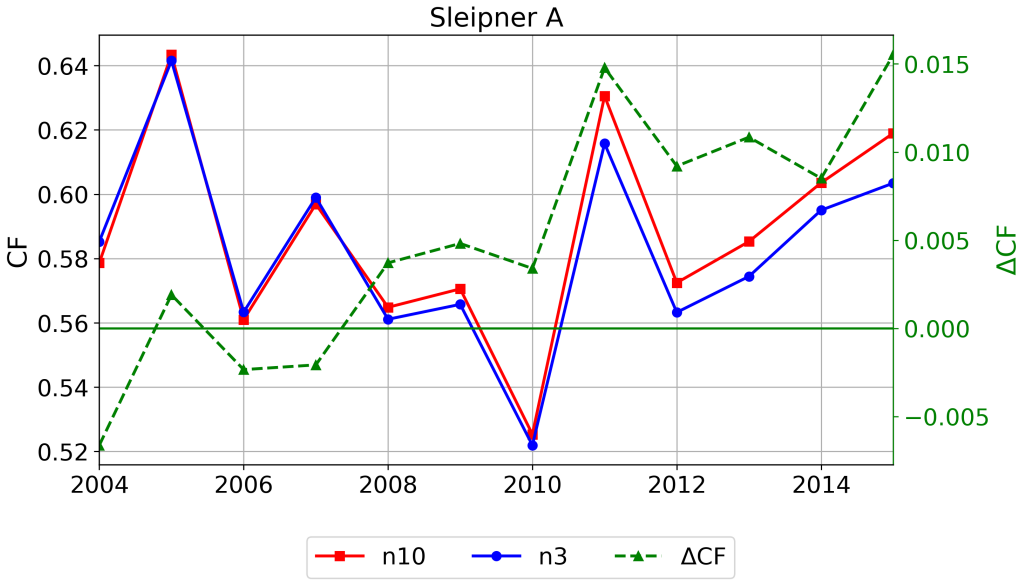

Figure H.2:

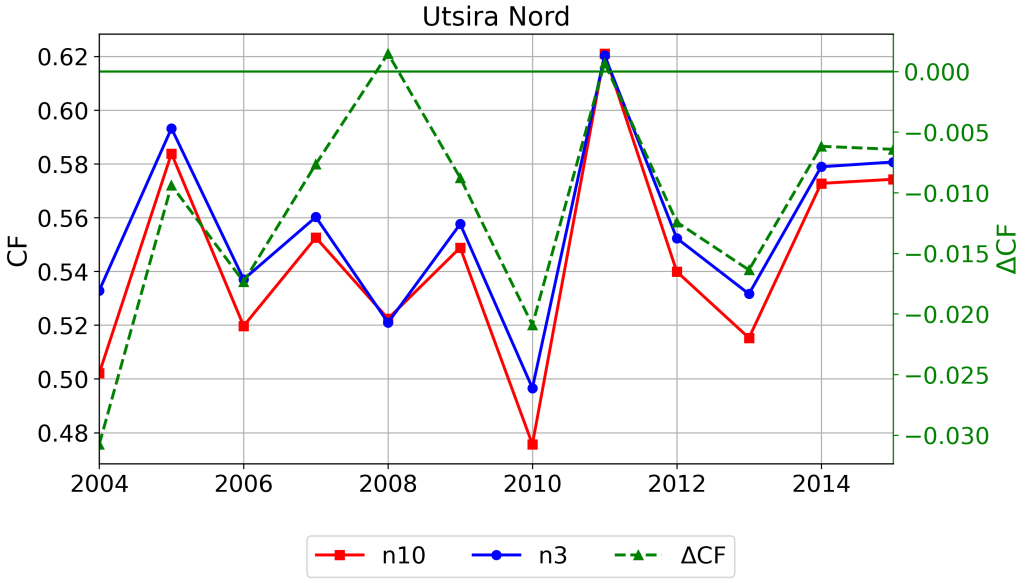

Figure H.3:

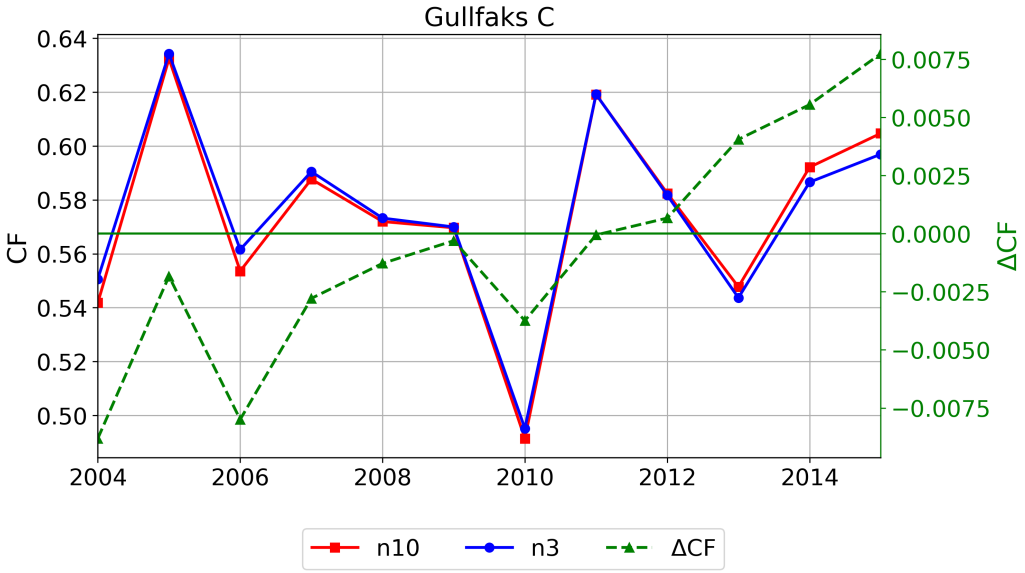

Figure H.4:

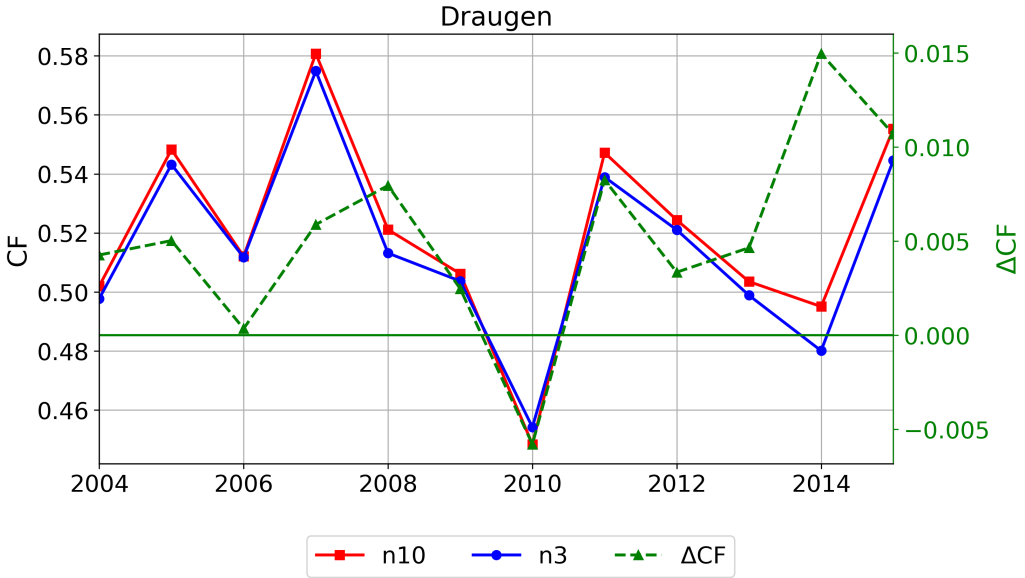

Figure H.5:

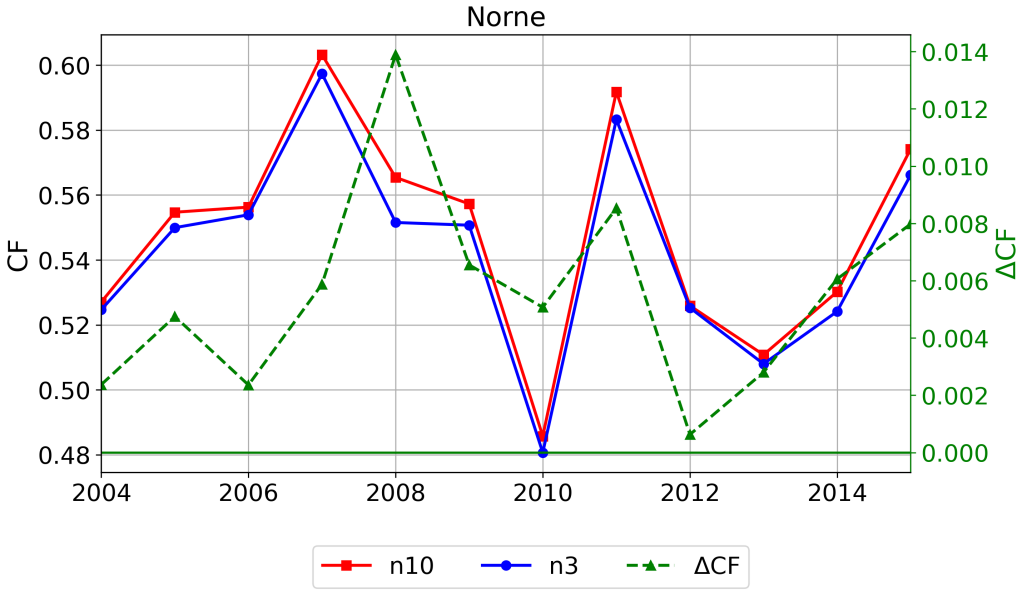
Norne
CF
ΔCF
0.60
0.58
0.56
0.54
0.52
0.50
0.48
0.014
0.012
0.010
0.008
0.006
0.004
0.002
0.000
2004
2006
2008
2010
2012
2014
n10
n3
ΔCF

Figure H.6:

Appendix I: Capacity factor for NREL 5 MW and NREL 15 MW

Figures I.1-I.6 show the monthly capacity factor (CF) computed for the NREL 5 MW turbine and the NREL 15 MW turbine with the difference (ΔCF) between the curves (NREL 15 MW-NREL 5 MW) on the left axis. Sites: Sørlige Nordsjø II, Sleipner A, Utsira Nord, Gullfaks C, Draugen and Norne. Time period: 2004-2015.

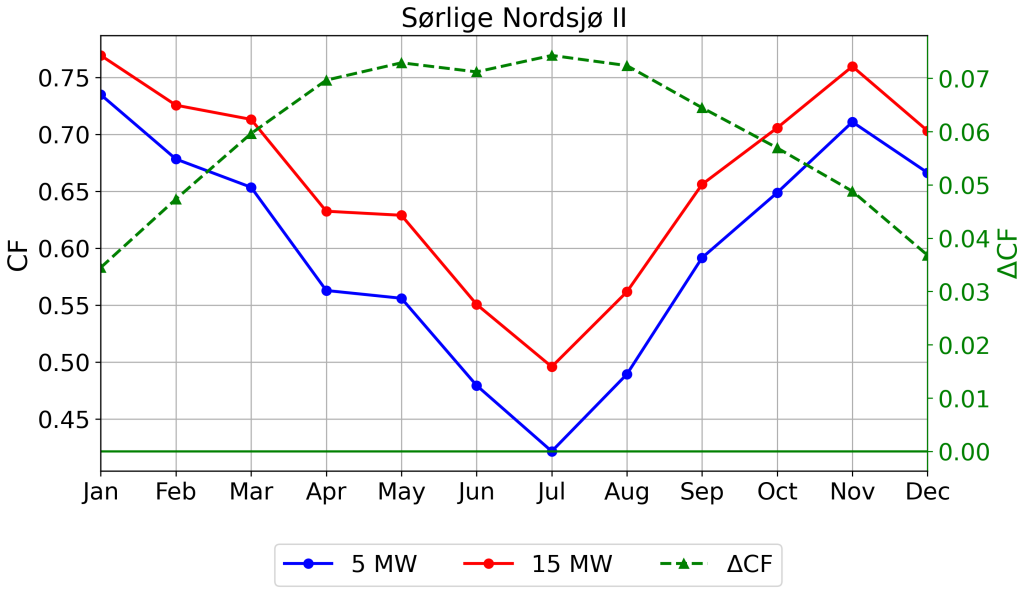

Figure I.1:

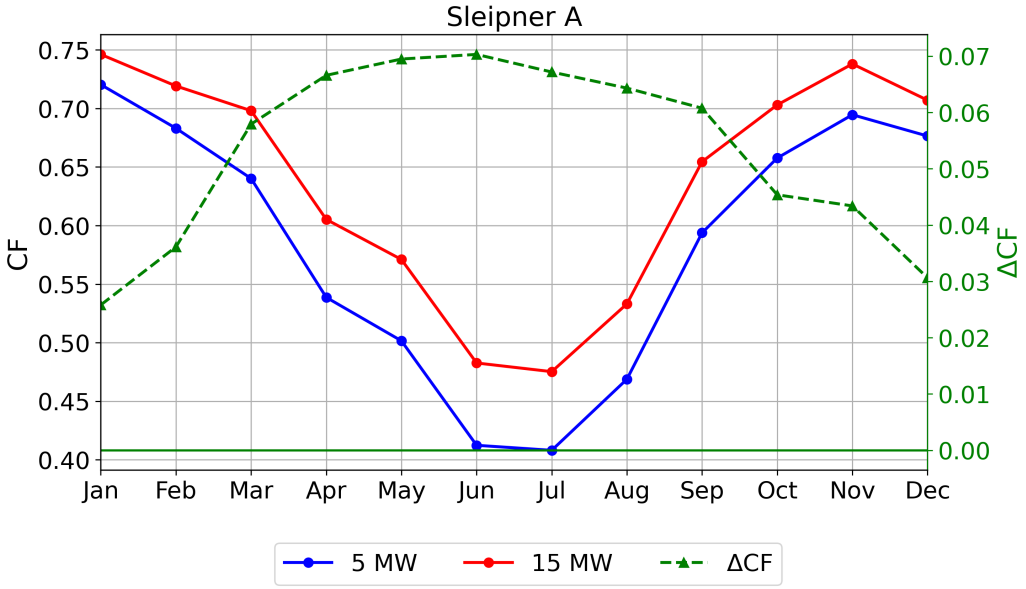

Figure I.2:

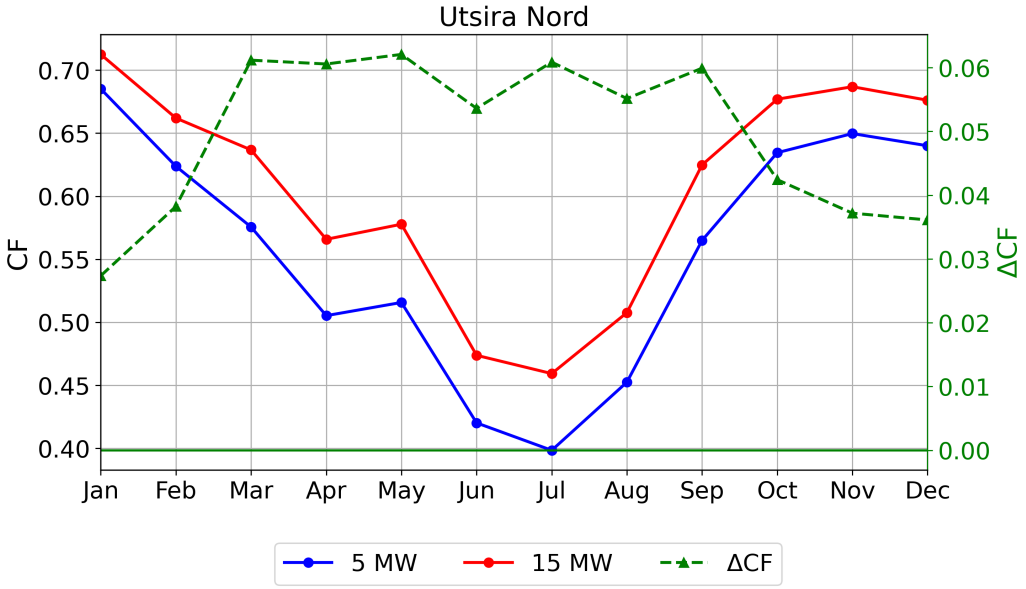

Figure I.3:

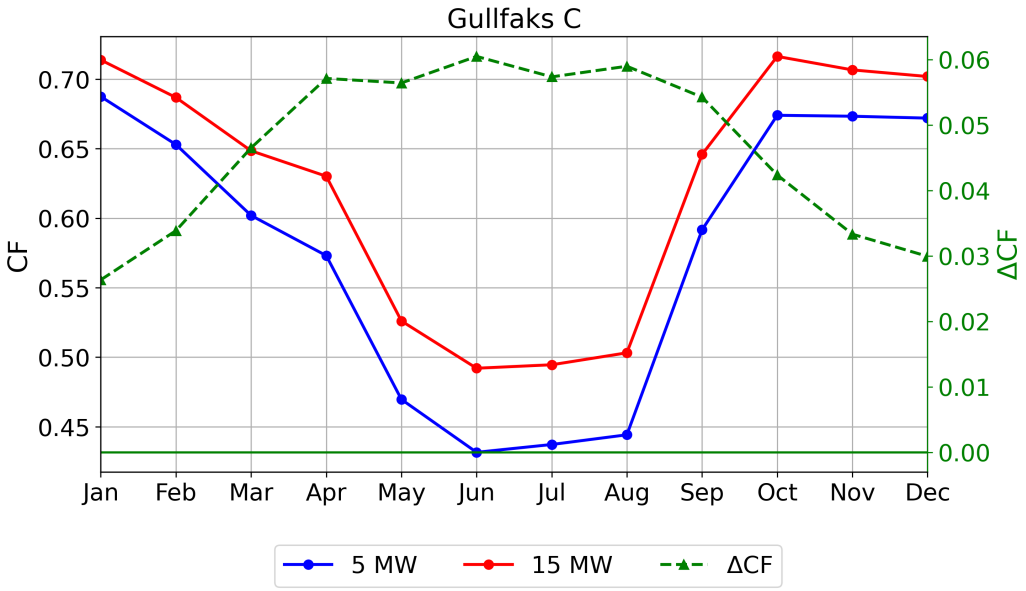

Figure I.4:

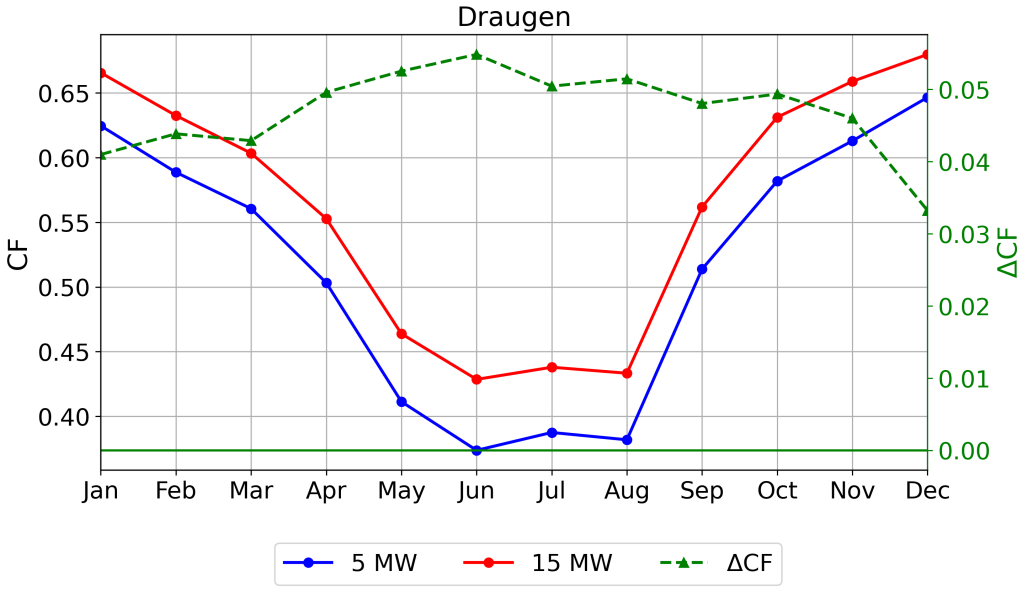

Figure I.5:

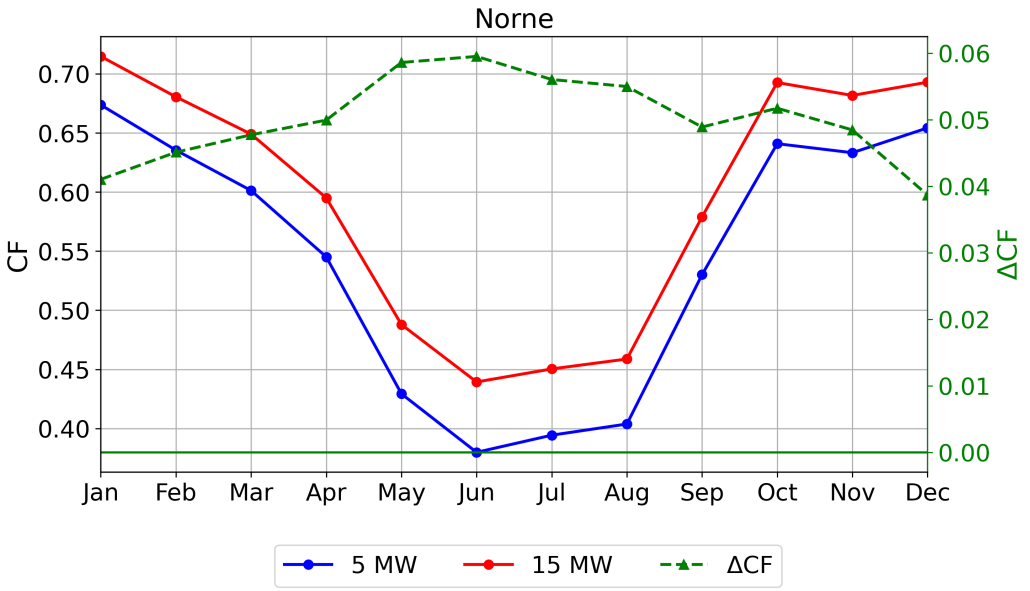
Norne
CF
ΔCF
0.70
0.65
0.60
0.55
0.50
0.45
0.40
0.06
0.05
0.04
0.03
0.02
0.01
0.00
Jan
Feb
Mar
Apr
May
Jun
Jul
Aug
Sep
Oct
Nov
Dec
5 MW
15 MW
ΔCF

Figure I.6:

Appendix J: Rotor equivalent wind speed

Figures J.1-J.6 show the monthly capacity factor (CF) computed for the NREL 5 MW turbine and the NREL 15 MW turbine using wind speed at hub height (Standard) and using rotor equivalent wind speed (REWS). Left axis: difference (ΔCF) between the curves (Standard-REWS). Sites: Sørlige Nordsjø II, Sleipner A, Utsira Nord, Gullfaks C, Draugen and Norne. Time period: 2004-2015.

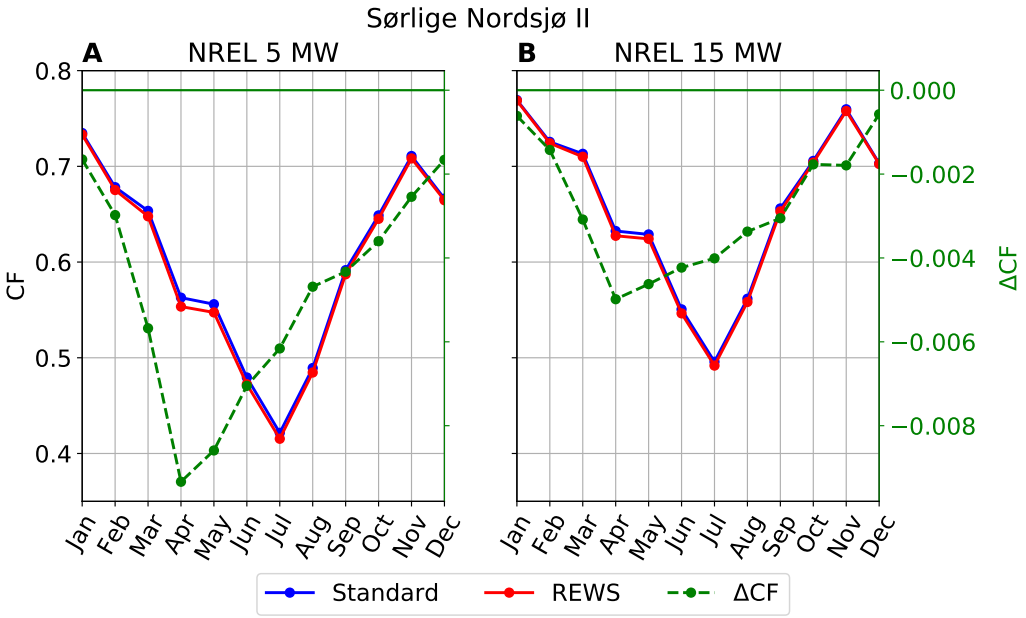

Figure J.1:

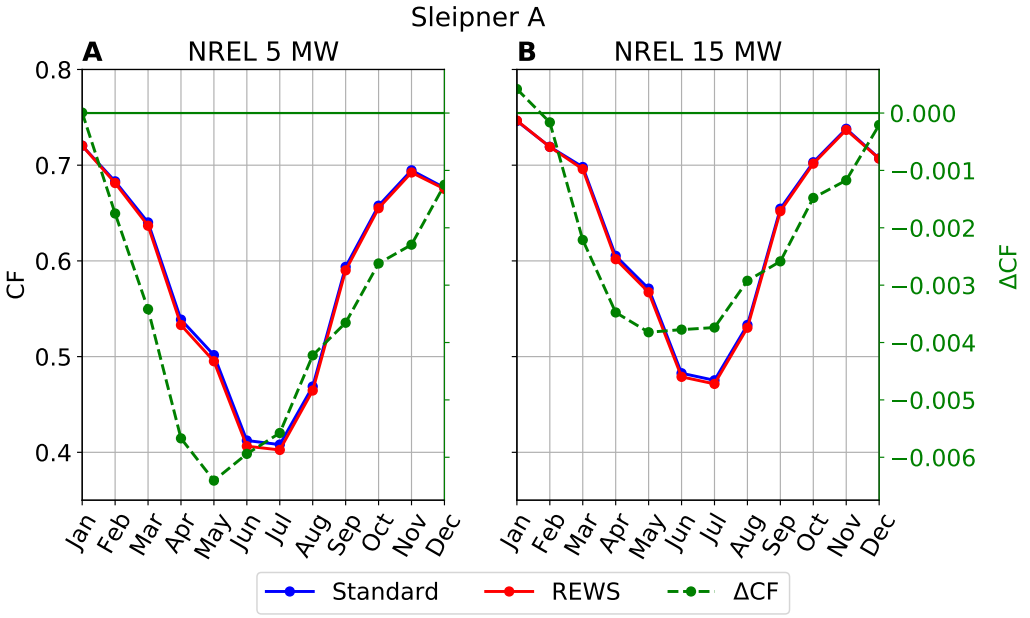

Figure J.2:

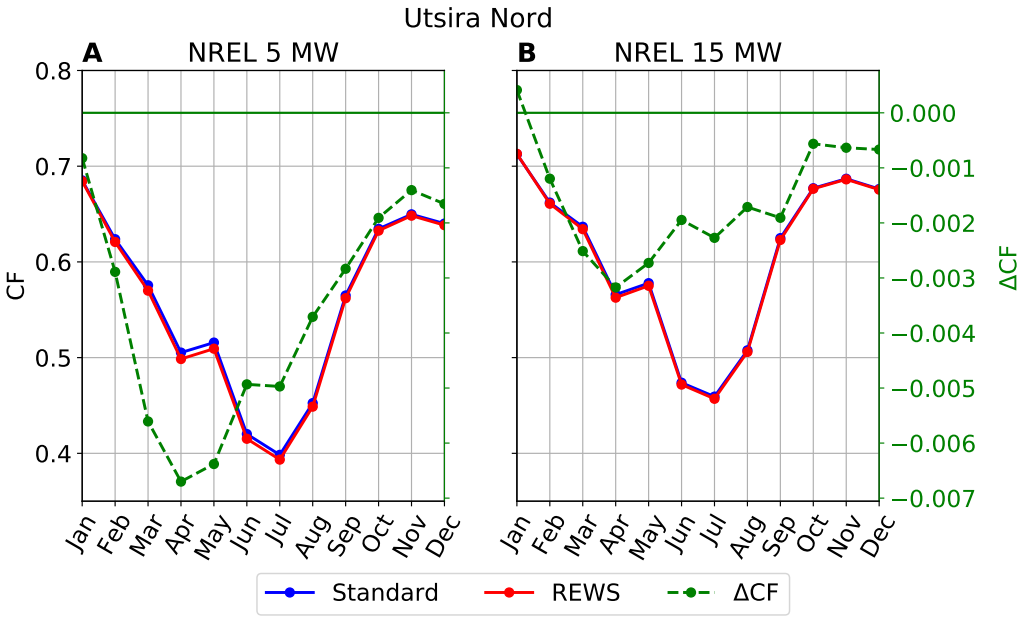

Figure J.3:

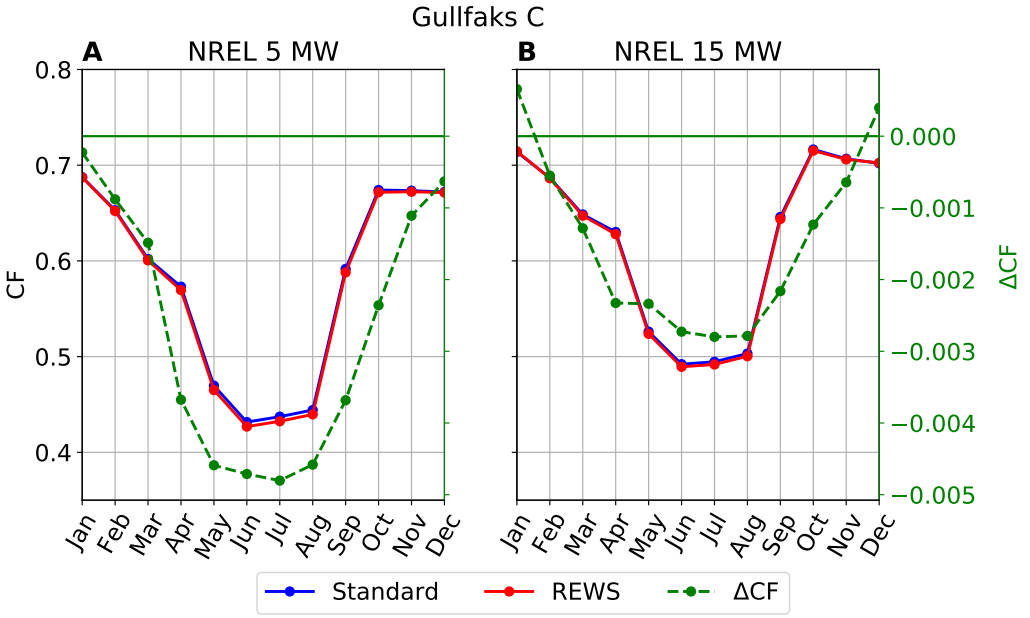

Figure J.4:

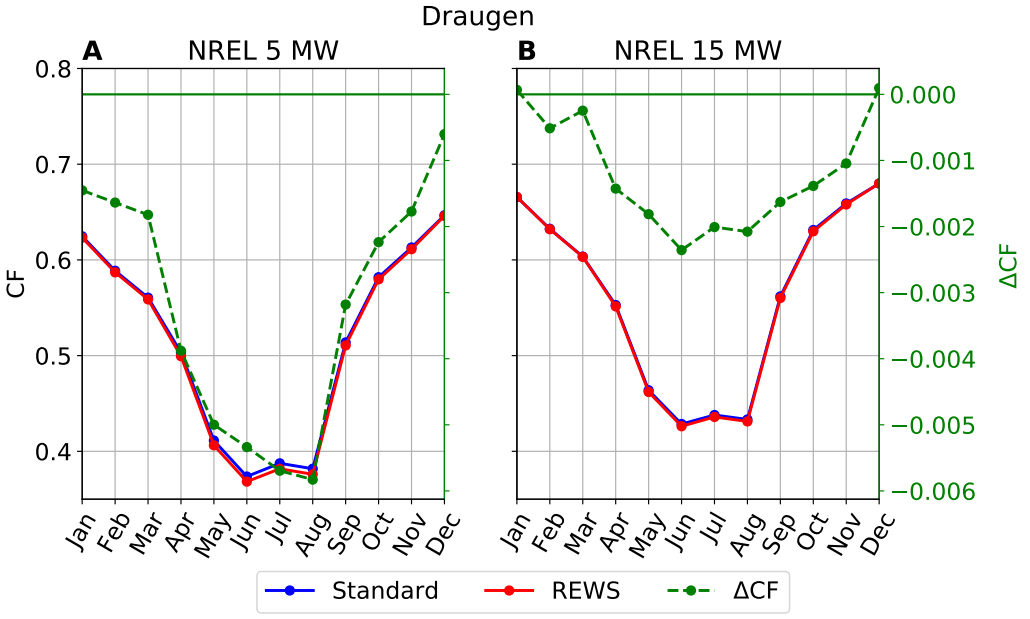

Figure J.5:

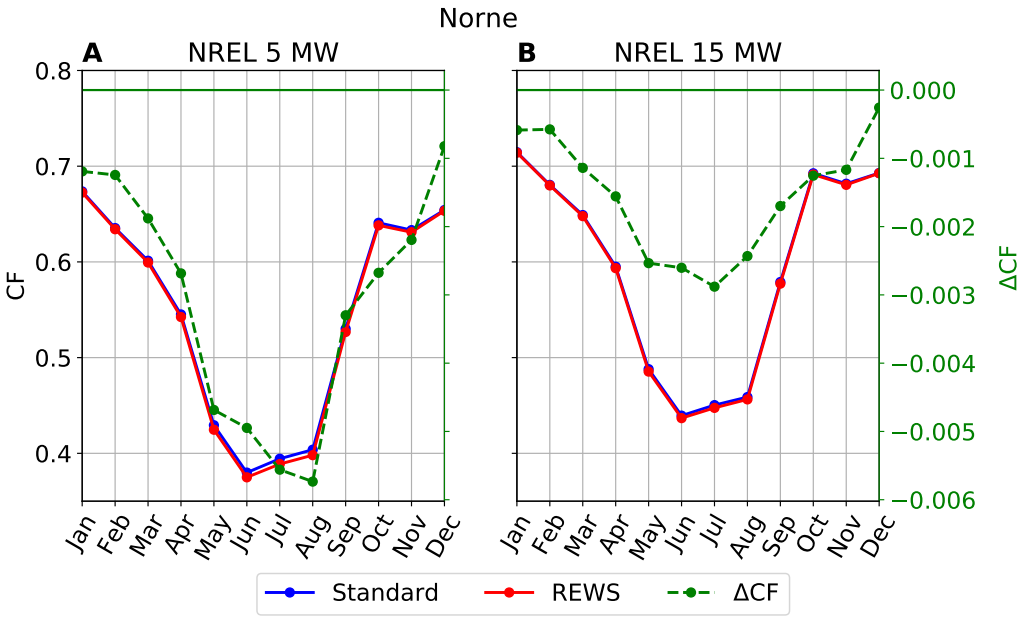
Norne
A
NREL 5 MW
B
NREL 15 MW
CF
ΔCF
0.8
0.7
0.6
0.5
0.4
0.000
−0.001
−0.002
−0.003
−0.004
−0.005
−0.006
Jan
Feb
Mar
Apr
May
Jun
Jul
Aug
Sep
Oct
Nov
Dec
Standard
REWS
ΔCF

Figure J.6:

Appendix K: Storm control 1

Figures K.1-K.6 show the monthly capacity factor (CF) computed for the NREL 5 MW turbine and the NREL 15 MW turbine using the standard power curve (Standard) and storm control 1 (SC1). Left axis: difference (ΔCF) between the curves (Standard-SC1). Sites: Sørlige Nordsjø II, Sleipner A, Utsira Nord, Gullfaks C, Draugen and Norne. Time period: 2004-2015.

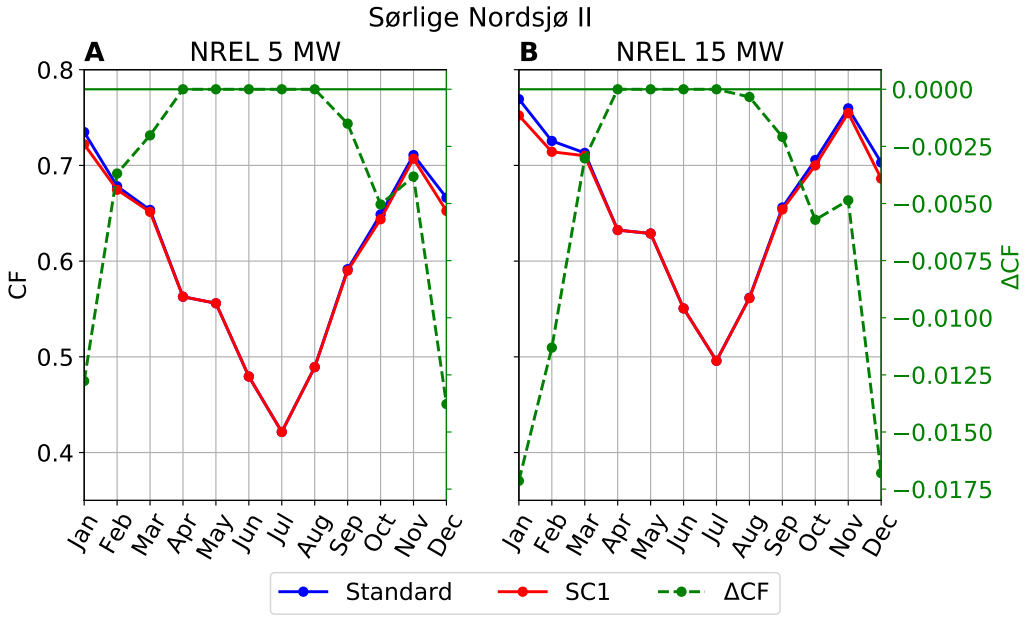

Figure K.1:

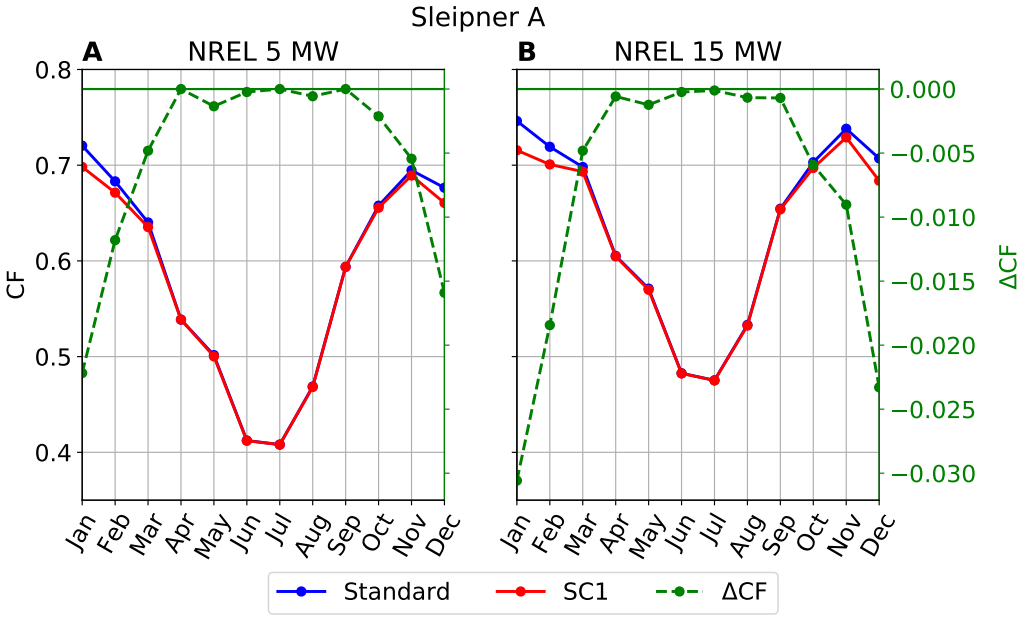

Figure K.2:

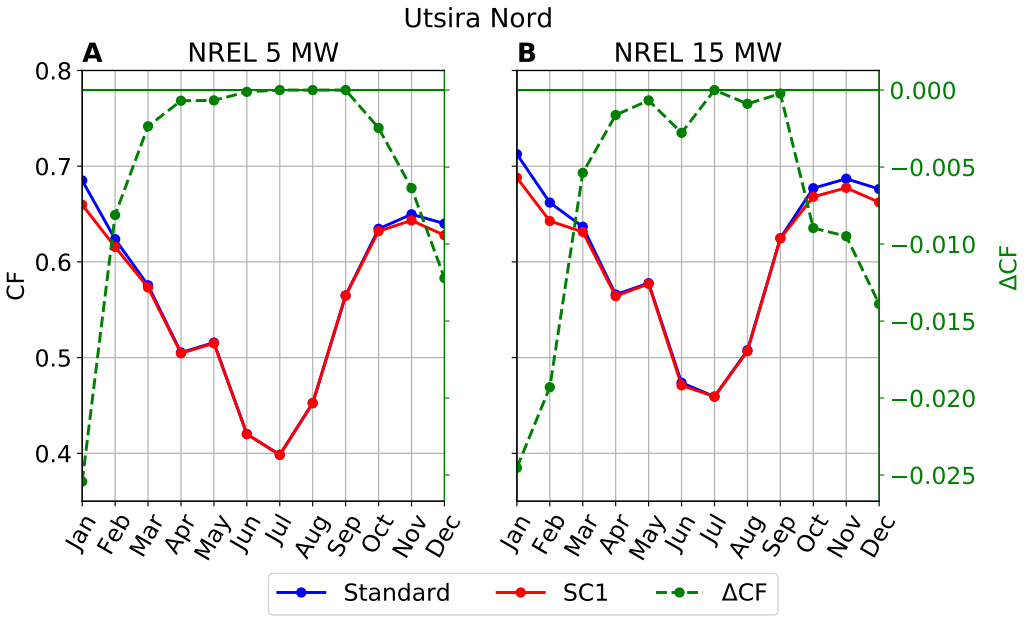

Figure K.3:

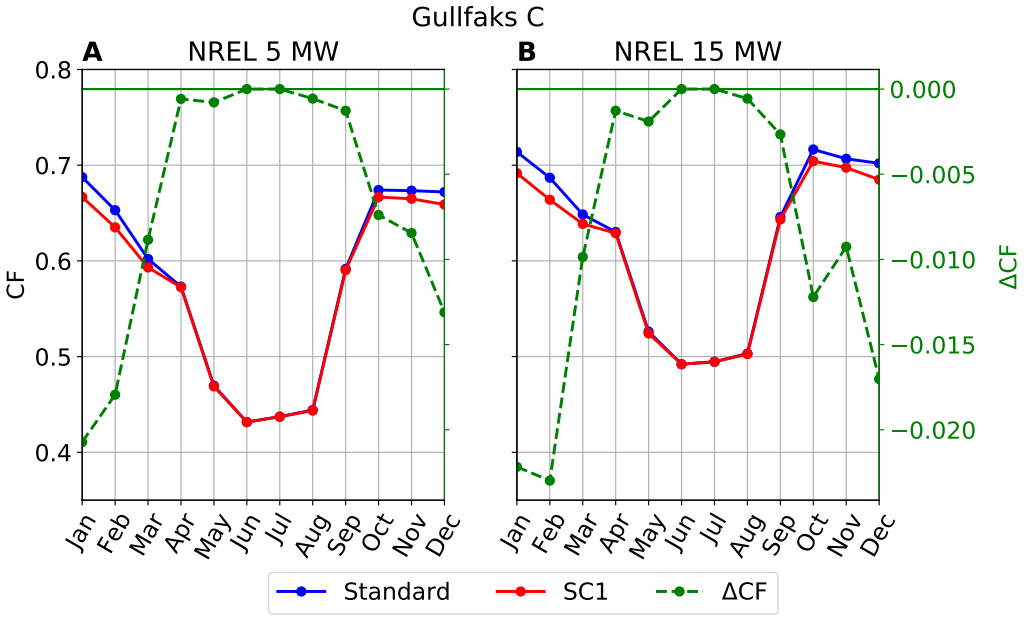

Figure K.4:

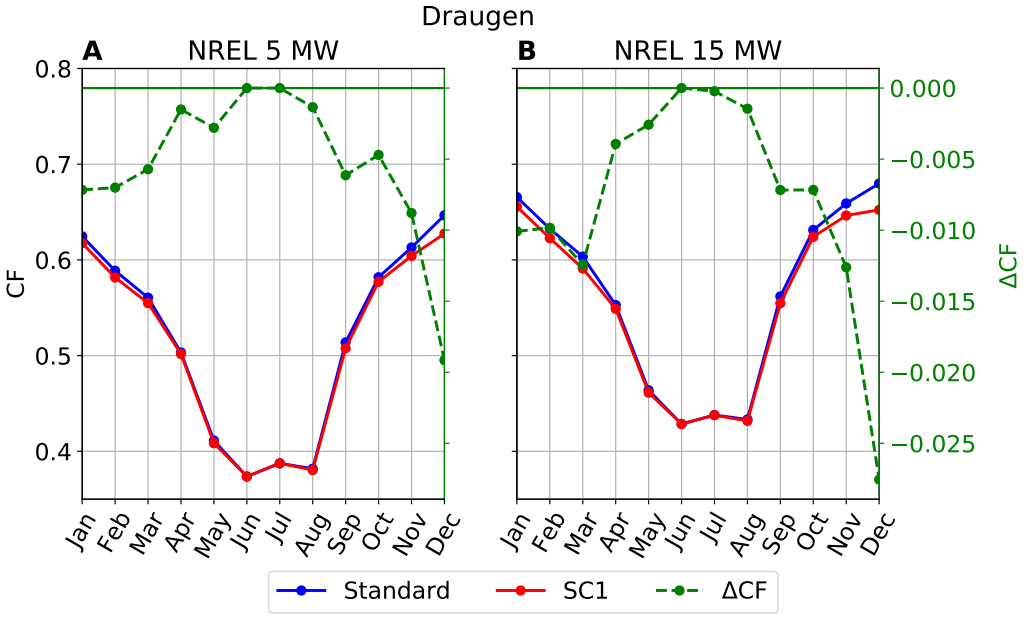

Figure K.5:

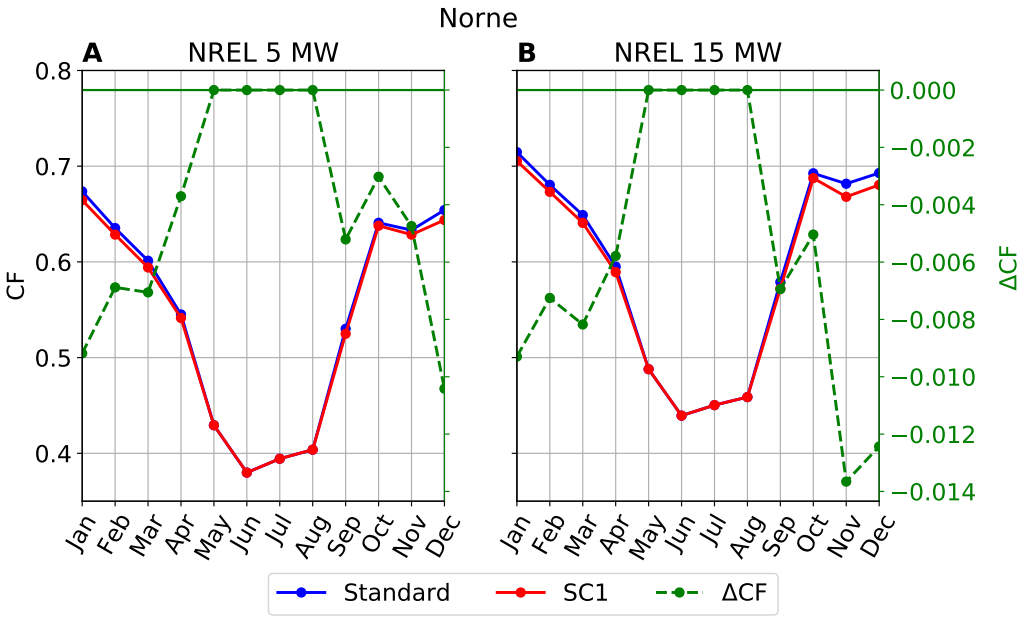
Norne
A
NREL 5 MW
B
NREL 15 MW
CF
ΔCF
0.8
0.7
0.6
0.5
0.4
0.000
−0.002
−0.004
−0.006
−0.008
−0.010
−0.012
−0.014
Jan
Feb
Mar
Apr
May
Jun
Jul
Aug
Sep
Oct
Nov
Dec
Standard
SC1
ΔCF

Figure K.6:

Appendix L: Storm control 2

Figures L.1-L.6 show the monthly capacity factor (CF) computed for the NREL 5 MW turbine and the NREL 15 MW turbine using the standard power curve (Standard) and storm control 2 (SC2). Left axis: difference (ΔCF) between the curves (Standard-SC2). Sites: Sørlige Nordsjø II, Sleipner A, Utsira Nord, Gullfaks C, Draugen and Norne. Time period: 2004-2015.

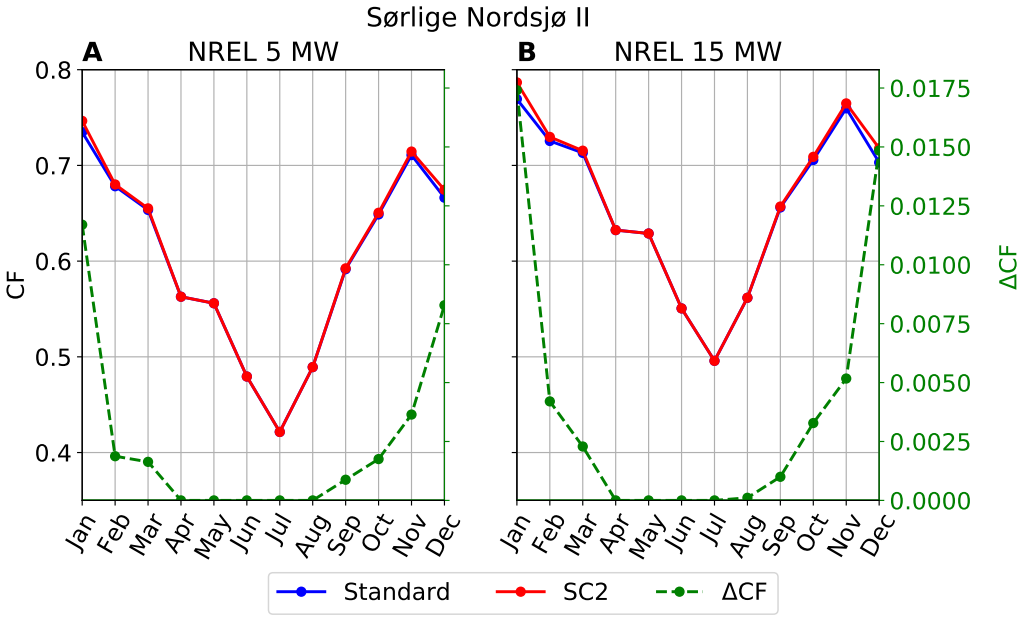

Figure L.1:

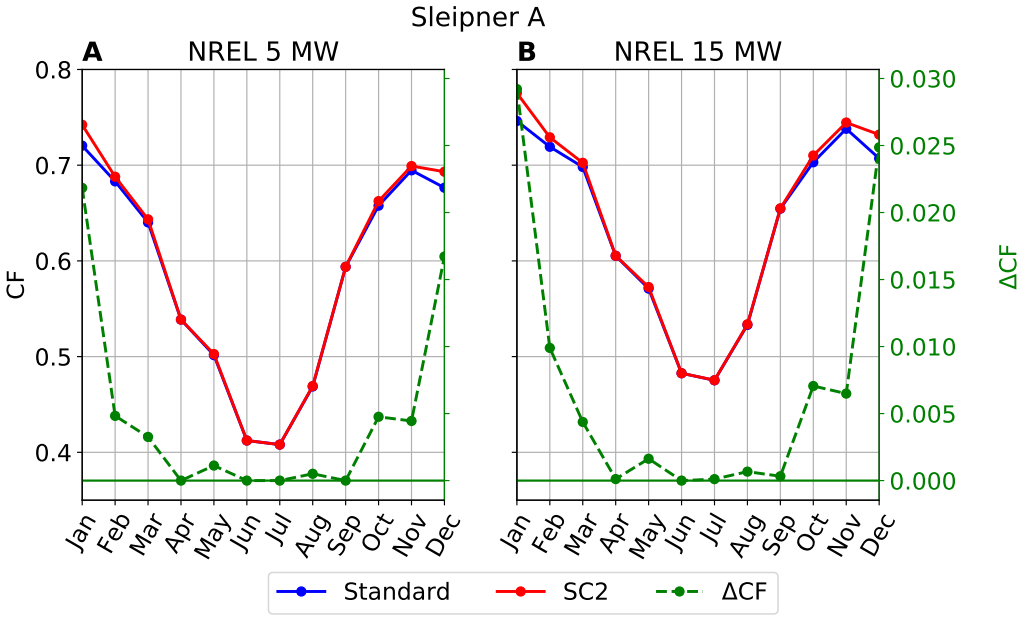

Figure L.2:

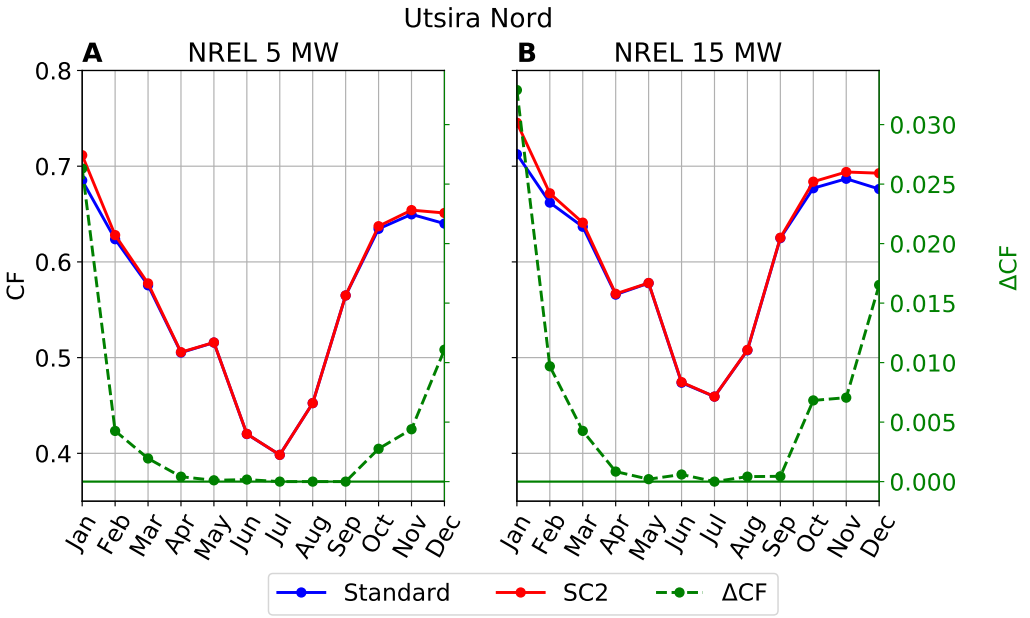

Figure L.3:

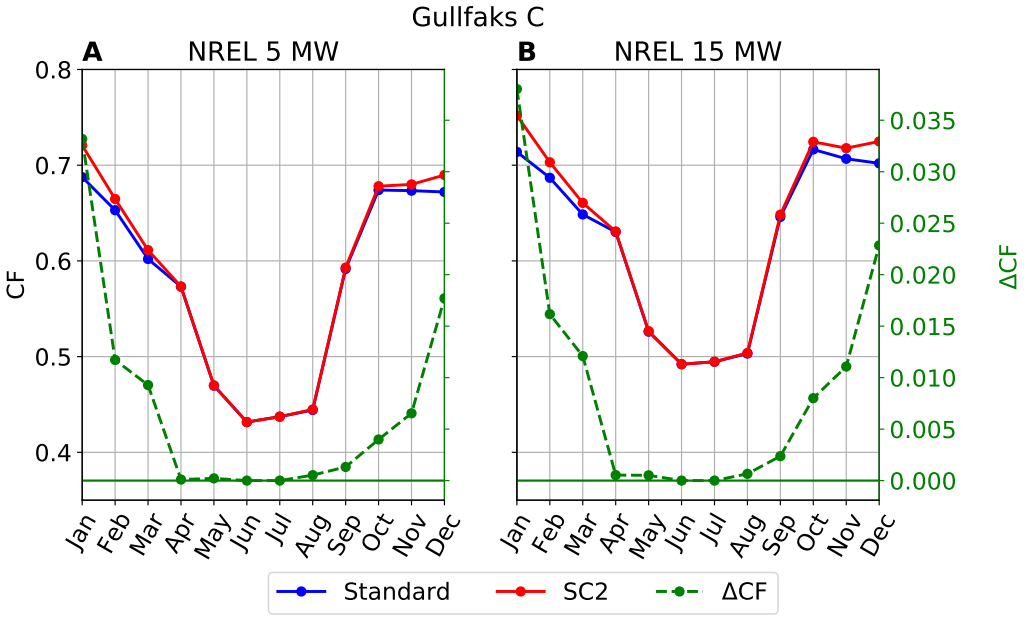

Figure L.4:

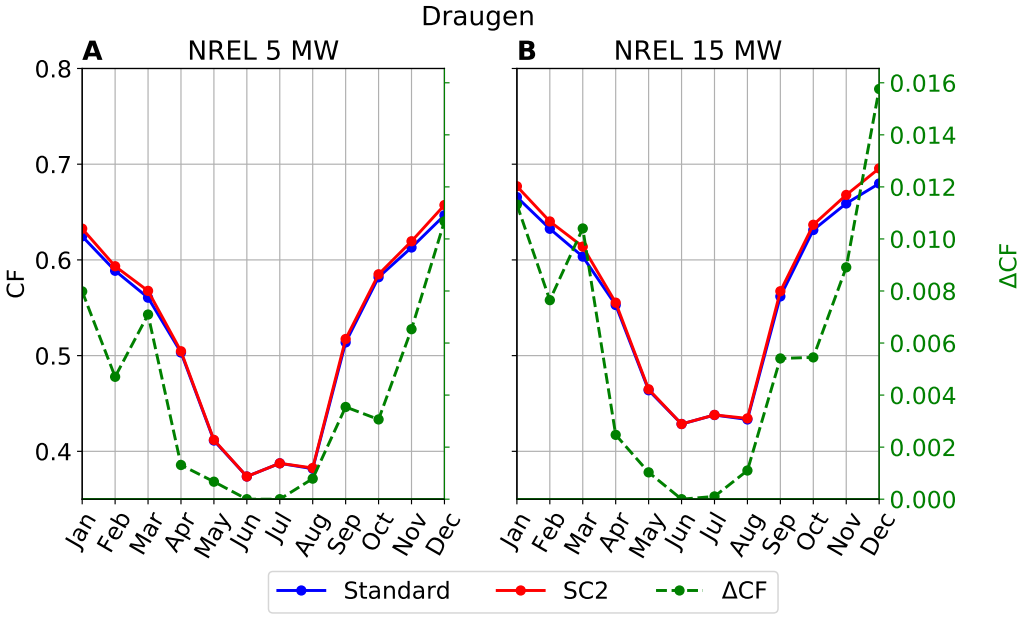

Figure L.5:

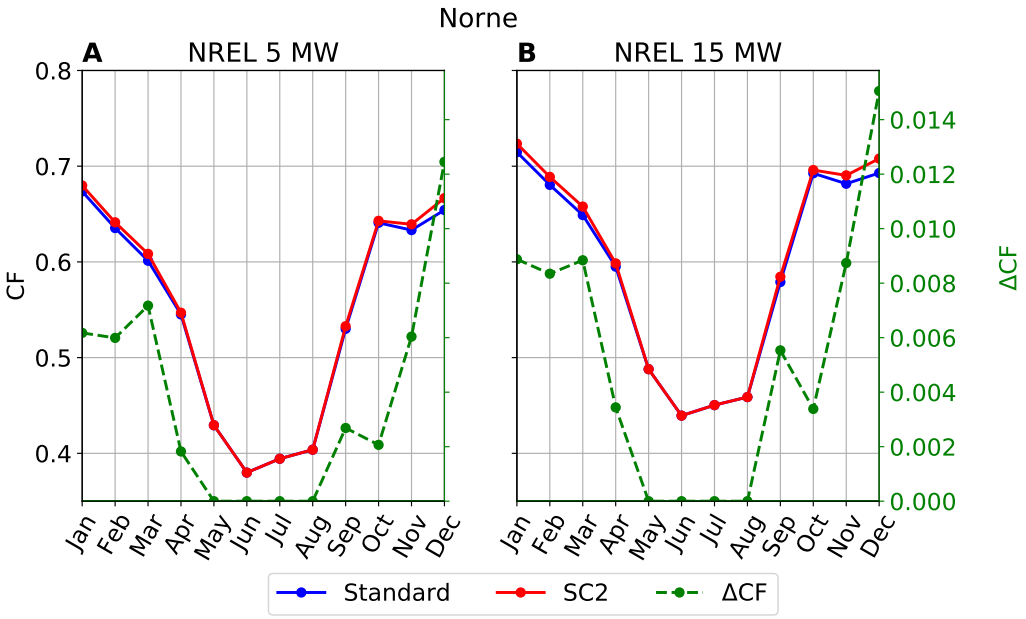
Norne
A
NREL 5 MW
B
NREL 15 MW
CF
ΔCF
0.8
0.7
0.6
0.5
0.4
0.014
0.012
0.010
0.008
0.006
0.004
0.002
0.000
Jan
Feb
Mar
Apr
May
Jun
Jul
Aug
Sep
Oct
Nov
Dec
Standard
SC2
ΔCF

Figure L.6:

Appendix M: Ramp rate for NREL 5 MW and NREL 15 MW

Figures M.1-M.6 show the ramp rate computed for the NREL 5 MW turbine and the NREL 15 MW turbine for wind speeds at hub height above 20 m/s. Table M.1 lists the ratio of wind speeds above 20 m/s for each site. Sites: Sørlige Nordsjø II, Sleipner A, Utsira Nord, Gullfaks C, Draugen and Norne. Time period: 2004-2015.

Site	NREL 5 MW	NREL 15 MW
Sørlige Nordsjø II	2.7	4.3
Sleipner A	4.1	5.8
Utsira Nord	4.1	5.5
Gullfaks C	4.9	6.4
Draugen	3.5	4.6
Norne	3.1	4.2
Average	3.7	5.1

Table M.1: Ratio [%] of wind speeds above 20 m/s for NREL 5 MW (90 m) and NREL 15 MW (150 m). Time period: 2004-2015.

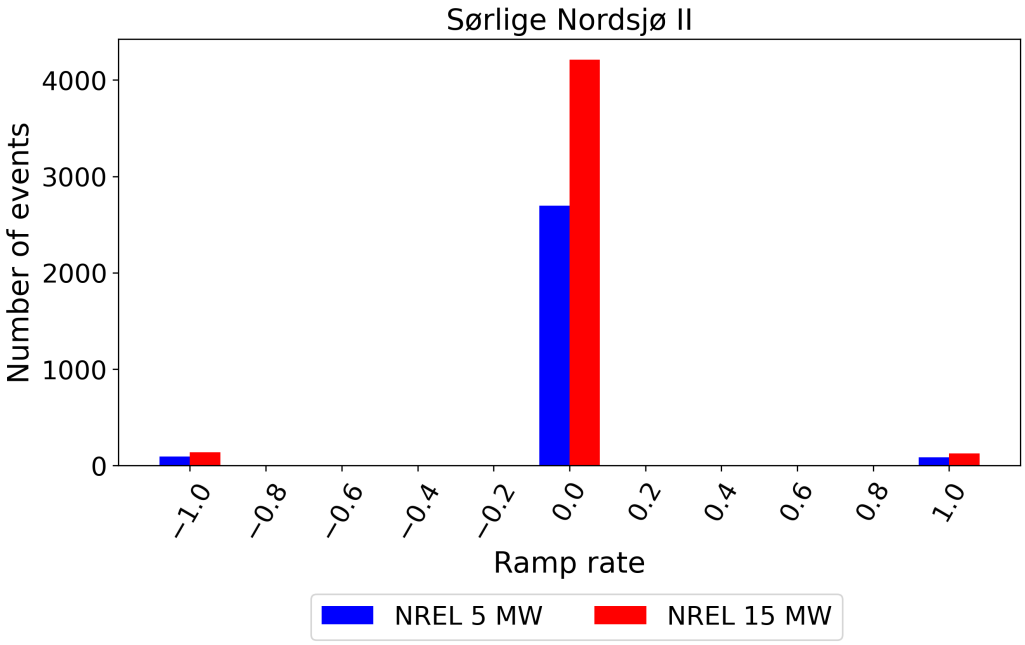

Figure M.1:

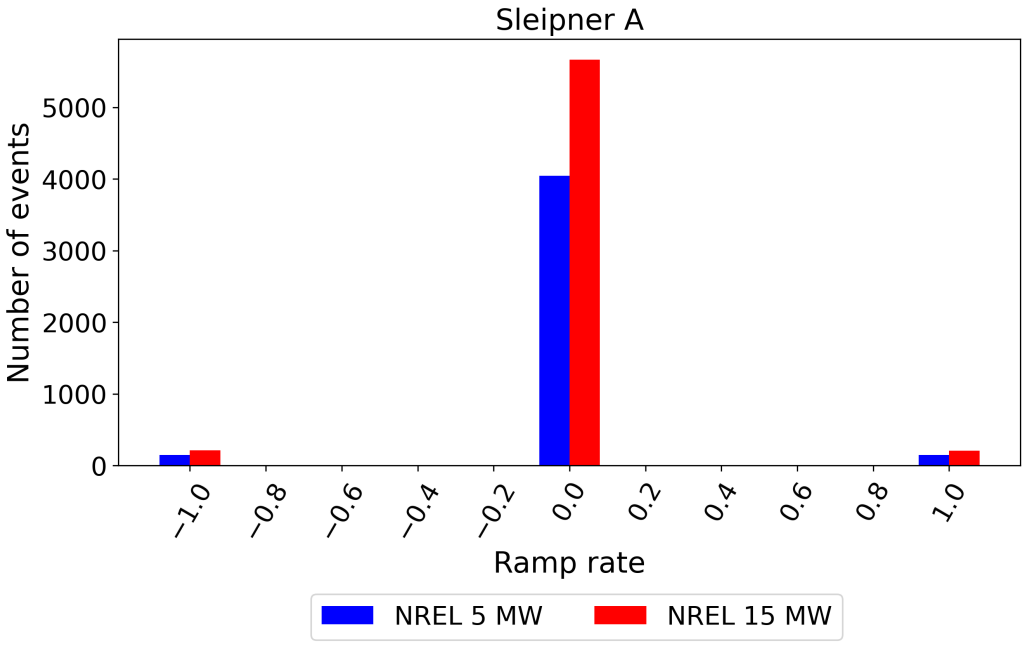

Figure M.2:

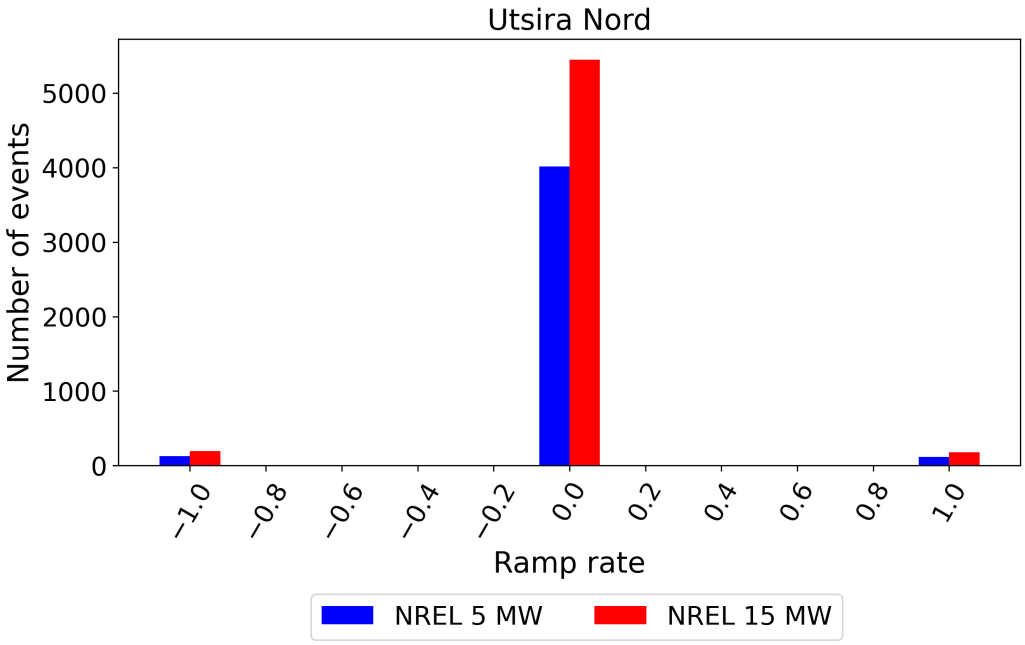

Figure M.3:

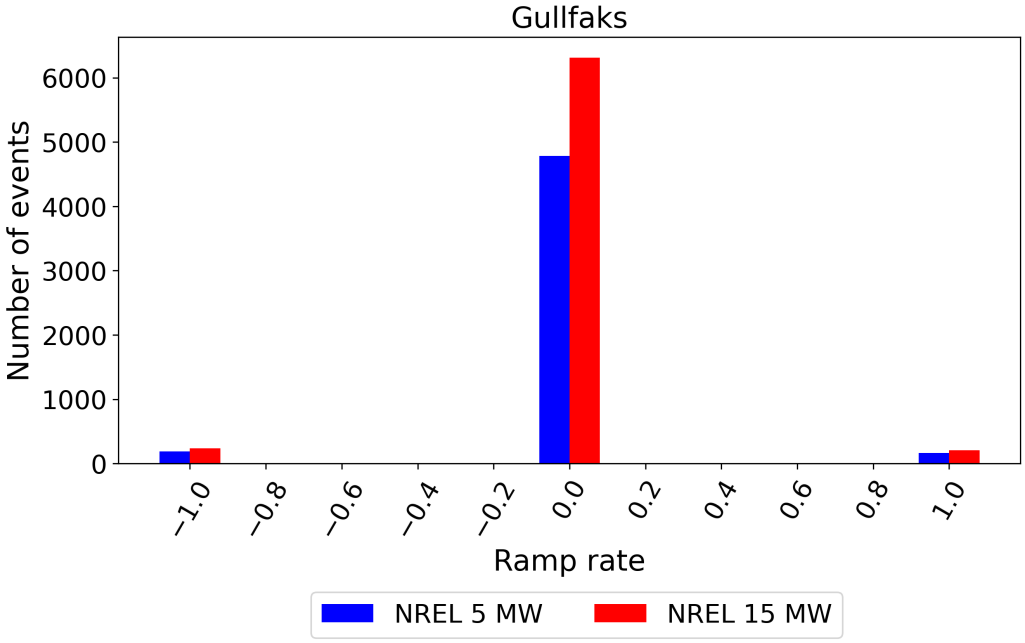

Figure M.4:

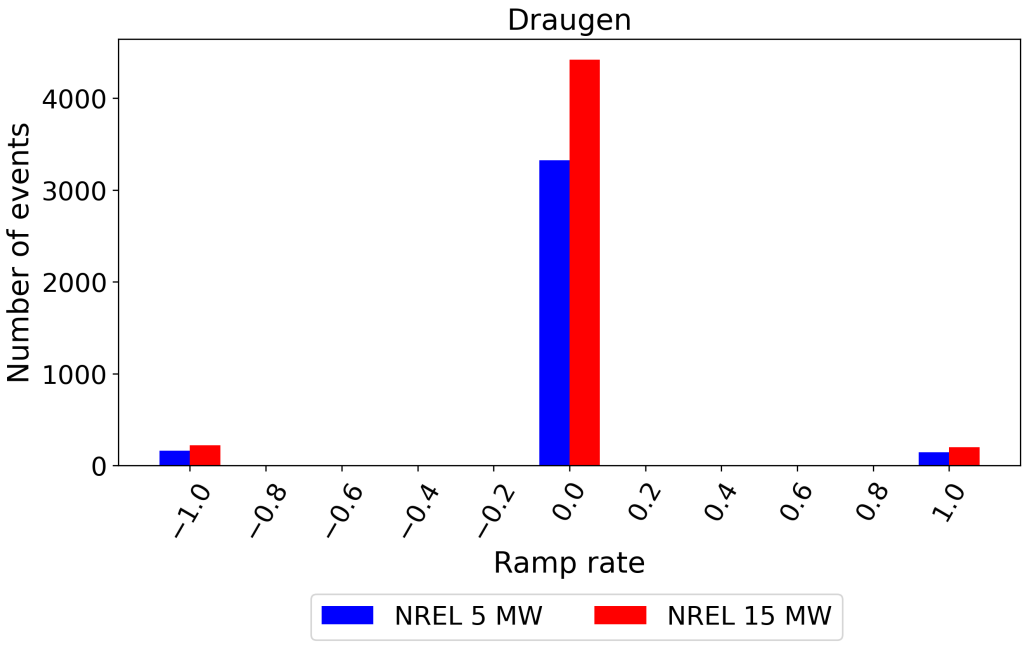

Figure M.5:

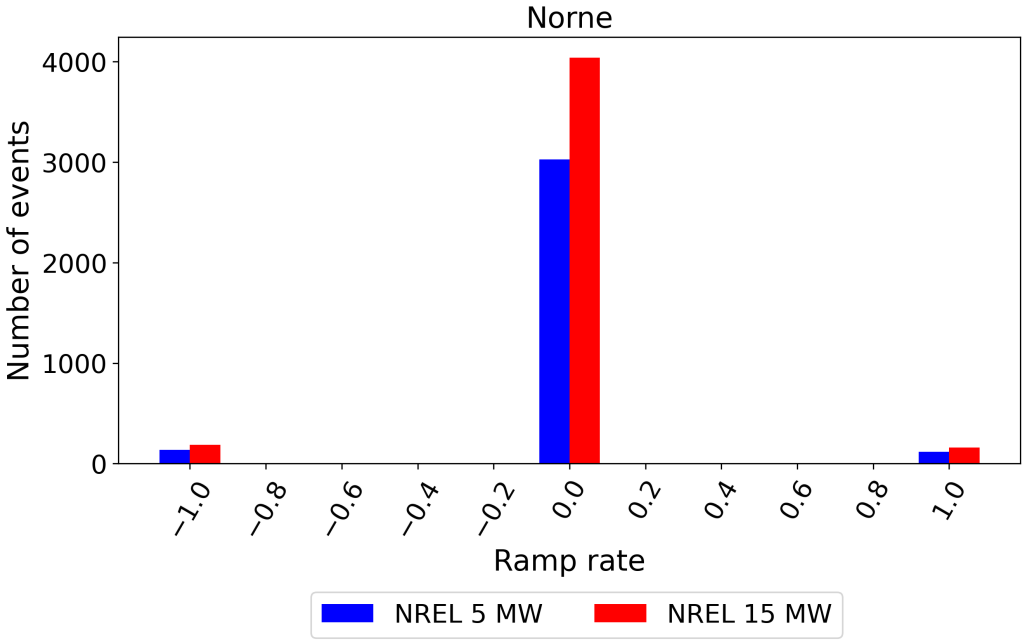

Figure M.6:

Appendix N: Ramp rate Standard, SC1 and SC2

Figures N.1-N.6 show the ramp rate computed for the NREL 5 MW turbine using the standard power curve (Standard), storm control 1 (SC1) and storm control 2 (SC2) for wind speeds at hub height above 20 m/s. Sites: Sørlige Nordsjø II, Sleipner A, Utsira Nord, Gullfaks C, Draugen and Norne. Time period: 2004-2015.

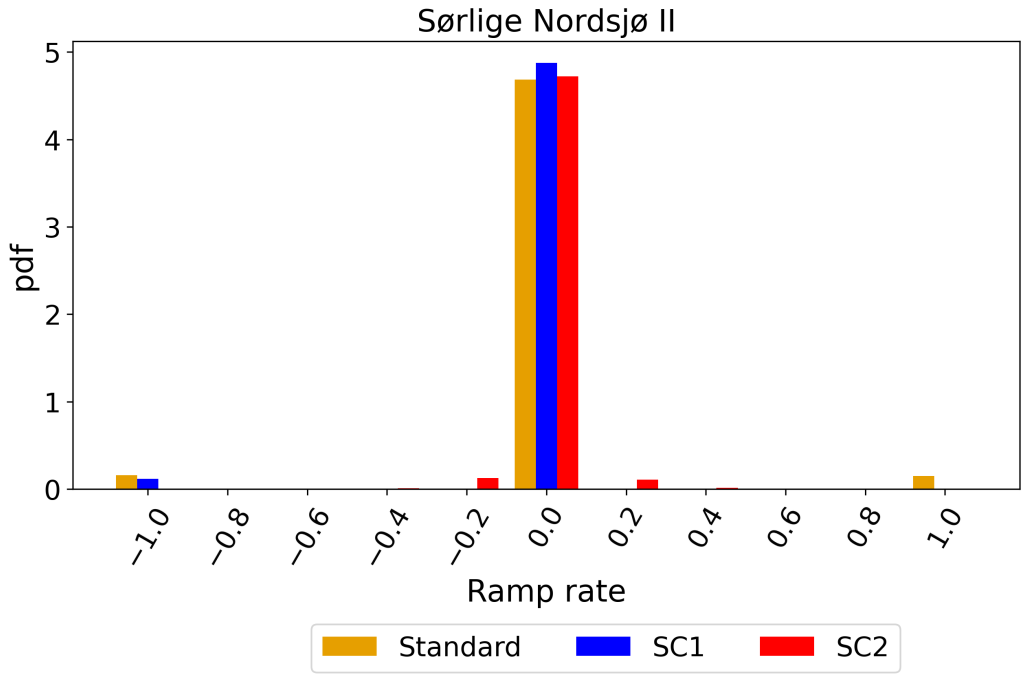

Figure N.1:

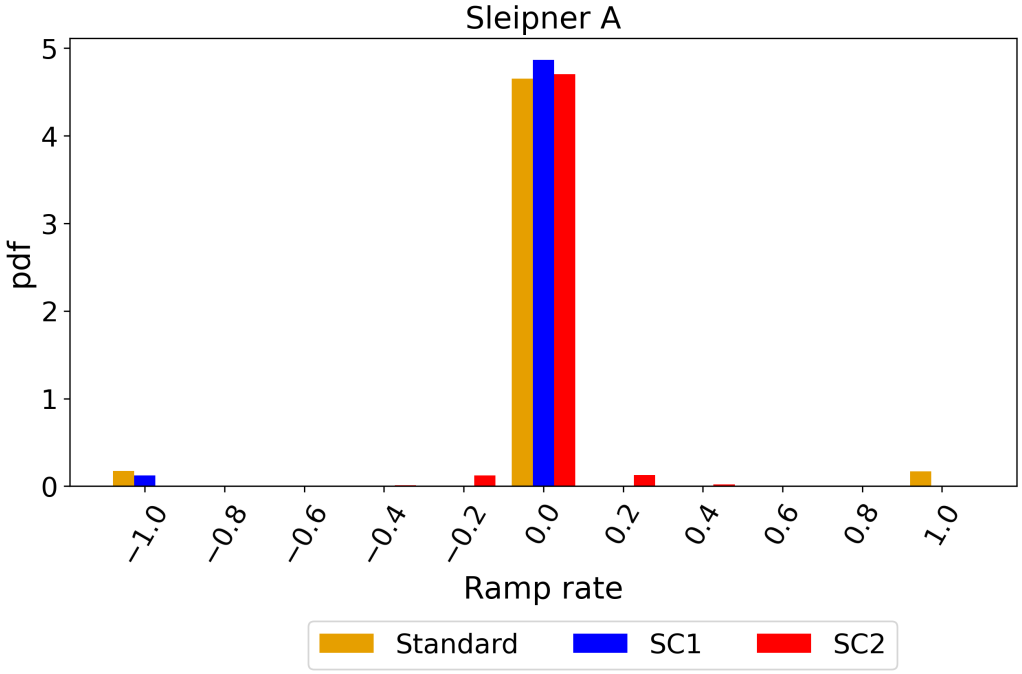

Figure N.2:

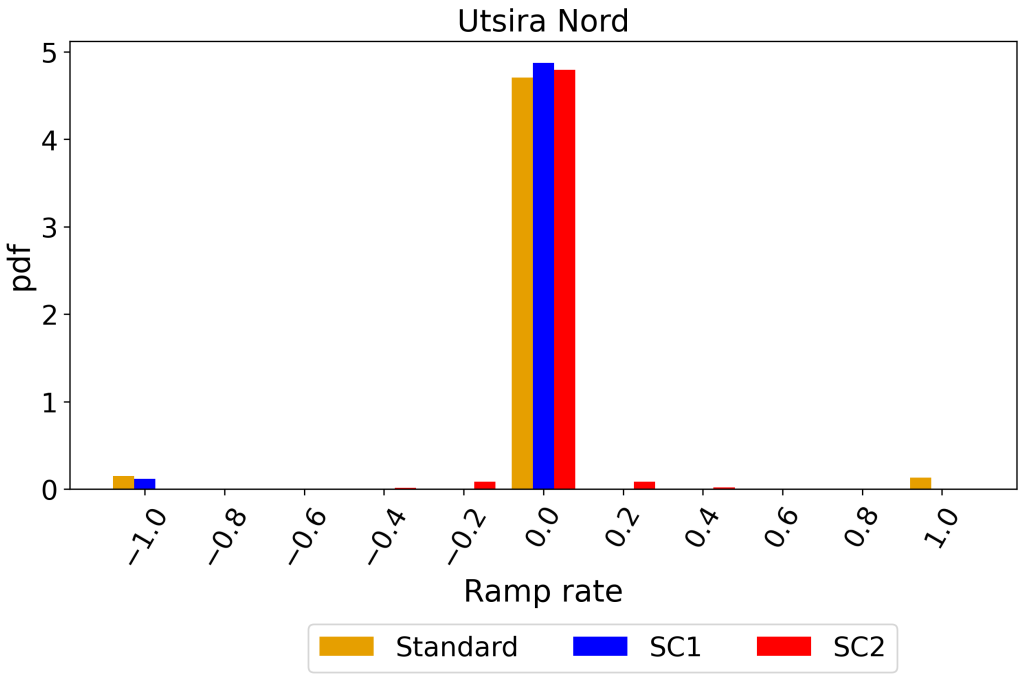

Figure N.3:

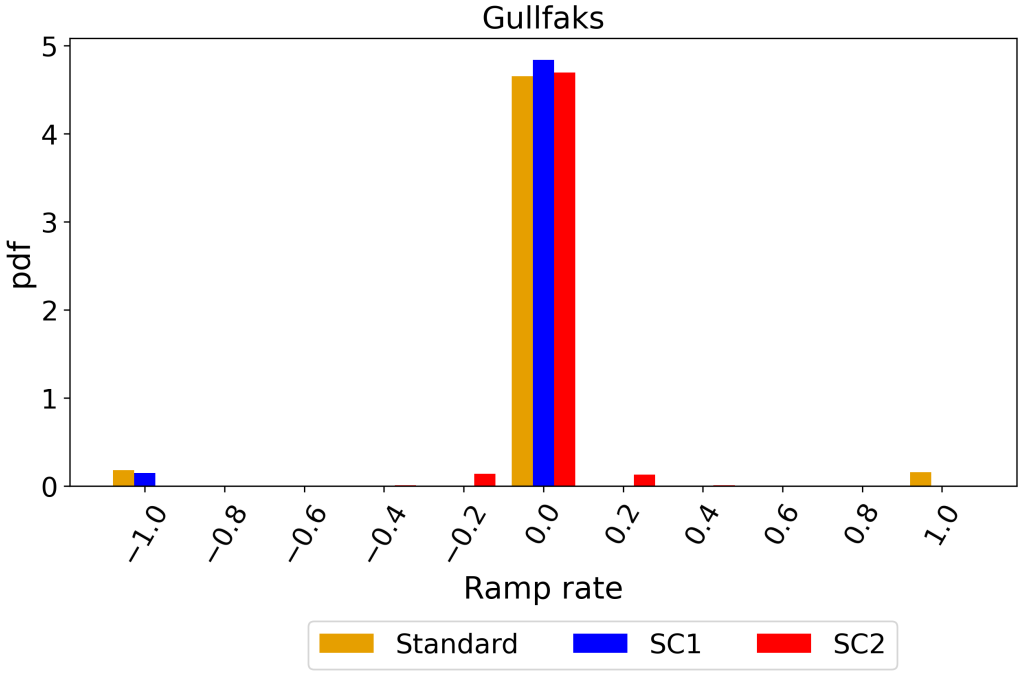

Figure N.4:

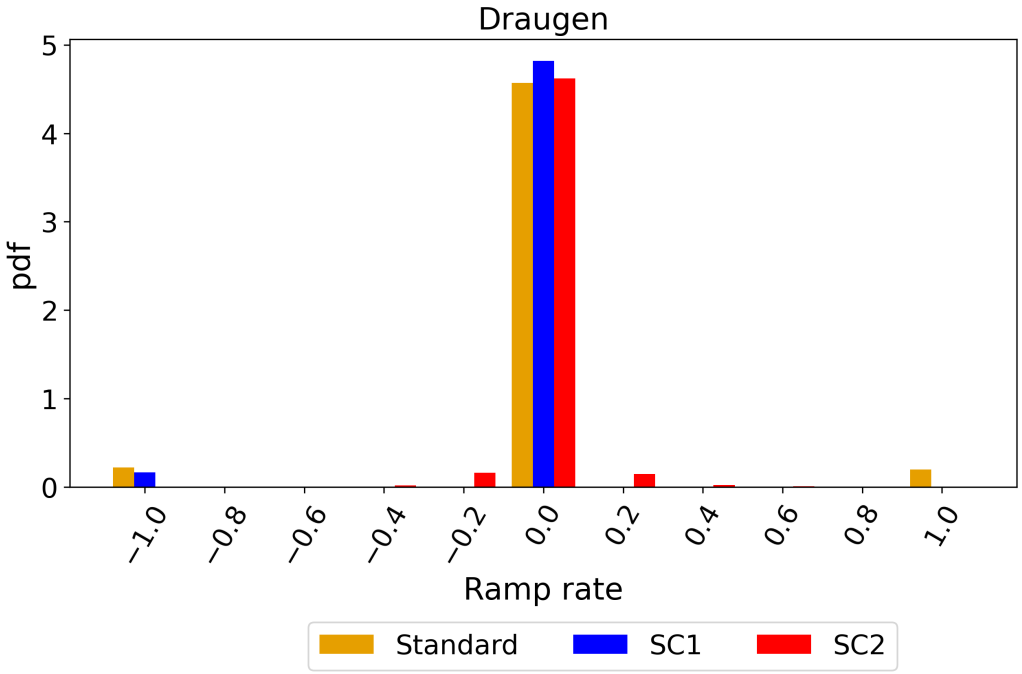

Figure N.5:

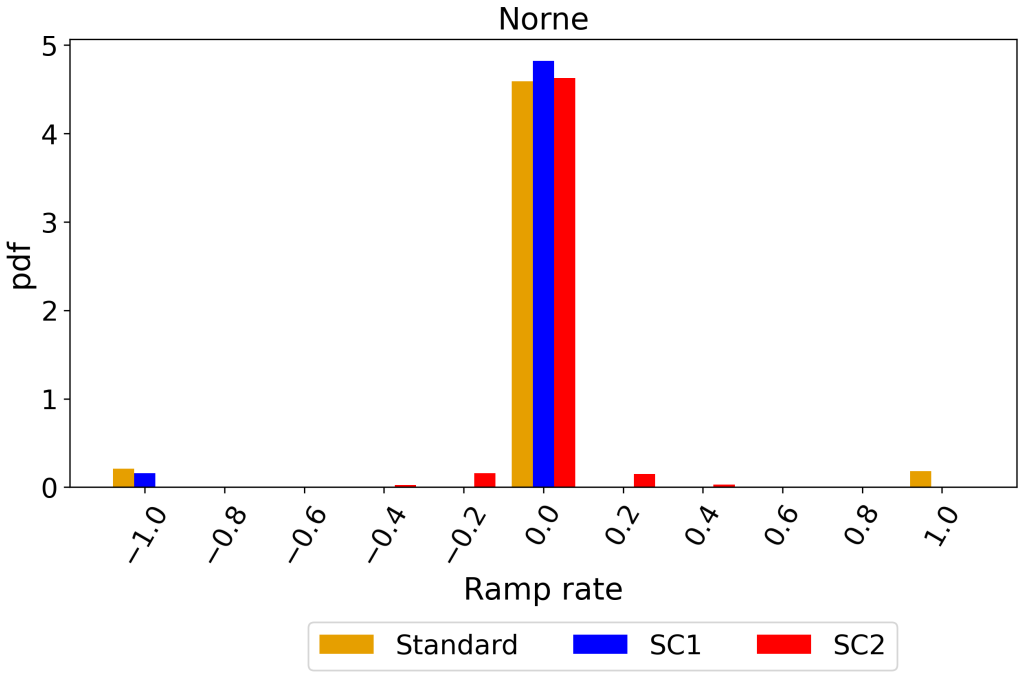
Norne
pdf
0
1
2
3
4
5
−1.0
−0.8
−0.6
−0.4
−0.2
0.0
0.2
0.4
0.6
0.8
1.0
Ramp rate
Standard
SC1
SC2

Figure N.6: